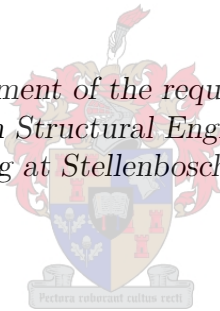


Tensile and Shear Characterisation of the Joint Interface of Alternative Masonry

by

Jacob Michal Schmidt

*Thesis presented in fulfilment of the requirements for the degree of
Master of Engineering in Structural Engineering in the Faculty of
Engineering at Stellenbosch University*



*The financial assistance of the National Research Foundation (NRF) towards this
research is hereby acknowledged. Opinions expressed and conclusions arrived at, are
those of the author and are not necessarily to be attributed to the NRF.*

Supervisor: Dr. Wibke de Villiers

March 2020

Declaration

By submitting this thesis electronically, I declare that the entirety of the work contained therein is my own, original work, that I am the sole author thereof (save to the extent explicitly otherwise stated), that reproduction and publication thereof by Stellenbosch University will not infringe any third party rights and that I have not previously in its entirety or in part submitted it for obtaining any qualification.

Jacob Michal Schmidt
March 2020

Copyright © 2020 Stellenbosch University
All rights reserved

Abstract

Tensile and Shear Characterisation of the Joint Interface of Alternative Masonry

J.M. Schmidt

*Department of Structural Engineering,
University of Stellenbosch,
Private Bag X1, Matieland 7602, South Africa.*

Thesis: MEng (Civil)

March 2020

One of the biggest challenges that the South African government is confronted with is providing adequate housing for approximately 2.3 million households still living in informal settlements. Currently, the most popular building material for low income housing (LIH) in South Africa is cement-based masonry units. However, the cement manufacturing industry is considered to be one of the largest carbon dioxide releasing industries in the world. This shows that the usage of cement-based masonry, as construction material, is unsustainable and alternative masonry materials are required. Nonetheless, if alternative masonry units (AMUs) are to replace conventional masonry units (CMUs), these AMUs would need to be structurally viable, environmentally friendly and socially and economically acceptable.

If AMUs should replace CMUs in the South African housing market, minimum mechanical specifications are required. The goal is to develop performance-based regulation for AMU construction. Common mechanical properties like strength and stiffness, of different AMUs are regularly studied. However, concepts like the tensile and shear characterisation of the masonry unit/mortar interface are not researched frequently.

This study investigates whether certain standards and benchmark tests used on conventional masonry can be successfully applied to alternative masonry. It also aims to determine certain mechanical properties. The focus of this study is the tensile and shear characterisation of the masonry unit/mortar interface on three different types of AMUs with two different mortars. These AMUs include the geopolymer (GEO) unit, cement stabilised earth (CSE) unit and adobe (ADB) unit. Results from the AMUs are compared to conventional concrete (CON) units which act as the benchmark material in this study.

The main mechanical properties investigated in this study include the following:

- Tensile strength and tensile fracture energy of masonry units/mortar interfaces.
- Initial shear strength, friction angle, shear fracture energy and initial dilatancy angle of masonry units/mortar interfaces.

Results from the tensile tests show that the water absorption characteristics of the masonry unit have a larger influence on the bond strength than the surface roughness. The shear tests indicate that the linear relationship defined by the Mohr-Coulomb friction law, between the shear stress and the pre-compression stress, continues for a higher pre-compression load of 2 N/mm^2 . The tensile and shear tests caused complications for determining the respective fracture energies in tension and shear. In contradiction to suggestions from literature, non-zero dilatancy values were obtained for shear tests at a pre-compression load of 2 N/mm^2 for CON and GEO masonry. The tests were conducted successfully in most cases and this confirmed the test setups as satisfactory, bar certain aspects, which are recommended for future studies.

The findings of this study can be used to add reliable data to literature, of the mechanical properties of the masonry unit/mortar interface of alternative masonry. This can complement other studies in developing a finite element model to simulate and analyse structures with different geometries constructed of AMUs on a performance basis. Additionally it can contribute towards the regulation of construction with AMUs in South Africa.

Opsomming

Trek- en Skuifkarakterisering van die Messelwerk Eenheid/Mortel Skeidingsvlak van Alternatiewe Messelwerk

J.M. Schmidt

*Departement Struktuur Ingenieurswese,
Universiteit van Stellenbosch,
Private Bag X1, Matieland 7602, Suid Afrika.*

Thesis: MIng (Siviël)

Maart 2020

Een van die grootste uitdagings waarmee die Suid-Afrikaanse regering gekonfronteer word is die voorsiening van voldoende behuising aan sowat 2.3 miljoen huishoudings wat steeds binne informele nedersettings woon. Tans is sement-gebaseerde messelwerkeenhede die gewildste boumateriaal vir lae inkomste behuising (LIH) in Suid-Afrika. Die sement vervaardigingsnywerheid is egter een van die nywerhede wat die meeste koolstofdiksied vrystel ter wêreld. Dit wys dat die gebruik van sement-gebaseerde messelwerk as konstruksiemateriaal onvolhoubaar is en alternatiewe messelwerk materiaal benodig word. Nietemin, as alternatiewe messelwerkeenhede (AMU's) konvensionele messelwerkeenhede (CMU's) vervang, moet hierdie AMU's struktureel lewensvatbaar, omgewingsvriendelik en sosiaal en ekonomies aanvaarbaar wees.

As AMU's CMU's sou vervang in die Suid-Afrikaanse behuisingsmark, is minimum meganiese spesifikasies nodig. Die doel is om prestasie-baseerde regulasie vir AMU-konstruksie te ontwikkel. Algemene meganiese eienskappe soos sterkte en styfheid van verskillende AMU's word gereeld bestudeer. Konsepte soos die trek- en skuifkarakterisering van die messelwerkeenhede/mortel skeidingsvlak word egter nie gereeld ondersoek nie.

Hierdie studie ondersoek die moontlikheid dat sekere standarde en normtoetse wat op konvensionele messelwerk gebruik word, suksesvol op alternatiewe messelwerk toegepas kan word. Dit het ook ten doel om sekere meganiese eienskappe te bepaal. Die fokus van hierdie studie is die trek- en skuifkarakterisering van die messelwerkeenhede/mortel skeidingsvlak op drie verskillende AMU's met twee verskillende mortels. Hierdie AMU's is onder meer die alkali-geaktiveerde betonblokke (GEO), die sement-gestabiliseerde grondblokke (CSE) en die adobeblokke (ADB). Resultate van die AMU's word vergelyk met konvensionele beton eenhede (CON) wat as die maatstaf materiaal in hierdie studie dien.

Die hoof meganiese eienskappe wat in hierdie studie ondersoek word, sluit die volgende in:

- Treksterkte en trekfraktuurenergie van messelwerkeenhede/mortel skeidingsvlakke.

- Aanvanklike skuifsterkte, samehorigheid, wrywingshoek, skuiffraktuurenergie en aanvanklike dilatansiehoek van messelwerkeenhede/mortel skeidingsvlakke.

Die resultate van die trektoetse het getoon dat die waterabsorpsie-eienskappe van die messelwerk 'n groter invloed op die bindingssterkte het as die oppervlakte se grofheid. Die skuiftoetse het aangedui dat die lineêre verhouding, gedefinieër deur die Mohr-Coulomb wrywingswet, tussen die skuifspanning en die normaalspanning, volgehou word vir 'n hoër normaal-las van 2 N/mm^2 . Dit is bevind vir die CON-messelwerk en alternatiewe messelwerkmateriale, behalwe die ADB-materiaal. Die opstellings van die trek en skuif toetse het komplikasies veroorsaak tydens die bepaling van die onderskeie fraktuurenergieë in trek en skuif. In teenstelling met literatuur, is daar geen nul-dilatansie waardes vir skuiftoetse verkry met 'n normaal-las van 2 N/mm^2 vir CON- en GEO-messelwerk nie. Die toetse is in die meeste gevalle suksesvol uitgevoer en dit het bevestig dat die toetsopstellings bevredigend is behalwe vir sekere aspekte, wat aanbeveel word vir toekomstige studies.

Die bevindinge van hierdie studie kan gebruik word om betroubare gegewens aan die literatuur te voeg oor die meganiese eienskappe van die messelwerkeenhede/mortel skeidingsvlak van alternatiewe messelwerk. Dit kan ander studies aanvul in die ontwikkeling van 'n prestasiegebaseerde eindige-elementmodel (FEM) om strukture te simuleer en te analiseer met verskillende geometrie wat uit AMU's saamgestel is. Dit kan ook bydra tot die ontwikkeling van streeks- en nasionale standaarde vir AMU-konstruksie binne Suid-Afrika.

Acknowledgements

I, hereby, want to thank the following people for their assistance in the completion of this study:

- Charlton and Leroi, thank you for your assistance in the laboratory and for reducing my workload when I needed it most.
- Deon, I appreciate your help in the workshop.
- Oom Johan, your general knowledge is astonishing. Thank you for all the wisdom you shared, and the many hours of helping me in the laboratory and workshop. I will miss our lengthy conversations and your stories about the South African history.
- Timmy, thank you for the many hours you helped me in the concrete lab.
- Bongani, thank you for decreasing my workload. You helped a lot and I enjoy all our conversations.
- Prince Shiso, I value all the knowledge you shared with me regarding the practical side of my thesis.
- To my colleagues, Divan, Marnu, Gerius, Vital, Seung and JP. Thanks for all the coffee's, conversations and laboratory help when I needed it.
- To my supervisor Wibke de Villiers, thank you for your patience, valuable feedback and support.
- To my friends, there are too many to name here. Thank you for your encouragement and motivation throughout these two years.
- To my mom and dad, thank you for your prayer and financial support. I am thankful for such parents.
- Ebard, from one wombat to another: it started with Simonsrust number 4 and a few adam runs, went to the Cheetahs winning the Currie Cup and the Springboks the World Cup, I can't wait to see what next year holds!

To my wife, Tanya Schmidt. You really are a champion, a gift and blessing to me. I value you so much. Thank you for standing by my side from 2 August 2013, and especially for the last two years. Thank you for all the small things you do for me, for keeping me fed, for every coffee with rusks in the mornings and milo's in the evenings. Thank you for understanding my sometimes-weird time schedule, for staying positive and motivating me to the end. Your unselfishness reminds me of our Lord Jesus Christ.

Lastly, to our Father in heaven and our Lord Jesus Christ. I would not be able to express my thanks in words. Your faithfulness exceeds all my understanding. Thank you for your love and what you taught me in these last two to years. You truly are, "the great I AM".

Contents

Declaration	i
Abstract	ii
Opsomming	iv
Acknowledgements	vi
Contents	vii
List of Figures	x
List of Tables	xiii
Nomenclature	xv
1 Introduction	1
1.1 Outline	1
1.2 Motivation for Research	1
1.3 Scope	2
1.4 Objectives	3
1.5 Methodology	3
1.6 Thesis Structure	4
2 Background	6
2.1 Environmental Concerns of Conventional Masonry Units (CMUs)	6
2.2 Low Income Housing (LIH) and CMUs in South Africa	7
2.3 Alternative Masonry Units (AMUs)	9
2.3.1 Adobe (ADB) Unit	12
2.3.2 Cement Stabilised Earth (CSE) Unit	15
2.3.3 Geopolymer (GEO) Unit	19
2.4 Conclusion	23
3 Literature Review	24
3.1 Tensile and Shear Characterisation of the Joint Interface	24
3.1.1 The Concept of Fracture Energy	25
3.1.2 Tensile Characteristics of the Joint Interface	27
3.1.3 Shear Characteristics of the Joint Interface	30
3.1.4 Concluding Remarks	36
3.2 Factors Influencing the Bond Strength of the Joint Interface	37
3.2.1 Masonry Unit Characteristics Affecting the Bond Development of the Joint Interface	37
3.2.2 Mortar Parameters Affecting the Bond Development of the Joint Interface	39

3.2.3	Concluding Remarks	40
3.3	Different Testing Procedures	40
3.3.1	Direct Tensile Test	40
3.3.2	Bond Wrench Test	41
3.3.3	Wedge Splitting Test	44
3.3.4	Concluding Remarks	46
3.4	Conclusion	46
4	Materials and Masonry Unit Production	47
4.1	Materials	47
4.1.1	Aggregates	47
4.1.2	Binders	49
4.1.3	Alkaline Solution	49
4.1.4	Water	50
4.2	Masonry Unit Production	50
4.2.1	Concrete (CON) Units	51
4.2.2	Geopolymer (GEO) Units	54
4.2.3	Cement Stabilised Earth (CSE) Units	58
4.2.4	Adobe (ADB) Units	61
4.3	Mortar Design	64
4.4	Conclusion	66
5	Experimental Procedure	67
5.1	Masonry Unit Tests	67
5.1.1	Compressive Strength Test Specifications	68
5.1.2	Modulus of Elasticity Test Specifications	70
5.1.3	Dry Density Test Specifications	74
5.1.4	Water Absorption Test Specifications	75
5.1.5	Determination of Surface Roughness	78
5.2	Mortar Tests	79
5.2.1	Consistence (Flow value) Test Specifications	79
5.2.2	Dry Density Test Specifications	80
5.2.3	Flexural and Compressive Strength Test Specifications	81
5.3	Joint Interface Tests	83
5.3.1	Direct Tensile Strength Test Specifications	84
5.3.2	Shear Strength Test Specifications	87
5.4	Conclusion	95
6	Results, Comparisons and Discussion	96
6.1	Masonry Unit Test Results	97
6.1.1	Compressive Strength	97
6.1.2	Modulus of Elasticity	100
6.1.3	Dry Density	102
6.1.4	Water Absorption	103
6.1.5	Surface Roughness	106
6.2	Mortar Test Results	107
6.2.1	Flow Value of Mortar	108
6.2.2	Dry Density of Mortar	108
6.2.3	Flexural and Compressive Strength of Mortar	109
6.2.4	Modulus of Elasticity of Mortar	110
6.3	Joint Interface Test Results	111
6.3.1	Direct Tensile Strength	111

6.3.2	Shear Strength	115
6.4	Conclusion	127
7	Conclusions and Recommendations	128
7.1	Conclusions	129
7.2	Recommendations	132
	References	134

List of Figures

2.1	CON units for LIH in South Africa, with a) the maxi-concrete block on the left and b) the hollow concrete block on the right	8
2.2	Standard low income house built with (a) fired clay bricks in Phuthaditjhaba and with (b) hollow concrete blocks near Kleimond (Leading Architecture, 2011), South Africa	9
2.3	Two storey load bearing soil-cement block masonry building in India (Reddy and Jagadish, 2003)	11
2.4	Distribution of earth buildings across the globe (Fratini <i>et al.</i> , 2011).	12
2.5	Eroded earth building near Kokstad in Kwazulu-Natal province, South Africa.	13
2.6	Sun drying ADB units (Dowling, 2004).	15
2.7	CSE units compaction process: a) Filling mould with mix b) Compacting soil c) Removing final unit (Reddy, 2012)	18
2.8	The effect of a) mixing time, b) retention time and c) curing conditions on a CSEB unit (<i>based on data from Rigassi (1995)</i>)	19
2.9	Alkali-activated binders, from the raw materials to the final binder product (Provis, 2013).	20
3.1	Wedge splitting test on drilled specimen (Brühwiler and Wittmann, 1990)	26
3.2	Typical load-deformation graph for stable fracture mechanics test (Schneemayer <i>et al.</i> , 2014)	26
3.3	Standard test methods for determining bond strength of mortar to masonry units (ASTM C 952-12, 2012)	27
3.4	Crossed couplet test recommended by NEN 3835 (1991) (<i>adapted from Van der Pluijm (1999)</i>)	28
3.5	General stress-deformation graph of the: a) compression- and b) tensile strength test on masonry units (Lourenço, 1998)	28
3.6	Flexural bond strength vs compressive strength relationship (Lumantarna <i>et al.</i> , 2014)	29
3.7	Shear behaviour of the joint interface with and without a normal confining load (Lourenço, 1998)	31
3.8	Horizontal masonry joint shear test methods: a) the couplet test, b) van der Pluijm test and c) triplet test.	32
3.9	Cohesion vs compressive strength relationship (Lumantarna <i>et al.</i> , 2014)	34
3.10	Visual interpretation of the concept of dilatancy with ratio $\Delta v/\Delta u$ (De Vasconcelos, 2005)	34
3.11	Dilatancy displacement at the joint interface upon inelastic shear of masonry (Van der Pluijm, 1992a)	35
3.12	Front and top view of the crossed-brick couplet specimen in test setup configuration (<i>adapted from Katiyar (2015)</i>)	41
3.13	Example of a) suitable support structure and b) clamp for the bond wrench test (<i>adapted from EN 1052-5 (2005)</i>)	42

3.14	Failure modes providing valid bond strength results as per Annex A of EN 1052-5 (2005)	43
3.15	Steps of assembly for the wedge splitting test set-up (Brühwiler and Wittmann, 1990)	44
3.16	Wedge splitting test with mortar-brick interface in the middle of the specimen (Schneemayer <i>et al.</i> , 2014)	45
4.1	Grading of Materials	48
4.2	Sieve analysis of Malmesbury sand #3	48
4.3	Manual block press, from Hydraform, with wooden boards	51
4.4	CON units weight batched into steel bowels on a trolley	53
4.5	Curing process of CON unit	54
4.6	Mixing procedure of GEO unit	57
4.7	GEO unit after curing	57
4.8	Crystal-like substance brushed of GEO unit	58
4.9	The maximum dry density and OMC of the CSE unit as per SANS 3001-GR30 (2015)	59
4.10	CSE unit after demoulding	60
4.11	Curing process of CSE unit	61
4.12	Combined gradings of first ADB mix design vs new ADB mix design	63
4.13	Manufacturing procedure of ADB unit	64
4.14	Curing process of ADB unit	64
5.1	GEO unit in industrial grinder from MATEST	69
5.2	CSE unit in compressive strength test setup	70
5.3	Loading cycles for the determination of the secant modulus of elasticity (<i>adopted from EN 12390-13 (2013)</i>)	71
5.4	The CON, CSE and ADB prism for the modulus of elasticity test	72
5.5	Elastic modulus test setup	73
5.6	Elastic Modulus testing frames	73
5.7	Water absorption test procedure	76
5.8	Water absorption of CSE unit at different time periods	77
5.9	ADB unit surface after immersion	78
5.10	Surface roughness specimens	79
5.11	Flow table test procedure	80
5.12	Four point bending test	82
5.13	The (a) CSE crossed-brick couplet specimen and the (b) CON triplet specimen after curing for 7 days	83
5.14	Crossed-brick couplet construction procedure of CSE material	85
5.15	Crossed-brick couplet of each material investigated in this study	86
5.16	Crossed-brick couplet test setup with GEO couplet	86
5.17	Triplet test loading and pre-compression configuration (<i>adapted from EN 1052-3 (2002)</i>)	88
5.18	Failure modes providing a valid bond strength results as per Annex A of EN 1052-5 (2005)	89
5.19	ADB triplet specimen	90
5.20	Triplet test setup at zero pre-compression	91
5.21	Triplet test setup for applying pre-compression	92
5.22	Triplet test setup for levels of high pre-compression	93
5.23	Back view of triplet test setup	94
6.1	Average compressive strengths measured at 28 days for CON, GEO, CSE and ADB units	98
6.2	Average modulus of elasticity measured at 28 days for CON, GEO, CSE and ADB units	100

6.3	Average dry density measured at 28 days for CON, GEO, CSE and ADB units . . .	102
6.4	Water absorption of different masonry units by weight	105
6.5	Surface images of typical CON, GEO, CSE and ADB unit	106
6.6	Average compressive (f_{cm}) and flexural (f_{fm}) strength of mortar measured at 7 days .	109
6.7	Average modulus of elasticity measured at 7 days for 7M and 20M	111
6.8	Average tensile bond strength of the joint interface measured at 7 days	112
6.9	Crossed brick couplet test failure types (a) B1 and (b) B5	114
6.10	Shear bond strength of the joint interface at different pre-compression levels from the triplet tests for both mortars	116
6.11	Shear bond strength of the joint interface at different pre-compression levels for all materials and both mortars	117
6.12	Triplet test failure types (a) A1/1 and (b) A1/2	119
6.13	Load vs displacement diagrams for each triplet test and each mortar	121
6.14	Load vs displacement diagrams for triplet test with sudden failure vs triplet test with descending branch	123
6.15	Dilatancy results of the joint interface from triplet tests	125

List of Tables

2.1	Compressive strength requirements for CON units (SANS 1215, 2008)	9
2.2	Factors that influence AAC strength (Barnard, 2014)	22
3.1	Flexural bond strength (f_f) results from literature	29
3.2	Tensile bond strength (f_t) results from literature	30
3.3	Tensile fracture energy ($G_{f,t}$) results from literature	30
3.4	Shear bond strength results from literature	33
3.5	Shear fracture energy ($G_{f,s}$) results from literature	34
3.6	Dilatancy results from literature	36
4.1	Characterisation of aggregates	49
4.2	Chemical composition of Fly ash (FA) and Ground granulated corex slag (GGCS) (Fourie, 2017)	49
4.3	Comparison of aggregate materials in CON Unit	52
4.4	Mix design of CON unit	53
4.5	Factors that influence AAC strength of the mix used in this study	55
4.6	Mix design of GEO unit	56
4.7	Mix design of CSE unit	60
4.8	Combined FM of ADB Unit	62
4.9	Mix design of ADB unit	63
4.10	Mortar mix proportions	65
6.1	Average compressive strengths (f_c) values presented in Figure 6.1 and the coefficient of variation (COV)	98
6.2	Normalised average compressive strength (f_{nc}) values	99
6.3	Average modulus of elasticity values presented in Figure 6.2 and the coefficient of variation (COV)	101
6.4	Average dry density values presented in Figure 6.3 and the coefficient of variation (COV)	103
6.5	Average water absorption results and the coefficient of variation (COV)	104
6.6	Surface characteristics of masonry units	107
6.7	Flow value results of mortars	108
6.8	Average dry density results of mortars and the coefficient of variation (COV)	108
6.9	Average compressive (f_{cm}) and flexural strength (f_{fm}) values presented in Figure 6.6 and the coefficient of variation (COV)	110
6.10	Average modulus of elasticity values presented in Figure 6.7 and the coefficient of variation (COV)	111
6.11	Average tensile bond strength values presented in Figure 6.8 and the coefficient of variation (COV) for each mortar	113
6.12	Triplet test results	118
6.13	Summary of change in pre-compression during triplet tests	120
6.14	Shear fracture energy results	122

6.15 Dilatancy results 126

Nomenclature

Acronyms

Acronym	Description
AAB	Alkali-activated binder
AAC	Alkali-activated concrete
AACBB	Alkali-activated cement based binder
ABM	Alternative building material
ADB	Adobe
AMU	Alternative masonry unit
ASTM	American Section of the International Association for Testing Materials
BS EN	British Standard European Norm
CMOD	Crack mouth opening displacement
CMU	Conventional masonry units
CON	Concrete
CSE	Compressed stabilised earth
CSH	Calcium silicate hydrates
EBANZ	Earth Building Association of New Zealand
FA	Fly ash
FEM	Finite element model
GEO	Geopolymer
GGBS	Ground granulated blast-furnace slag
GGCS	Ground granulated corex slag
GHG	Greenhouse gasses
IMTM	Instron Materials Testing Machine
LIH	Low income housing
LVDT	Linear variable differential transducers
NBR	National Building Regulations
OPC	Ordinary Portland cement

OMC	Optimum moisture content
SABS	South African Bureau of Standards
SAICE	South African Institution of Civil Engineering
SANS	South African National Standard
SEM	Scanning electron microscopy
SH	Sodium hydroxide
SHRA	Social Housing Regulatory Authority
SHS	Sodium hydroxide solution
SS	Sodium silicate
URM	Unreinforced brick masonry

Symbols

Latin Letters	Units	Description
A_b	mm ²	Cross-sectional area of joint interface for direct tensile test
A_F	mm ²	Fracture area of wedge splitting test
A_i	mm ²	Cross-sectional area of joint interface parallel to specimen for triplet test
d	-	Shape factor of masonry unit
F_1	N	Applied load for bond wrench test
F_2	N	Weight of the bond wrench
$F_{applied}$	N	Total applied load for direct tensile tests
f_c	MPa	Compressive strength of masonry units
f_{ck}	MPa	Characteristic compressive strength of masonry
f_{cm}	MPa	Compressive strength of mortar
f_{fm}	MPa	Flexure strength of mortar
f_t	MPa	Tensile bond strength
f_{nc}	MPa	Normalised compressive strength
F_f	N	Total applied load for flexural strength test
F_h	N	Horizontal splitting force for wedge splitting tests
$F_{h,max}$	N	Maximum horizontal splitting force for wedge splitting tests
FM	-	Fineness modulus
F_{max}	N	Maximum shear force applied for triplet test
F_p	N	Pre-compression force applied for triplet test
F_t	N	Tensile splitting force

F_v	N	Vertical force for wedge splitting test
G_f	N/m	Specific fracture energy
$G_{f,t}$	N/m	Specific tensile fracture energy
$G_{f,s}$	N/m	Specific shear fracture energy
h	mm	Ligament length of wedge splitting test specimen
IRA	kg/m ² /min	Initial rate of absorption
K_E	-	Constant used for the prediction of the modulus of elasticity of masonry
l	mm	Support span for flexural strength test
M_b	Nm	Bending moment introduced from wedge splitting test
m	kg	Mass of masonry unit after air-dried in laboratory
m_d	kg	Dry mass of masonry unit
Ra	μm	Mean roughness value
RD	-	Relative density
t	s	Time
t_s	s	Immersion time
V	m ³	Volume
W	N	Weight of top unit after bond wrench test
$w_{initial}$	%	Initial moisture content of masonry units after air dry condition
Greek Letters	Units	Description
φ	degrees	Internal angle of friction
μ	-	Coefficient of friction
ψ	degrees	Dilatancy angle
ρ_d	kg/m ³	Dry density
σ_n	MPa	Normal compression stress
τ_c	MPa	Pure shear strength (cohesion)
τ_a	MPa	Shear strength at a certain normal stress

Chapter 1

Introduction

1.1 Outline

This study focuses on determining the tensile and shear characterisation of the joint interface of three types of alternative masonry units (AMUs). Namely, the geopolymer (GEO) unit, cement stabilised earth (CSE) unit and adobe (ADB) unit. These AMUs were specifically chosen due to this study being an extension of research previously conducted at Stellenbosch University.

Laboratory tests are performed on these AMUs as well as on concrete (CON) units, which are used as a benchmark material. Mechanical properties that are tested include the tensile strength, tensile fracture energy, initial shear strength and shear fracture energy of the joint interface. Additional interface parameters also tested for are dilatancy, cohesion and friction angle. The compressive strength and modulus of elasticity of the different AMUs, and mortars used to construct the masonry, are also tested to compare their quality to previous research on the same materials. Two mortars are compared throughout this study, a stronger and weaker mortar of approximately 20 MPa and 7 MPa. Further applicable tests are conducted on each type of AMU and mortar that would better characterise the bond strength of the joint interface.

An important concept to define, for use throughout the rest of this document, is masonry. The European testing standard EN 1052-1 (1999) defines masonry as, "An assemblage of masonry units laid in a specific bonding pattern jointed together with mortar." Lourenço (1998) states that masonry is a heterogeneous material consisting of units and joints. For this study masonry is defined by these two sources.

1.2 Motivation for Research

Cement based masonry units, also referred to as CON units, are currently the most popular building material, alongside fired clay bricks, used for construction of low income housing (LIH) in South Africa. The production of CON units, however, has a negative impact on the environment. This is due to emissions from the production process of cement and the usage of non-renewable natural resources. The cement production industry is one of the leading carbon emitting industries worldwide (Benhelal *et al.*, 2013).

Ample research has been conducted that considers these environmental concerns. The study done by Hasanbeigi *et al.* (2010) indicated that 900 kg CO₂ is emitted for every ton of cement produced and other literature states that approximately 5 % of global CO₂ emissions originate from the manufacturing process of cement (Huntzinger and Eatmon, 2009). This, with the growing universal awareness of being more environmentally conscious raises the need for construction companies to start considering alternative materials for masonry production to limit

the volumes of cement used in construction. Cement is one of the main constituents of CON units. More environmental concerns are discussed in Section 2.1.

However, for alternative masonry units to get into industry and compete with CON units these units have to meet certain regulations and requirements and outperform CON units. AMUs would have to keep the advantages of CON units and negate the disadvantages. Certain requirements these AMUs have to meet are:

- Structural viability
- Reduce the environmental impact
- Social and economic acceptability

To determine if AMUs are structurally viable, the characterisation and evaluation of their mechanical properties are of importance. Research in AMUs from the last two decades shows that there is still a shortage of knowledge when it comes to fully understanding their mechanical properties and structural behaviour in certain applications (Tennant *et al.*, 2012; Illampas *et al.*, 2011; Walker and Stace, 1996; Walker, 1999; Reddy and Gupta, 2006; Rao *et al.*, 1996; Lourenço, 1996; De Almeida, 2012; Schneemayer *et al.*, 2014; Van der Pluijm, 1999; Varum *et al.*, 2007). Most research and literature on AMUs focus on finding alternative building materials (ABMs) that best comply with the three requirements named earlier, especially being environmentally friendly.

Well known mechanical properties are regularly studied like strength and stiffness, but concepts concerning the tensile and shear characterisation of the masonry unit/mortar interface not as much. The masonry unit/mortar interface is referred to as the joint interface further in this study. A possible reason for the lack of research in this field can be due to more complex test setups needed to obtain these properties. The brittle nature of most masonry materials causes these tests to be even more difficult to execute.

For AMUs to replace CON units in the housing market in South Africa minimum mechanical specifications would need to be determined, with standards for construction. The end goal is to develop standardised codes for use in AMU construction. Even though standards are widely available for use on conventional masonry these standards cannot always be applied to alternative masonry due to the differences in their material properties. Therefore, a focus of this study is to either select appropriate benchmark tests and/or develop new ones, to determine accurate tensile and shear characteristics of the joint interface of alternative masonry.

Further motivation for this study is threefold. Firstly, to improve the understanding of the mechanical properties of different AMUs and to compliment further studies in informing a finite element model (FEM) to simulate and analyse different structures constructed out of AMUs. Secondly, to use these numerical modelling tools with actual test results to assist with the introduction and application of AMUs into the housing market in South Africa. Lastly, to add reliable data to literature, of the mechanical properties of alternative masonry, to contribute towards the development of regional and national standards for AMU construction.

1.3 Scope

The scope of this study consists of two parts. Firstly, the aim of this study is not to obtain the best AMUs for replacing CON units or optimising the mix design thereof, but rather to increase the knowledge of specific mechanical properties of AMUs. Therefore, less time was

spent on developing different mix designs but rather using mix designs from previous research done on these materials, at Stellenbosch University, to get an in-depth understanding of these mechanical properties. Developing a FEM is not part of this study, but rather determining some of the parameters needed to develop one in future studies.

Secondly, only certain mechanical properties of AMUs are determined in this study and therefore not a wide range of tests are conducted to avoid duplicating previous research. Time is rather spent on developing an in-depth understanding of available test methods to select either appropriate benchmark tests and/or developing new ones that would give accurate results for different AMUs.

1.4 Objectives

The two main objectives of this study are as follows:

1. The first objective is to determine whether standards and benchmark tests used on conventional masonry can be successfully applied on different AMUs to determine certain mechanical properties and if not, to develop tests which would deliver accurate results.
2. The second objective is the tensile and shear characterisation of three types of AMUs on the joint interface of the masonry.

In compliance with the first objective as three different AMUs were selected due to this study being an extension on previous research. The original aim of selecting these AMUs was to represent a range of materials with different material properties. This was done for a specific reason, and that is, to comprehensively analyse the applicability of conventional standards and tests on a group or range of different AMUs.

To meet the second objective tests included in this study are tests determining the tensile and shear strength of the joint interface. The tensile and shear fracture energy of the joint interface are also tested for, but can be determined from the strength tests on the interface. Tests for the compressive strength and modulus of elasticity are also conducted.

1.5 Methodology

The criterias for selecting these three specific AMUs in previous research, of which this study is an extension, are twofold. Firstly, as stated in Section 1.4, to display a range of materials with different mechanical properties and secondly to represent masonry materials that will be widely available, economically acceptable and practically implementable in South Africa in the housing market. The mix designs of the different AMUs are also obtained from previous research. However, trial mixes are first conducted on these mix designs to ensure that masonry units with similar fresh and hardened attributes, to those used in the previous research, are created. This is done to ensure that the different soil batches used to create the AMUs are accounted for. When trial mix attributes differ from previous research the mix is adjusted until similar attributes are obtained.

To accomplish the first objective stated in Section 1.4, conventional masonry units (CMUs) are created and used as a benchmark material for the AMUs. The CMUs are used to test the validity of the different test setups. The CON unit was used as the CMU for this study. Results obtained from testing the CON units are compared with widely available literature to determine if the tests are functioning properly. Conventional standards are first considered to find test methods for determining the mechanical properties of the AMUs that are sought after. If the

conventional tests are seen as functional but the results seem erroneous, literature is considered and other tests are developed which give more accurate results. If conventional tests are found to be dysfunctional, literature is also considered to develop new test setups.

A number of tests are conducted on the CON units and three types of AMUs to reach the second objective of this study. These tests can be grouped as follows:

- Companion tests
- Joint interface tensile test
- Joint interface shear test

Different mechanical properties are investigated for each test. Companion tests consist of compressive strength and modulus of elasticity tests on individual masonry units and mortar used to construct the masonry being tested. The joint interface tensile test considers the tensile strength and tensile fracture energy of the interface. The initial shear strength, shear fracture energy, friction angle, cohesion and dilatancy of the interface are investigated as joint interface shear tests. Tests from both the South African National Standard (SANS) and European Norm (EN) are mainly considered. If both these standards fail to provide an appropriate test setup the American standard, American Section of the International Association for Testing Materials (ASTM), are considered. The European Norm (EN) is, however, mostly used in this study due to South Africa likely adopting these standards in the near future. Most of the tests are displacement regulated from crack formations. The cracks are localised by specimen geometry and load configuration. Test methods investigated in this study to determine the mentioned parameters include the compressive strength test, secant modulus of elasticity test, bond wrench test, wedge splitting test, direct tensile test, cross couplet test and triplet test.

After approving the functionality of the tests the mechanical properties are determined from the test results. These results can then contribute towards future research for informing a FEM used to analyse different structures built with AMUs.

1.6 Thesis Structure

The structure for this research thesis is as follows. Chapter 2 examines the current state of LIH in South Africa and the environmental concerns associated with the use of CON units. Thereafter, the different available test methods for determining the tensile and shear characterisation of the joint interface of alternative masonry is investigated.

Chapter 3 discusses different test methods available in standards and/or literature for the tensile and shear characterisations of the joint interface. The test methods chosen for this study and the reason/s for selecting them are further explained.

Chapter 4 discusses the materials used for production of the CON units and three types of AMUs. The materials used for the masonry unit production consist of different aggregates and binders, and their respective properties are discussed. The mix design, mixing procedure and curing of the each type masonry unit are also explained. Lastly, the mix designs of the two different mortars are discussed.

Chapter 5 investigates the test specifications of the test methods chosen in Chapter 2 for this study. If an international standard is available for the chosen test method, the test specification of that standard is thoroughly discussed. In the case where no standard is available, literature is

considered to predict how the test would be conducted. The tests are aimed at determining the mechanical characterisation of each type of masonry unit, mortar and joint interface. Chapter 5 explains the testing methodology for this study. Tests investigated in Chapter 5 are applied to the masonry units produced in Chapter 4. The setup and execution of each test is documented, as well as any adjustments or deviations made.

Chapter 6 documents the results obtained from the tests discussed in Chapter 5. Results from the three types of alternative materials are compared to the benchmark material. The results are also compared to available literature to determine if the results fall within an acceptable range of results to ultimately conclude if standard and benchmark tests can be applied successfully to AMUs. Emphasis is put on factors influencing the bond strength of the joint interface, the second objective of this study.

Chapter 7 concludes this research study. This chapter aims to summarise the discoveries and observations made in this study. Recommendations are made for forthcoming work based on these findings.

Chapter 2

Background

2.1 Environmental Concerns of Conventional Masonry Units (CMUs)

It is widely accepted that global warming is one of the biggest environmental concerns of our time. Global warming is caused by the emissions of greenhouse gasses (GHG) due to human activities which can have threatening consequences if not mitigated and controlled (Benhelal *et al.*, 2013). The five primary GHGs consists of water vapour, carbon dioxide (CO₂), ozone, methane and nitrous oxide (Annenberg Foundation, 2017). CO₂ is known to be the most significant GHG, it is not only the most abundant GHG but also makes the biggest contribution towards global warming (Benhelal *et al.*, 2013).

The cement manufacturing industry is considered to be one of the largest CO₂ releasing industries in the world. It is stated that 900 kg CO₂ is emitted for every tonne cement produced (Hasanbeigi *et al.*, 2010). Schneider *et al.* (2011) stated that globally 2.8 billion tonnes of cement are produced annually and this figure is expected to rise to near 4 billion tonnes per year. Major growth is foreseen for countries, like China and India, in Southern Asia and Northern Africa (Schneider *et al.*, 2011). It is estimated that China will need 40 billion square meters of combined residential and commercial floor space over the next 20 years to accommodate for the rapid population and industry growth (Dobbs, 2010).

Through research, Huntzinger and Eatmon (2009) found that approximately 5 % of global CO₂ emission originates from the manufacturing process of cement. The chemical reaction that is responsible for half of the CO₂ emitted is the calcination process which removes CO₂ from CaCO₃ to form CaO and the remaining carbon stems from energy usage during the production process (Huntzinger and Eatmon, 2009). However, this research was conducted in the year 2009 and 2011 and with the exponential growth in world population a rapid increase is expected in both the manufacturing and production of cement and concrete respectively. Research estimates that the global production of cement reached near 4.1 billion tonnes in 2018 (Wang, 2019). Pacheco-Torgal and Jalali (2012) approximate that in the context of environmental pollution the global construction industry is responsible for 30 % of the earth's carbon dioxide emissions, causing this industry to be clearly unsustainable.

Concrete (CON) units and fired clay bricks are two of the most widely used building materials to construct low income housing (LIH) in South Africa (Laing, 2011). This is due to a few reasons, concrete (CON) units and fired clay bricks are the most socially acceptable and the skills required to build with them are usually locally available (Boshoff *et al.*, 2013). However, even though CON units and fired clay bricks are the most popular building materials, they still have a few disadvantages. Two specific disadvantages of CON units are their negative impact

on the environment and usage of non-renewable natural resources in their production process. A disadvantage of fired clay bricks is their high embodied energy. After the clay mixture has been removed from the brick moulds these bricks are dried at between 900 °C and 1000 °C to reach the final product (Fourie, 2017). Therefore, due to the high energy usage of fired clay bricks, CON units are predominantly used in South Africa. Reddy and Jagadish (2003) states that hollow CON block masonry requires between 38 and 45% of fired brick masonry energy.

This phenomenon is not only the case in South Africa but all over the globe as literature has shown that concrete is the most widely used construction material in the world (Shafiqh *et al.*, 2014). Literature also states that cement (the dominant binder in concrete masonry (Jablonski, 1996)) will remain the key material to satisfy the universal growing need for housing and infrastructure (Schneider *et al.*, 2011).

Lippiatt and Ahmad (2004) found that on average more or less 1 tonne of concrete is produced each year for each human being in the world and in 2004 this amounted to some 6 billions tonnes of concrete produced per year. Meyer (2009) stated that approximately 10 billion tonnes of concrete were produced annually with the demand expected to grow to about 18 billion tonnes produced annually by 2050. Therefore, concrete is one of the most significant produced building material worldwide (Huntzinger and Eatmon, 2009; Lippiatt and Ahmad, 2004). However, due to the universal growing awareness of being more environmentally friendly in all types of industry, especially the construction industry, this could cause that the disadvantages of concrete masonry production to outweigh their advantages in the near future.

A way to mitigate the negative environmental impact of concrete as building material is to consider alternative materials and methods to create building materials that reduce the use of cement and non-renewable natural resources. These alternative materials and methods, however, need to comply with certain requirements like being structurally viable, environmentally friendly and socially and economically acceptable. One way to do this is to consider alternative masonry units (AMUs).

2.2 Low Income Housing (LIH) and CMUs in South Africa

Currently one of the biggest challenges that the South African government is faced with is the housing backlog (i.e. demand outstripping supply) of approximately 2.3 million units, for households living in informal settlements. The reason for this many households living in informal settlements is largely due to the growth in household numbers and the relocation of population to urban areas, this putting additional pressures on limited housing supply (Centre for Affordable Housing Finance in Africa, 2019).

The largest concentrations of informal settlements are located near the metropolitan areas, especially in Gauteng and Western Cape, where large migrations are experienced from poorer provinces. Informal settlements grew from 300 settlements in 1994 to 2700 in 2011. Section 26 of the Constitution of South Africa states that everyone has a right to adequate housing as it is part of their right for an adequate standard of living (South African Human Rights Commission, 1997).

The Deputy Minister of Human Settlements Kota-Fredericks (2013) stated that the government since 1994, housed over 11 million people through the government's housing programme and built over 3 million LIH units since. However, the General Household Survey 2018 showed that, from the population of 57.77 million people in South Africa, 13.1% still lives in informal dwellings. A further 81.1% of South African households resides in formal dwellings and 5% in

traditional dwellings (Centre for Affordable Housing Finance in Africa, 2019). Kota-Fredericks (2013) also said that even though there is an increase in demand for LIH, the delivery thereof has decreased, due to building cost, lack of suitable well located land and rising land costs. The delivery of government-subsidised housing units, by the Social Housing Regulatory Authority (SHRA), dropped to only 2284 units in 2018/2019 from 3519 in 2017/2018 (Centre for Affordable Housing Finance in Africa, 2019).

Therefore, the South African government is not only restricted due to financial restraints, but also due to environmental issues regarding the current construction methods and conventional construction materials like CON units and fired clay bricks. As stated in Section 2.1 the use of CON units is not sustainable and therefore, alternative building materials need to be considered. A solution to this problem is considering adequate AMUs which can replace CON units and fired clay bricks while keeping the specific advantages of conventional building materials, thereby reducing the use of CON units and fired clay bricks for the construction of LIH in South Africa. However, for further development and acceptance of AMUs and getting AMUs into the housing market the characterisation and evaluation of their mechanical properties is necessary. Therefore, research on different AMUs is very important to widen the available knowledge of these materials as a possible building material in the future.

In 2016 the South African Bureau of Standards (SABS) in conjunction with the South African Institution of Civil Engineering (SAICE) and other industry bodies for the application of the National Building Regulations (NRB) revised the existing standard SANS 10400-A (2016) and introduced a new category 1 building with the goal of making buildings more affordable to construct for poorer communities. These buildings have the same safety and structural performance standards but different resistance standards against water penetrations, deflections, local damage etc. than other non-category 1 buildings. The main differences between category 1 buildings and non-category 1 buildings are shown Table C.1 in SANS 10400-A (2016).

At the moment two type of blocks (CON units) are mostly used for the construction of LIH in South Africa namely, the maxi block and the hollow concrete block (Laing, 2011). Figure 2.1 displays these two block.



(a) The "maxi-block"



(b) The hollow concrete block

Figure 2.1: CON units for LIH in South Africa, with a) the maxi-concrete block on the left and b) the hollow concrete block on the right

The gross compression strength of these blocks for single-storey buildings can be found in SANS 0400 (1990). Hollow and solid masonry units are limited in gross compression strength to not less than 3.5 MPa and 7 MPa, respectively, for single-storey houses. Figure 2.2 displays two standard LIH's, one built with fired clay bricks in the Free State province and another built with hollow concrete blocks in the Western Cape province, of South Africa.

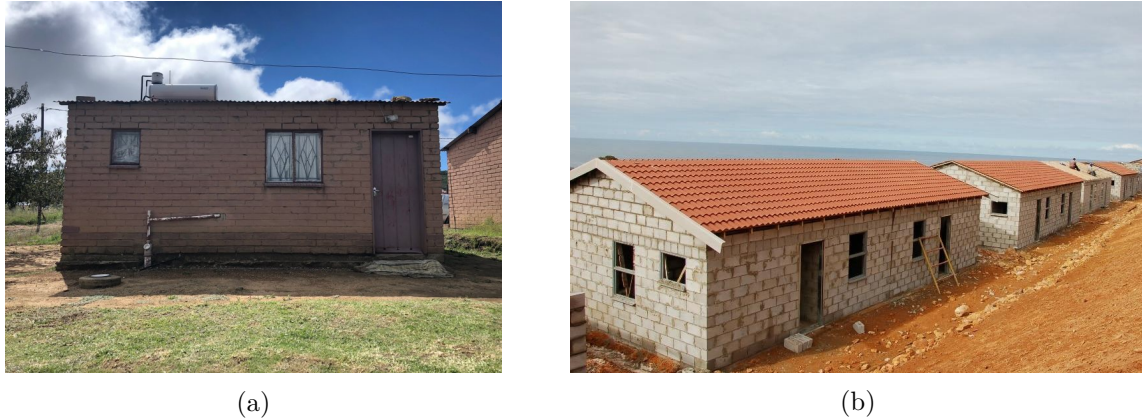


Figure 2.2: Standard low income house built with (a) fired clay bricks in Phuthaditjhaba and with (b) hollow concrete blocks near Kleimond (Leading Architecture, 2011), South Africa

Recently an existing part of SANS 0400 (1990) was revised, SANS 10400-K (2015) with regards to wall requirements. The revised standard, SANS 10400-K (2015) states that for single-storey houses an average compressive strength of not less than 3 MPa and 4 MPa is required for hollow and solid masonry units respectively. SANS 1215 (2008) gives requirements for both hollow and solid CON units. Appearance, shape with dimensions, surface texture and strength requirements are all included. Table 2.1 (Table 2 in SANS 1215 (2008)) displays the compressive strength requirements for CON units.

Table 2.1: Compressive strength requirements for CON units (SANS 1215, 2008)

Nominal compressive strength [MPa]	Minimum compressive strength [MPa]	
	Average (for 5* units)	Individual units
3.5	4	3
7	8	5.5
10.5	11.5	8.5
14.5	15.5	11
21	23.5	17

*In case of units having an overall length of 290 mm or less, an average of 12 units is taken

2.3 Alternative Masonry Units (AMUs)

The universal growing awareness of becoming more environmentally friendly or "green" raises the need for companies and businesses all over the world to reduce their carbon footprint. This, with the introduction of carbon tax in certain countries, forces industries to become more sustainable in their conduct. Carbon tax came into affect on 1 June 2019 in South Africa (Government Gazette No.42483, 2019).

Even though conventional masonry (CON units and fired clay bricks) is seen as the most popular building material for residential construction, in South Africa, it is not considered environmentally friendly. Therefore, the need to consider AMUs to replace conventional masonry units

(CMUs) is motivated, especially to keep the advantages of CMUs and negate their disadvantages. This section briefly discusses AMUs found in literature and explains the process behind choosing the three types of AMUs investigated in this study.

A common problem most developing countries are faced with is a severe housing shortage for the growing millions without proper shelter. A developing country where this phenomenon is widely present is India. Therefore, considerable research has been conducted in India to find a viable solution to this problem. Harrison and Sinha (1995) found that India's population grew with more than 150 million in only 10 years between 1981 and 1991. Bloom (2011) estimated that the population of India grew from 448 million in 1960 to 1.2 billion in 2011 and would reach approximately 1.6 billion in 2050. The vast population growth in India causes severe constraints on resources of all kinds and the resources utilised in the construction industry are of no exception (Harrison and Sinha, 1995).

As a result of these resource constraints on the economy and building materials the construction industry would have to adopt different measures to provide shelter and low-rise buildings for housing the homeless (Harrison and Sinha, 1995). These measures include thinking of alternative building materials (ABMs) and new building technologies that either replace or complement conventional building materials and are also more environmentally friendly. Harrison and Sinha (1995) conclude, for ABMs to be appropriate for use in developing countries, they must be locally available in abundance, have a low energy input in terms of production, be environmentally friendly and labour intensive. For developing countries with high unemployment rates labour intensive construction methods are of high demand to complement those who need an income to provide for their families.

One of the procedures for determining the impact of a building material on an economic and environmental level is to measure its embodied energy. The embodied energy of a building material refers to the amount of energy spent on that material in its manufacturing process. Buchanan and Honey (1994) define embodied energy as the energy requirements for the production processes of a building material in its final state which leads to CO₂ emissions and adverse implications on the environment. Conservation of energy comes to be important in the setting of limiting the carbon footprint and cost of materials (Reddy and Jagadish, 2003). In a highly populated country like India the phenomenon of limiting the greenhouse gas CO₂ emissions is important due to the large volumes of building materials that are produced annually. Research estimates that the construction sector in India is responsible for the largest input of energy resulting in 22 % of India's total CO₂ emissions into the atmosphere (Debnath *et al.*, 1995).

Reddy and Jagadish (2003) compared the embodied energy of common building materials to alternative building materials in the quest for discovering which alternative material performs the best. Reddy and Jagadish (2003) focused on masonry materials and compared the embodied energy of the stone block, burnt clay brick (commonly used in South Africa), soil-cement block, hollow concrete block and steam cured block. From all the materials considered, the soil-cement block was found to be the most energy efficient among the alternative materials, especially for application in walling. Reddy and Jagadish (2003) estimated that with an alternative building materials like soil-cement block masonry the embodied energy of a building (measured in MJ/m³) can be reduced by 66% compared to conventional masonry. It should be noted that the energy in transportation is not included for the previous statement. Figure 2.3 displays a two storey load bearing soil-cement block masonry building.



Figure 2.3: Two storey load bearing soil-cement block masonry building in India (Reddy and Jagadish, 2003)

Buchanan and Honey (1994) examined the embodied energy and CO₂ emissions associated with the construction industry in New Zealand. It was estimated that the greater use of wood and a decrease in the use of steel, concrete and aluminium would lead to a significant decrease in carbon emissions. Wood, however, is not as widely available in South Africa and especially not for mass housing and is, therefore, not considered as a viable alternative building material in this study. This study rather focuses on AMUs and literature thereof that would be a viable replacement for CON units, considering that CON units are the most popular building material for the construction of LIH in South Africa.

Harrison and Sinha (1995) studied alternative building materials and technologies that are implemented in Bangalore, India, through considering different case studies. The research focused on comparing AMUs, of which soil-cement blocks were one, to burnt clay bricks and concluded that soil-cement blocks were the most economical in terms of material costs. The study of Shakir and Mohammed (2013) investigated more efficient, durable and sustainable alternatives which would reach far beyond the limitations of the conventional brick in the construction industry. Shakir and Mohammed studied the hazardous impacts of the conventional brick manufacturing process and also supplied a broad list of research on sustainable masonry units which could treat the current problems. The hazardous impacts of the conventional brick manufacturing process are not discussed here as it is already touched on in Section 2.1. The focus of discussing some of the research provided by Shakir and Mohammed is not to find the best suitable AMU for this study, as this is not the aim, but rather to indicate and explain the process behind choosing the three types of AMUs chosen for this study in previous research, of which this study is an extension.

One of the main focus points of the study of Shakir and Mohammed is to attempt to fill the gap of past studies and suggest sustainable solutions for brick manufacturing in the future. Their research can be broadly divided into two categories. Firstly, to enhance the clay brick quality and properties by mixing clay with post-consumer wastes and industrial by-products. Secondly, to create bricks out of wholly waste materials without utilising any natural resources. The first category of research looked at recycled wastes like foundry sand, granite sawing waste, harbour sediment, sewage sludge and other wastes. This category, however, provides a more economical option to brick production due to the utilisation of industrial wastes but falls short in the context of natural resource conservation and limiting greenhouse gas emissions. The second category provides a more environmentally friendly and sustainable solution, avoiding resource depletion and the use of valuable top soils and clays, yet this still does not solve the issue of decreasing the embodied energy of masonry units and the emission of GHG in their manufacturing process.

In research conducted by Fourie (2017), of which this study is an extension, there were three main reasons why specific AMUs were chosen for this research. They were:

- Selecting AMUs with different material properties to represent a wide variety of AMUs.
- Finding AMUs that are environmentally friendly through utilising waste materials, avoiding natural resource depletion and reducing the carbon footprint of the masonry unit.
- Choosing cost-effective masonry units with lower embodied energy.

The first objective of this study is to determine if standards and benchmark tests used on conventional masonry can be successfully applied to different AMUs. Therefore, three AMUs were chosen with different material properties to represent a broad group of AMUs and test the validity of these tests on such a variety of materials. The second reason for choosing these specific AMUs is choosing masonry units that utilise industrial waste products, conserve non-renewable natural resources and valuable biodiversity's and reduce the emission of GHG in their manufacturing process. Lastly, choosing AMUs suitable for the implementation of LIH in South Africa. Therefore, they have to be more, or at least as, economical as CON units and the raw materials needed for their production must be locally and widely available with the skills in labour and equipment needed for the production process.

The three different types of AMUs chosen for this study are cement stabilised earth (CSE) units, geopolymer (GEO) units and adobe (ADB) units. These masonry units comply mostly with all of the requirements above and can be seen as a viable replacement for CON units in LIH construction in South Africa (Fourie, 2017). Sections 2.3.1 to 2.3.3 briefly discuss these three AMUs.

2.3.1 Adobe (ADB) Unit

Earth has been used as a construction material for thousands of years and is still a popular building material in developing countries (Pacheco-Torgal and Jalali, 2012). Literature estimates that about 30 % of the world's population lives in earthen buildings and about 50 % of the population in third world or developing countries live in buildings constructed from earth (Fratini *et al.*, 2011). Their study indicated that a wide range of earthen buildings can be found in the Middle East and Europe. Through studying the past of earthen construction Pacheco-Torgal and Jalali found that countless earth buildings were built 1000 years ago and made in to the 21st century. Even popular ancient structures like the great wall of China consist of sections built with Earth (Pacheco-Torgal and Jalali, 2012). Figure 2.4 displays the estimated distribution of earth buildings across the globe.



Figure 2.4: Distribution of earth buildings across the globe (Fratini *et al.*, 2011).

This material has recently again gained popularity due to the universal growing interest of low embodied energy and sustainable building materials. Earthen materials present several advantages as a building material, namely local availability, low costs, recyclable, good acoustic and thermal properties and reduced embodied energy in manufacturing processes (De Almeida, 2012). Earthen construction materials, however, have a number of disadvantages. These disadvantages are linked to earth-based materials, namely shrinkage occurring during the drying phase leading to surface cracks, poor tensile and flexural strength attributes, low dimensional stability, poor ductility and a low resistance against wind and water erosion (Deboucha and Hashim, 2011). Stabilisers are usually added to the earth to prevent these issues from occurring (Aymerich *et al.*, 2011). Figure 2.5 displays an earth building in Kwazulu-Natal, South Africa that has been eroded over the years by rain.



Figure 2.5: Eroded earth building near Kokstad in Kwazulu-Natal province, South Africa.

There are four basic earth construction techniques discussed in literature (Pacheco-Torgal and Jalali, 2012). They are:

- ADB and compressed earth block;
- Cob;
- Pressed earth;
- Wattle and daub;

The wattle and daub technique includes pressing earth onto a woven lattice of wooden strips (Pacheco-Torgal and Jalali, 2012). Cob consists of earth mixed with straws and water to form a layer by layer masonry wall (Quagliarini *et al.*, 2010). The technique of pressed earth involves compacting moist earth into wooden form-work. This earth can be stabilised or not (Pacheco-Torgal and Jalali, 2012). As stated previously, for this study the ADB unit and CSE unit are considered. The ADB unit, also known as the "mud brick" is a simplified earth masonry unit (De Almeida, 2012). The word adobe originates from the Arab "attob" meaning sun-dried brick (Rogers and Smalley, 1995).

Soil Characteristics

Soil utilised for earth construction consists usually of the mineral layer (second layer) and not the top soil (first layer) to avoid organic matter occurring within the soil. Organic matter can rot after implementation leaving cavities in the soil structure which reduces the soil strength (Pacheco-Torgal and Jalali, 2012). Soils consist of varying proportions of four types of particle sizes, namely gravel, sand, silt and clay (Rigassi, 1995). The European testing standard standardises soil with the following gradings (EN 5930, 2015):

Gravel	60.00 mm to 2.00 mm
Sands	2.00 mm to 0.06 mm
Silt	0.06 mm to 0.002 mm
Clay	less than 0.002 mm

Rigassi (1995) states that the first two types of soil can be seen as stable and the latter two as unstable. A soil type is seen as stable when it comes into contact with moisture without changing volume. Therefore, a soil is labelled as unstable when moisture affects its volume. Gravel has the biggest particle size and undergoes no change in mechanical properties and volume when in contact with water. Sand, also seen as stable, obtains a high degree of surface tension but lacks cohesion in its raw material form. Gravel and sand give the soil its strength. The clay content in soil, however, provides a solution for the lack of cohesion and is the essential element of formation in the ADB unit (Rigassi, 1995). The shrinking characteristic of clay, when dried out, forms a compact and resistant mass giving stability to the end product (Velde, 2008). The specific role of silt in a soil mixture is not completely known and more research is still required in this area (Rigassi, 1995).

The ADB unit consists of a mixture of gravel, sand, silt and clay. To obtain the best performing ADB unit the balance between different soil type gradings are important. Rigassi (1995) states that it is not always necessary to have extensive knowledge of the physical properties of the soil, but rather to understand three fundamental properties. These three properties are:

- Soil grading;
- Plasticity of the soil;
- Compressibility of the soil;

The latter is most favourable at the optimum water content. This implies the amount of water needed to ensure maximum density when compressed, leading to maximum strength (Rigassi, 1995). A fair amount of literature discusses some of the mechanical characteristics of the ADB unit. As stated, ADB is seen as a weak masonry material, especially when coming in contact with water. Minke (2009) states that generally ADB units vary between 0.5 and 5 MPa in compressive strength depending on the grading, preparation technique and method of curing. Extensive research on ADB characterisation was conducted in the Aveiro region, Portugal, and compressive strengths between 0.3 to 2.4 MPa were found (Varum *et al.*, 2007). Research at Stellenbosch University found ADB units with compressive strengths of between 0.75 and 0.85 MPa (Fourie, 2017).

Adobe Unit Creation

ADB units are produced through filling wooden moulds with moist earth and compressing it into the mould either by hand or mechanically. To prevent the soil from sticking to the inside of the moulds the mould can be dipped in water just before adding the ADB material. The unit is usually de-moulded just after being compacted into the mould. After the units are de-moulded they are placed in the sun to dry (Pacheco-Torgal and Jalali, 2012). However, with a large clay content shrinking cracks can occur on the unit's surface. To prevent shrinkage cracks literature suggests drying the units under a layer of straw or under a roof, avoiding direct sunlight. In addition, adding fibres (straw or vegetable fibres) to prevent surface cracking is also suggested (Neumann *et al.*, 1984). Figure 2.6 displays ADB units being sun dried to construct a child care centre in El Salvador. Fourie (2017) suggests that the unit should be dried for more or less three days and then left to rest on their side until construction.



Figure 2.6: Sun drying ADB units (Dowling, 2004).

Few international standards exist for earth or ADB construction. New Zealand, however, has put in effort over the past two decades to develop standards and today has one of the most advanced legal regulations on earth construction, which is structured in three different parts (Pacheco-Torgal and Jalali, 2012; EBANZ, 2015):

- NZS 4297:1998 - Engineering design and earth buildings (establish performance criteria for mechanical properties)
- NZS 4298:1998 - Materials and workmanship for earth buildings (describe requirements for materials and workmanship)
- NZS 4299:1998 - Earth buildings not requiring specific design (applicable for buildings with less than 600 m² area per floor)

2.3.2 Cement Stabilised Earth (CSE) Unit

The CSE unit is a modern successor of the moulded earth block, better known as the ADB unit (Deboucha and Hashim, 2011). As stated in Section 2.3.1 the interest in using earth and specifically ADB as a building material has recently increased due to the global movement towards sustainability and being environmentally friendly. The ADB unit, however, has a few shortcomings as discussed in Section 2.3.1. Therefore, the idea of compacting earth was introduced. Compacting earth into blocks to improve its performance and quality as building material is, however, far from new and this technique dates back to the 18th century where Francois Cointeraux, promoter of pressed earth as a building technique, designed the "crecise" a

device built from an idea of a wine-press used to compress earth (Rigassi, 1995). Nonetheless, it was not until the 20th century when the first mechanical presses, using heavy lids forced down into moulds, were produced. The turning point and start of the evolution of compressed earth began in 1952 when Raul Ramirez, an engineer, designed the CINVA-RAM press. This design was then used throughout the world (Rigassi, 1995).

Sitton *et al.* (2018) states that a possible reason for the constraint on the proliferation of CSE unit production is due to a lack of international standardisation and agreement. A reason for this can be because of the large differences in soil types across the world, as well as different construction techniques.

Soil Stabilisation

Soil has specific properties such as strength, swelling, shrinkage and plasticity and when these properties are altered to obtain a soil more suitable for building applications it is termed "soil stabilisation" (Reddy, 2012). Rigassi (1995) states that there are three stabilisation processes namely, mechanical, physical and chemical stabilisation.

Mechanical stabilisation is when the properties of the soil are changed by means of compression. This changes the structure of the soil and modifies its density, strength and permeability (Rigassi, 1995).

Physical stabilisation is referred to as changing the properties of the soil by changing the texture or grading of the soil by adding a certain amount of another soil. This is usually done to control the amounts of sand and clay in the soil which contribute the most to the final soil properties (Rigassi, 1995).

Chemical stabilisation, usually the most expensive form of stabilisation, is achieved by altering the properties of a soil through the addition of chemicals or specific type of materials to the soil. This form of stabilisation normally causes the largest amount of change to the soil properties and contributes greatly to the quality of the final product (Rigassi, 1995). Portland cement and lime are usually used as chemical stabilisers.

All three forms of stabilisation are used for CSE unit production. When cement is used as chemical stabiliser it adds cohesion to the mix and increases the weather resistance of the final product (Sitton *et al.*, 2018). In addition, the use of cement as chemical stabiliser also increases strength and reduces shrinkage, both improving properties that lack in the ADB unit. Cement highly affects soils with a large amount of sand and gravel. Soils with high clay content are to be avoided and it is preferred that the clay content in the soil is limited (<20%) (Rigassi, 1995). Soils with a higher clay content require more cement and more cement defeats the purpose of finding environmentally friendly AMUs. The presence of organic matter is undesirable when using cement as stabiliser because it inhibits the cementing action and could give unwanted structural properties in the end product. The presence of iron oxide in the soil is however desired. This allows efficient stabilisation due to the pozzolanic reaction of the iron oxides with the soil in the presence of moisture (Meukam *et al.*, 2004).

Rigassi (1995) stated that at least 5 to 6% cement by mass is needed in a mix to acquire the desired outcome and low proportions of cement under 3% can cause certain soils to perform inferior to the same soil without cement. Meukam *et al.* (2004) suggests that a well graded soil only requires 4% cement by mass for optimum performance. Sitton *et al.* (2018) found that the optimum cement content needed to achieve the maximum compressive strength of a CSE unit is 10.91%. CON units have a cement content of about 16% by mass if not lower (Jablonski, 1996).

The focus of this study is not to design a mix for CSE units with high a compressive strength, but rather to obtain a CSE unit that is structurally viable and environmentally friendly. The latter could be achieved by reducing the cement content in the unit.

The CSE unit has several advantages due to the alteration of its soil properties. Some advantages that negate the disadvantages of the ADB unit are:

- Soil, the primarily used material in CSE unit production, is a readily abundant resource mostly everywhere in the world (Sitton *et al.*, 2018). Soil utilised for CSE unit production is less dependant on clay and is, therefore, more versatile.
- CSE unit is seen as a more sustainable alternative to traditional masonry units when compared to the ADB unit and pressed earth, due to the binder increasing cohesion and water resistance (Sitton *et al.*, 2018).
- The use of mechanical compaction results in a unit with a higher density and increased consistent quality. The increased quality improves the social acceptability of the unit and the higher density increases the unit's resistance to water and wind erosion (Rigassi, 1995).
- CSE units can be consistently produced in a variety of shapes and sizes depending on the need of the project. This, with the increased quality, regular shape and sharp edges, is appreciated by builders (Rigassi, 1995).
- CSE unit can be produced locally, therefore, reducing product and transportation costs. CSE unit production also promotes local job creation which has a positive influence on the countries economical sector, especially in South Africa with high current unemployed rates (Centre for Affordable Housing Finance in Africa, 2019).
- Lessens the high demand for non-renewable resources (Walker and Stace, 1996).

CSE unit Creation

The production process of CSE units consists of five steps: soil selection, soil preparation, mixing, compaction and curing. Parameters that mainly influence the characteristics of these units are the percentage of clay, stabiliser content and final density (Pacheco-Torgal and Jalali, 2012).

The type and amount of clay normally determines the amount of stabiliser added to the mix. Numerous types of clay exist and each type has different properties. The most important property in terms of stabilised earth is the expansiveness of the clay. The three main types of clay that exist are montmorillonite, kaolinite and illite where the first is termed as being expansive and the latter two being less-expansive. Expansiveness of clay is measured in two parameters and these are, the amount the clay swells when coming in contact with water and the amount it shrinks when drying out. Less expansive soils are recommended for CSE unit production. The maximum strength of the final unit is increased if the clay content is optimised (Rigassi, 1995). Reddy and Gupta (2006) estimate that the optimum clay content, for CSE unit production, is between 10 and 15%.

Due to soil being the primary constituent of the CSE unit the soil selection step is of great importance. The soil gradation can provide a good indication if the soil is suited for use or not. The soil gradation can be altered by physical stabilisation.

Rigassi (1995), suggests that the following grading is suited for CSE unit production:

Gravel	0 to 40 %
Sands	25 to 80 %
Silt	10 to 25 %
Clay	8 to 30 %

Rigassi (1995) additionally recommends that gravel particles should not exceed 6 mm as this results in a poor surface finish of the final product. It is important to correctly process the soil before being mixed. The soil processing step consists of preparing the soil for mixing. As a result of moisture and clay in the excavated soil, lumps form which could, if not treated correctly, prevent the soil from reaching a state of full homogeneity. The excavated soil could also contain large gravel particles that could easily exceed 6 mm. It is therefore necessary that the soil is treated through means of sieving, crushing and drying to obtain the correct grading.

The mixing step consists of two phases. Firstly, mixing all the dry materials in a mixer for a few minutes, depending on the amount of stabiliser used, and thereafter further mixing for a few minutes after the water is added. If less stabiliser is used the dry materials should be mixed more thoroughly to ensure an even distribution of stabiliser. Another important factor is the retention time, which is known as the time between finishing the mixing process and compacting the moist soil into units. The moist soil, when compressed, forms a unit with higher density. The confined compaction is responsible for the increase in density. The compaction energy required, to obtain the most favourable unit, is dependent on the moisture content, soil grading and required density (Reddy, 2012). The compaction process is displayed in Figure 2.7.

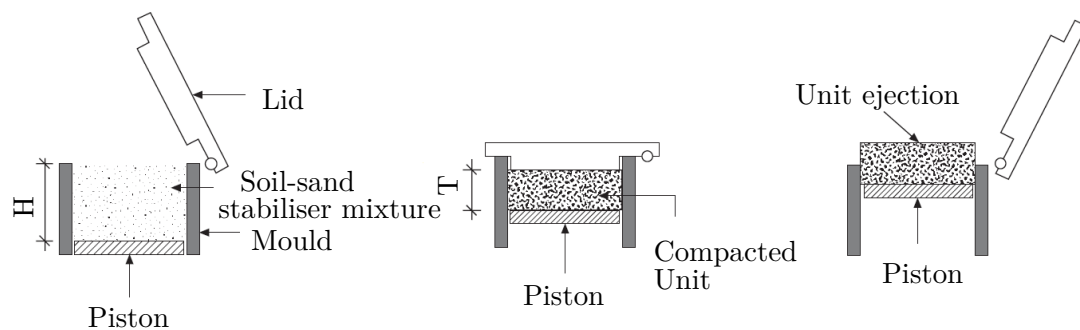


Figure 2.7: CSE units compaction process: a) Filling mould with mix b) Compacting soil c) Removing final unit (Reddy, 2012)

The last and final step in CSE unit production, curing, is important and, if not done correctly, can greatly damage the final product. The units must be kept humid for at least 7 days for proper hydration of the cement particles. Direct sunlight and wind must be avoided at all cost during the whole curing period as this can cause the unit to dry out too quickly and surface cracks can form. Units can be cured at elevated temperatures which would give them higher strengths, but this is not necessary and would defeat the purpose of producing low embodied energy masonry (Rigassi, 1995). The effect of direct sunlight and wind on a CSE unit while being cured is displayed in Figure 2.8.

It can be seen from Figure 2.8 that a lower cement content is influenced much more by varying curing condition than a higher cement content. Especially with direct exposure to the elements. This highlights the importance of curing conditions of CSE units.

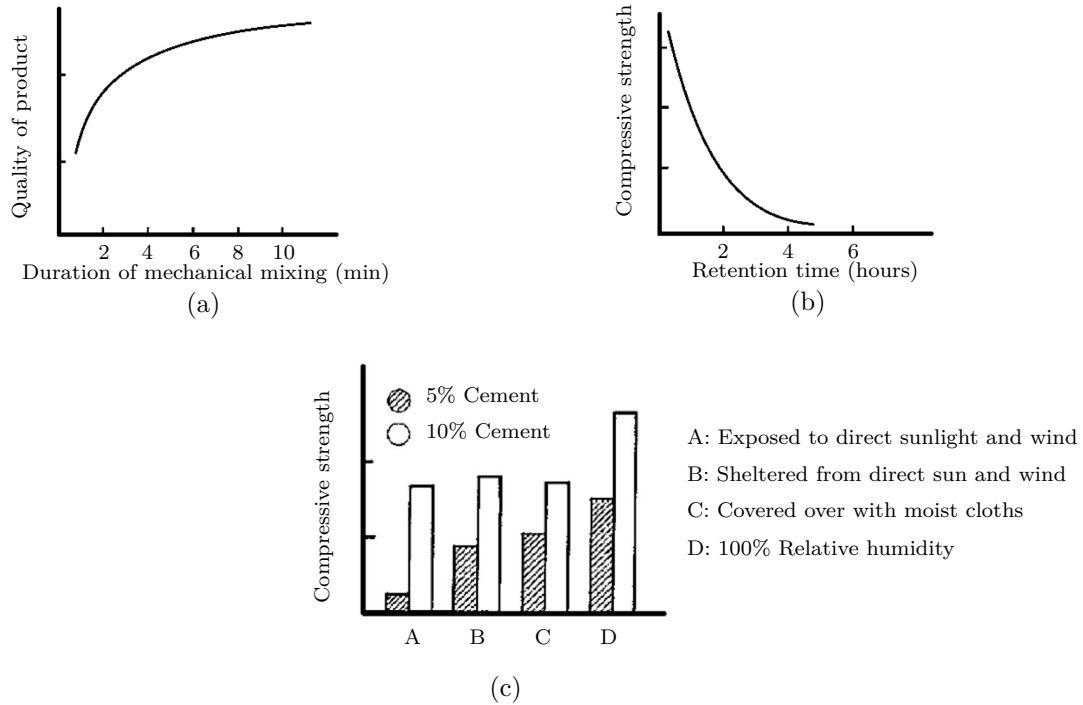


Figure 2.8: The effect of a) mixing time, b) retention time and c) curing conditions on a CSEB unit (based on data from Rigassi (1995))

2.3.3 Geopolymer (GEO) Unit

The first mention of alkali-activated binders (AABs) as an alternative to conventional concrete found in literature dates back to 1908 where Kuhl (1908) patented it. Further research was done by Purdon (1940) in Belgium from the 1930s to 1950s and after that by Glukhovsky in the Ukraine. However, it was only in 1978 where Davidovits (1989) introduces the term GEO. The development on GEOs was originally aimed at finding a fire resistant binder material that could replace Ordinary Portland Cement (OPC) after a series of large fires in France at that time (Davidovits, 1989). The material was first used as coating for cruise ships to increase their fire resistance and to increase thermal properties of wood structures. It was only thereafter introduced to the construction industry when it was observed that the material has high and reliable performance attributes when compared to conventional concretes (Provis and van Deventer, 2009).

Research on AABs increased enormously in the 21st century and this is mainly due to certain properties of this material namely, its low embodied energy, high compressive strength and resistance to fire. This, in conjunction with the universal growth of environmental awareness in the construction industry, made this material all the more popular (Pacheco-Torgal, 2015). Certain countries have been using alkali-activated cement based binders (AACBB) for almost half a century but they did not share this knowledge internationally. Only in 2006 has a book been written in English by Shi *et al.* (2006) that describes the past of AACBB.

There are also other reasons why the application of AACBB has not yet been presented as a viable alternative to conventional cements in the construction industry. One is due to the various terminologies of the material which is a result of different scientific research done in respective countries without being shared in the past. This vast amount of terminologies can cause new researchers to struggle in the field of AABs to get to grips with the material. Terminologies like mineral polymers, ash materials, cemented soils, zeocements and others are all used for AACBB

(Pacheco-Torgal, 2015). Another reason is due to the complexity of understanding how the material works. There is still a lack of understanding the behaviour parameters of AACBB. For instance, the major factor that influences the strength of conventional concrete is the water to binder ratio where the parameters influencing alkali-activated concrete (AAC) are much more complex and depend on a lot of different ratios and factors (Ahmari and Zhang, 2015).

Alkali-Activated Concrete Binders

To understand where the GEO unit comes from, alkali-activated materials and binders must first be understood. AABs consist of a broad group of materials. This makes it almost impossible to list properties that act as characteristics of the material. Provis (2013) suggests that to fully understand the material one has to obtain a detailed molecular understanding of the chemical and physical characteristics of the material. This, however, is not the focus of this study and therefore the chemistry behind the material is only touched on briefly.

GEO is known as a material that falls under alkali-activated materials. This means that GEO is one of the AABs. AABs are formed through the reaction of aluminosilicates with an alkaline activator. Aluminosilicates are usually industrial by-products and examples of these by-products are metakaolin, fly ash (FA) and blast furnace slag. Alkaline activators on the other hand are usually concentrated watery solutions of sodium hydroxide, sulphates, silicates and carbonates (Provis, 2013). Alkaline-activated binders can also be referred to as alkaline cements. Figure 2.9 displays a tree diagram of AABs, from the raw material to the final binder product. According to Garcia-Lodeiro *et al.* (2014), there are three categories of alkaline cements.

- The first consist of a calcium silicate alkaline-activated system. Calcium and silicon rich materials, such as blast furnace slag, are activated under moderate alkaline conditions. A calcium silicate hydrate gel is formed. This category is better suited for ambient curing.
- The second category consists of a low calcium alkali-activated system where aluminium and silicon rich materials, such as metakaolin and FA, are activated under aggressive alkaline conditions. Heat curing is normally required in the absence of slag. This category is known as GEO.
- The third and last category is a mixture between the two and has complex properties. Therefore, this category is avoided in this study.

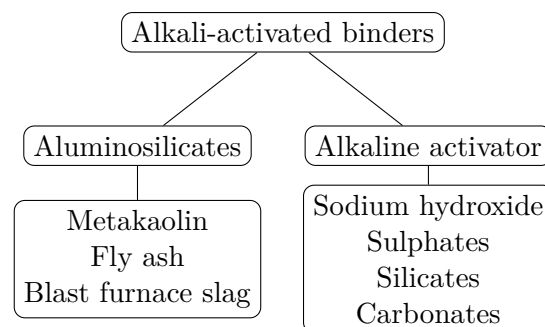


Figure 2.9: Alkali-activated binders, from the raw materials to the final binder product (Provis, 2013).

GEO concrete hardens due to the process called geopolymerisation. This process is described as follows. The binder is broken down by a dissolution process in which silica and aluminium ions are released. The binder consists mostly out of silica and aluminium. Next, the aluminosilicates

are interlocked with oxygen ions through a condensation process which hardens the material. This material usually has to be cured at heated temperatures. When slag is added to the mix, calcium silicate hydrates (CSH) form in conjunction with the aluminosilicate hydrate gel. This improves the compressive strength and allows for ambient temperature curing (Davidovits, 2008; Yip *et al.*, 2008). Research on the mechanical properties of FA/slag based GEOs by Barnard (2014) gives a full understanding of the chemistry behind GEO concrete.

Creation of GEO units

GEO units are one of the AMUs found in literature that has shown some of the most promising results as a viable, and more environment friendly, replacement for CON units. There are, however, some challenges to present this material on the housing market. These include health concerns, problems with the utilisation of the material as a masonry unit and expensiveness of the activators (Schneider *et al.*, 2011). Nonetheless, literature still suggests that the GEO unit can serve as a eco-friendly masonry unit (Ahmari and Zhang, 2015; Cheah *et al.*, 2015). A few advantages of AAC and GEO units are as follows:

- The production of AAC emits about 20% of the CO₂ that is emitted through the production of conventional concrete, making it more environmentally friendly (Sakulich, 2011).
- The production process of AAC consumes approximately 70% less energy compared to conventional concrete (Sakulich, 2011).
- The ability to pre-cast AAC allows for easy unit production.
- AAC has a high resistance against chemical attacks and a good passivation of reinforcement (Schneider *et al.*, 2011).
- AAC shows high early compressive strengths and can easily compete against conventional concrete on this basis (Provis and van Deventer, 2009).
- GEO unit can be produced on the basis of FA, a waste material of the coal burning process (Boshoff *et al.*, 2013).
- GEO unit is seen as more sustainable than CON units due to its natural resource conservation, low embodied energy and use of some local cost-effective materials (Ahmari and Zhang, 2015).
- GEO unit is one of the most fire resistant masonry types available (Davidovits, 1989).

Ahmari and Zhang (2015) state that the general production process of GEO units is as follows:

- Processing materials
- Mixing and forming units
- Curing at ambient temperature for one or more days
- Heat curing
- Storing and transportation

The second last step can be avoided when slag is included in the mix design. From this production process it can be seen that GEO units have a lower embodied energy than CON units due to the absence of cement and high temperature heat curing (Ahmari and Zhang, 2015). For this study curing at ambient temperatures is considered.

After studying different mix designs from literature, Barnard (2014) suggests a methodology for designing a GEO unit mix, based on an initial mix volume of 1 m^3 . The aggregate should consist of 59 to 65% of the volume of the mix while the remaining volume should be filled with binder material, alkaline solution and water. The binder should consist of between 60 and 80% FA and the alkaline solution ratio of sodium silicate (SS) to sodium hydroxide should be between 0.5 and 2.0. To give a better understanding of the complexity of this mix Barnard (2014) stated all the factors and ratios that have a direct influence on the strength of AAC. These factors are stated in Table 2.2 with the desired values to produce a GEO unit with more or less the same strength than that of the standard CON unit used for LIH in South Africa. According to Van Jaarsveld *et al.* (2003) the sodium hydroxide solution (SHS) is the most influential aspect regarding the compressive strength of the final product.

Table 2.2: Factors that influence AAC strength (Barnard, 2014)

Factors influencing AAC strength	Desired
Sodium silicate to sodium hydroxide ratio	0.6 to 2.5
Fine aggregate to total aggregate ratio	0.5
Alkali to binder ratio	0.55
Binder to sand ratio	0.85 - 1.1
Slag content	20%
Aggregate content	60%
SHS (sodium hydroxide and water)	3 - 6M
Percentage alkaline liquid replaced by water	25%

The characteristics of AAC are influenced largely by the type of binder material and the activation conditions (Schneider *et al.*, 2011). A frequently encountered problem with AAC is a low workability. The only reason for water being added to the mix design is to ensure workability of the fresh GEO concrete (Davidovits, 1994; Hardjito *et al.*, 2005). Literature estimates that the workability of fresh GEO concrete can be improved by the following (Hardjito *et al.*, 2005; Lloyd and Rangan, 2010; Yip *et al.*, 2008):

- Increase the water content
- Decrease the mixing time
- Lower the slag content
- Lower the alkaline concentration
- Lower the percentage of aggregate in the mix

Barnard (2014) states that the workability of a mix is increased at the cost of strength loss of the final product.

Health Concerns of AAC

The alkaline solution of alkali-activated materials often contains sodium hydroxide and SS. Alkaline solutions are classified in two categories, corrosive and irritant. The first is termed as user-hostile and the second user-friendly. Corrosive alkaline products must be handled with the

appropriate safety equipment and are harmful when coming in contact with skin or eyes. Corrosive products cannot be mass implemented without the necessary safety procedures (Davidovits, 2013). Sodium hydroxide is classified as highly corrosive and alkaline-activated cement based on FA is also normally of a corrosive nature. Sodium hydroxide is not carcinogenic or genotoxic, but a high intake via the mouth or exposure to large parts of the skin can be fatal. Alkaline solutions with a concentration below 0.5% with water is not harmful where concentrations of above 2% are harmful. A concentration of between 0.5% and 2% can cause serious skin and eye irritations (Evonik Industries, 2011). Sodium silicate and alkaline-activated cement based on slag is classified as an irritant alkaline product (Davidovits, 2013).

2.4 Conclusion

This chapter gave a brief overview of the environmental concerns associated with conventional masonry, the state of LIH in South Africa and the need for alternative masonry materials.

These AMUs were chosen due to the availability of these materials in South Africa and to represent a wide spectrum in terms of strength and stiffness. This study also forms part of wider research previously conducted on these three type of AMUs.

Chapter 3

Literature Review

3.1 Tensile and Shear Characterisation of the Joint Interface

In the last four decades large growth has been achieved in the area of numerical modelling as a tool for structural analysis. This rapid advance of numerical methods has given engineers the capability to model structures much more accurately than in the past. The use of these tools as an analysing technique demands access to a number of material and mechanical properties of the structure (Lourenço, 1998). A problem encountered with masonry structures, in this area, is finding constitutive methods to determine appropriate mechanical properties for these materials. A common method used to avoid this problem has been to apply the constitutive laws of concrete to masonry. This, however, disregards the composite nature of masonry and the fact that masonry is not as homogeneous as concrete and has specific locations of weakness, usually at the joint interface (D'Ayala, 2008).

Generally, well known mechanical properties of masonry are mostly studied and these mechanical properties are usually the compressive strength and modulus of elasticity, which give a good representation of the strength and stiffness of the material (De Almeida, 2012). Concepts like the tensile and shear characterisation are not studied that frequently and especially not of the joint interface. Different literature encountered similar problems with assessing the structural behaviour of historic earth masonry buildings with analytical tools, this is due to the lack of the characterisation of the mechanical properties of the joint interface (Lourenço, 1998; D'Ayala, 2008). Therefore, to successfully apply numerical models to masonry structures, the mechanical properties of the joint interface must be defined.

This study represents an experimental investigation for the tensile and shear characterisation of the joint interface of alternative masonry. This section focuses on defining different concepts in the field of tensile and shear characterisation of masonry. Section 3.1.1 defines fracture energy and explains the use of this mechanical property in this study. Sections 3.1.2 and 3.1.3 define these concepts and present findings from literature regarding each topic.

Literature discusses different parameters and their influence on the characteristics of the joint interface of masonry (Groot, 1993; Grenley, 1969; Reddy and Gupta, 2006; Sugo *et al.*, 2001). Section 3.2 investigates the influence of masonry unit characteristics and mortar parameters on the bond strength of the joint interface. When forces are applied to masonry structures the mortar is used to transfer these forces between the masonry units at the joint interface. In addition, the mortar also determines the cohesion between masonry units (Schneemayer *et al.*, 2014). The mechanical properties of mortar are characterised by the tensile strength, compressive strength, flexure strength and modulus of elasticity (Schubert, 1998).

As stated in Section 1.4, the first objective of this study is to determine if international standards and benchmark tests used on conventional masonry can be successfully applied on different types of alternative masonry to obtain certain mechanical properties and if not, to adjust or develop new tests which yield accurate results. The focus of this section is to examine different concepts regarding the tensile and shear characterisation of the joint interface of masonry and also to investigate different experimental setups and choose test methods for application in this study. Section 3.3 considers three different test methods available in literature and/or in international testing standards to experimentally characterise the tensile properties of the joint interface. Chapter 5 explains how test methods chosen for this study are adjusted or developed for application in this study.

This study investigates the initial shear strength, shear fracture energy, cohesion, friction angle, initial dilatancy angle and the dilatancy softening gradient of the joint interface for each type of alternative masonry unit (AMU).

3.1.1 The Concept of Fracture Energy

Fracture energy represents the inherent resistance of a material against cracking. It can also be termed as the fracture toughness of a material (Zhao *et al.*, 2008). Brühwiler and Wittmann (1990) did extensive research on stable fracture mechanics tests on concrete and concrete-like materials. The most direct way to determine a material's fracture energy would be a deformation controlled uni-axial tensile test. The problem with conducting such a test on brittle or quasi-brittle materials like masonry is the small deformations at rupture and extreme stiffness of these materials (Brühwiler and Wittmann, 1990). The aim is to determine test methods for obtaining stable fracture mechanics on these types of materials as there are not yet standard tests available. A test is seen as stable if no sudden drop of load occurs in the load-time plot. Stable fracture tests would, therefore, display a descending branch in the overall load-deformation diagram after reaching the peak load (Brühwiler and Wittmann, 1990). De Almeida (2012) estimates that the shape of the descending branch depends on the boundary conditions of the testing equipment, and consequently the fracture energy can be influenced by this. Fixed boundary conditions are associated with larger fracture energy values.

Other possible difficulties in standardising fracture mechanic tests, in conjunction with the behaviour of brittle materials at failure, are the size and the effect of self weight of specimens. This phenomenon is related to the loss of nominal strength of concrete, or concrete like materials, as the size of geometrically similar specimens is increased (Brühwiler and Wittmann, 1990; Barr *et al.*, 1998). Brühwiler and Wittmann (1990) proposed the wedge splitting test as the best method to determine stable fracture mechanics tests of individual masonry units. This test setup has a compact nature, reducing the negative effect of self weight, and a large fracture area. This has a positive influence on the size effect, and therefore outperforms other fracture mechanics tests like the uni-axial tensile test, notched three point bending test and compaction tension test (Brühwiler and Wittmann, 1990).

One of the main advantages of the wedge splitting test is the stable crack formation for quasi-brittle materials by introducing a load with constant rate. Section 3.3.3 investigates the wedge splitting test method. Figure 3.1 displays a wedge splitting test performed by Brühwiler and Wittmann (1990) on a prismatic specimen, drilled from a dam wall.

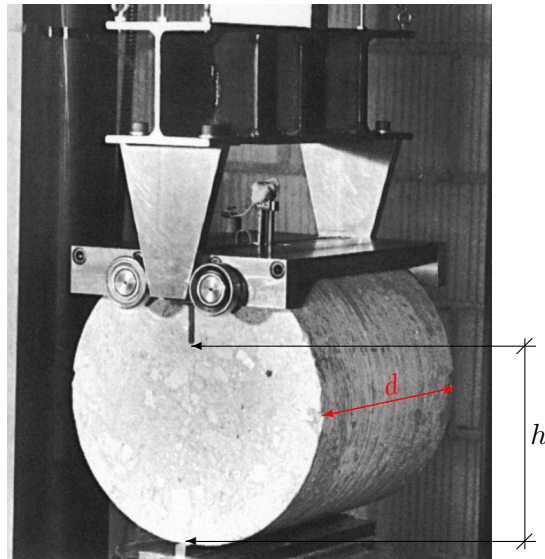


Figure 3.1: Wedge splitting test on drilled specimen (Brühwiler and Wittmann, 1990)

The aim of a stable fracture mechanics test is to measure the amount of energy needed to split a specimen in half. This energy is calculated as the area under the load-deformation graph after the peak load is reached. The material's specific fracture energy (G_f) is termed as the amount of energy required to form a unit area of crack surface (Lourenço, 1998). The G_f is determined by dividing the fracture energy by the projected fracture area (ligament length $h \times$ width of specimen d , Figure 3.1) (Brühwiler and Wittmann, 1990). Figure 3.2 displays a typical load deformation graph in a fracture mechanics test. It should be noted from Figure 3.2, that G_f is only calculated after the peak load.

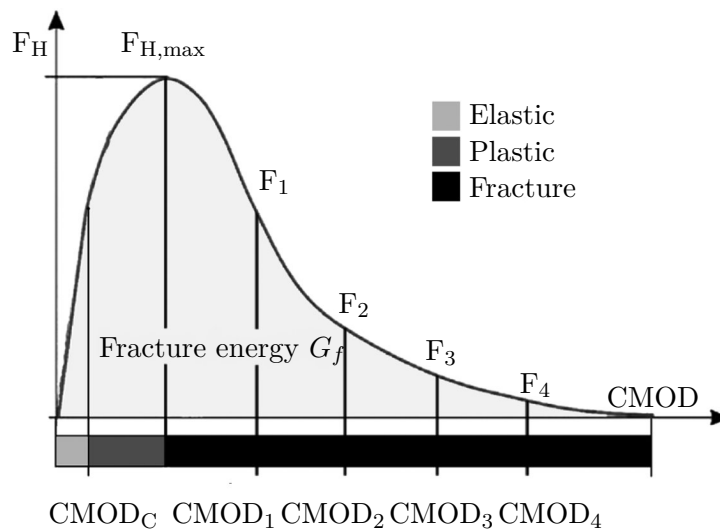


Figure 3.2: Typical load-deformation graph for stable fracture mechanics test (Schneemayer *et al.*, 2014)

One of the focus points of this study is to investigate test methods, from international standards and/or literature, which would best represent stable fracture tests. To obtain the tensile ($G_{f,t}$) and shear fracture energy ($G_{f,s}$) of the joint interface a load-deformation graph as displayed in Figure 3.2 is required. Stable fracture tests are central to this study and Section 3.3 investigates different test setups and explains the advantages and disadvantages of each in terms of being a stable fracture test.

3.1.2 Tensile Characteristics of the Joint Interface

Customarily, masonry is implemented in numerical models or building standards as a material with zero tensile strength at the joint interface (Schneemayer *et al.*, 2014). However, the study conducted by Najafgholipour *et al.* (2013) indicates that this is not true. In the case of in-plane shear failure and out-of-plane bending, the tensile strength of the joint interface becomes important. It was also found an evident interaction between the in-plane shear and out-of-plane bending capacities of masonry walls from test results. The resistance against these failure modes can be increased by improving the interface properties. Masonry failing in tension on the joint interface is known as mode I failure (Lourenço, 1998).

Literature frequently refers to the tensile strength of the joint interface as the bond strength. The bond strength, however, also influences the shear characteristics of the joint interface and is in this study not only related to the tensile strength but also the shear strength of the interface. Numerous factors influence the bond strength are elaborated on in Section 3.2.

Different research groups have created different test methods to measure the tensile strength of the joint interface of masonry over the years. The earliest tensile test was created by Baker (1902), which tested the tensile strength of cement mortars. The most direct way to determine the tensile strength of the joint interface is with a uni-axial tension test (also known as a direct tensile test). The United States of America published a standard test method for determining the bond strength of mortar to masonry units. Two test methods are provided to determine the bond strength, a crossed-brick couplet tensile test for evaluating the direct tensile strength of the mortar-brick interface and a stacked bond flexure test for evaluating the bond strength (indirect tensile strength) of the mortar-concrete block interface (ASTM C 952-12, 2012).

The crossed-brick test assembly represents the most direct method to determine the tensile strength of the joint interface. Figure 3.3 displays both the crossed-brick couplet tensile test and the stacked bond flexure test as per ASTM C 952-12 (2012).



(a) Crossed-brick test assembly



(b) Concrete block test assembly

Figure 3.3: Standard test methods for determining bond strength of mortar to masonry units (ASTM C 952-12, 2012)

The Dutch mortar standard, NEN 3835 (1991), also prescribes a cross couplet test to determine the tensile strength of the joint interface. See Figure 3.4 for the visual representation of the test setup. Although in principle this test is the same as the crossed-brick couplet test from ASTM C 952-12 (2012), the test assemblies differ. The crossed-brick couplet test setup from the American standard is seen as more stable than the one from the Dutch standard. The upper

and lower tripods ensure a more balanced test setup than the U-shaped steel plates used in NEN 3835 (1991). The tripods were probably used to better account for inequalities in the test setup. Therefore, the crossed-brick couplet test from ASTM C 952-12 (2012) is further discussed in this study.

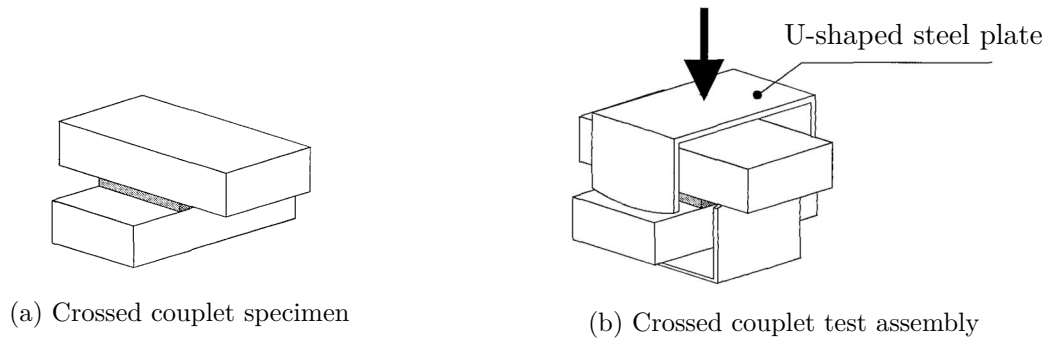


Figure 3.4: Crossed couplet test recommended by NEN 3835 (1991) (*adapted from Van der Pluijm (1999)*)

Obtaining a descending branch in the overall load-deformation diagram from the crossed-brick test would be difficult considering the quasi-brittle behaviour of masonry materials at failure. This could cause difficulties with determining the tensile fracture energy of the joint interface. If it is possible to obtain such a branch, accurate test equipment is required. Figure 3.5 displays the differences in the general load-deformation graph of a compressive and tensile test on quasi-brittle masonry materials (Lourenço, 1998). The graph displays the failure behaviour of general masonry units in compression and tension. Failure at the joint interface in tension could show an even more sudden failure as in Figure 3.5(b) due to the non-homogeneous nature of the interface.

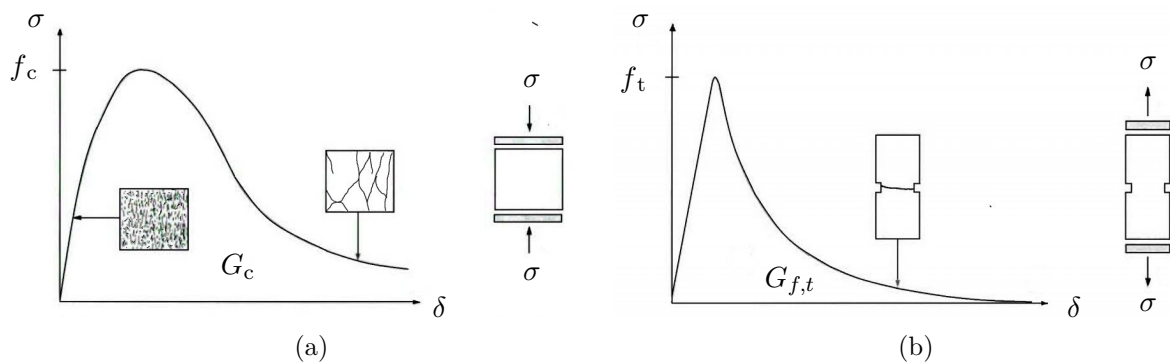


Figure 3.5: General stress-deformation graph of the: a) compression- and b) tensile strength test on masonry units (Lourenço, 1998)

Literature and the European testing standard suggest two other indirect tensile strength tests to obtain the bond strength of the joint interface namely, the wedge splitting test and bond wrench test (Brühwiler and Wittmann, 1990; Schneemayer *et al.*, 2014; EN 1052-5, 2005). The crossed-brick test, bond wrench test and wedge splitting test are investigated in Sections 3.3.1, 3.3.2 and 3.3.3. The bond wrench test from EN 1052-5 (2005) is similar to the stacked bond flexure test from ASTM C 952-12 (2012) and, therefore, only one of these tests is further investigated in this study.

Table 3.1 presents flexural bond strength results obtained from literature. Table 3.1 shows the masonry unit type used by each researcher, the mortar type and mortar compressive strength (f_{cm}). Only the most relevant information are given in this table. For example Rao *et al.* (1996) investigated not only cement-sand mortars, but also, cement-soil-sand mortars and cement-lime-sand mortars. However, cement-sand mortars are most relevant due to this being the mortar used in this study. Therefore, when a researcher investigates more than one type of masonry unit only the most relevant mortar results are given.

Table 3.1: Flexural bond strength (f_f) results from literature

Researcher	Unit Type	Mortar Type	f_{cm} (MPa)	f_f (MPa)	Test Method
Lumantarna <i>et al.</i> (2014)	URM clay	L:S	1.2 - 8.6	0.031 - 0.345	Bond Wrench
	Fired brick			0.05 - 0.1	
Rao <i>et al.</i> (1996)	Stabalised mud	C:S	0.9 - 8.4	0.02 - 0.23	Bond Wrench
	Stabalised soil-cement			0.02 - 0.12	
Nichols and Holland (2011)	Fired brick	C:L:S	unk	0.65 - 0.73	Bond Wrench

Note: C - Cement, L - Lime, S - Sand, unk - Unknown

Past investigations suggest that there is a relationship between the mortar compressive strength and the mortar flexural strength (Reddy and Gupta, 2006; Sarangapani *et al.*, 2005). Lumantarna *et al.* (2014), therefore, related the masonry flexural bond strength to the mortar compressive strength as most of the test samples showed bond failures within the mortar joint and not at the joint interface. Lumantarna *et al.* (2014) indicated that the masonry flexural bond strength is better characterised by the mortar compressive strength than by the masonry compressive strength. Figure 3.6 shows these relationships. Results show that the average masonry flexural bond strength increased with an increase in the average mortar compressive strength.

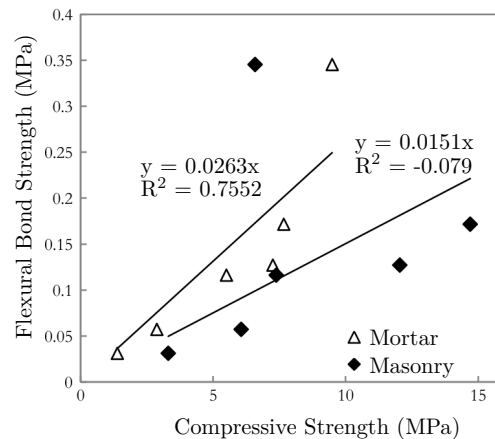
Figure 3.6: Flexural bond strength vs compressive strength relationship (Lumantarna *et al.*, 2014)

Table 3.2 shows the tensile bond strength results obtained from different studies in literature. Again, results that are more relevant to this study are shown. The test specimens of Schneemayer *et al.* (2014) consisted of bricks with different roughness's joint together with mortar. To vary the surface roughness of the brick the surface was physically altered by sawing three grooves into the brick at the joint interface. Only test results from bricks with plain surfaces (without grooves) are considered for this study, due to this being more relevant to this study. The

surfaces of the concrete (CON) units and different type of AMUs employed in this study are left unchanged throughout. Reddy and Gupta (2006) examined the tensile bond strength of masonry couplets using different mortars, with the crossed-brick test method as per ASTM C 952-12 (2012). Tensile bond strengths obtained by Reddy and Gupta is presented in Table 3.2. Reddy and Gupta also considered a few other parameters and their influence on the bond strength, this is discussed in Section 3.2. It should be noted that this is not exhaustive literature on the tensile strength of the joint interface, but rather literature that are relevant to this study.

Table 3.2: Tensile bond strength (f_t) results from literature

Researcher	Unit Type	Mortar Type	f_{cm} (MPa)	f_t (MPa)	Test Method
Hamid (1978)	CON	C:L:S	10.3 - 27.2	0.75 - 0.84	Circular Masonry Discs
Schneemayer <i>et al.</i> (2014)	Standard Austrian	C:L:S	4.8 - 18.9	0.30 - 1.10	Wedge Splitting Test
	brick	C:S	29.8	0.5	
Sugo <i>et al.</i> (2001)	Extruded clay			0.93	Uniaxial Tensile Test
	Dry-pressed clay	C:S	unk	0.84	
	CON			0.51	
	Calcium silicate			0.87	
De Almeida (2012)	ADB	L:S	2.7	0.01	Uniaxial Tensile Test
Reddy and Gupta (2006)	Soil-cement	C:S	5.4 - 6.0	0.09 - 0.18	Crossed-brick Test

Literature investigating the tensile fracture energy of the joint interface of masonry is not often obtained. However, some literature investigates this mechanical property and the findings are presented in Table 3.3.

Table 3.3: Tensile fracture energy ($G_{f,t}$) results from literature

Researcher	Unit Type	Mortar Type	f_{cm} (MPa)	$G_{f,t}$ (N/m)	Test Method
Schneemayer <i>et al.</i> (2014)	Standard Austrian	C:L:S	4.8 - 18.9	5.10 - 11.10	Wedge Splitting Test
	brick	C:S	29.8	4.8	
De Almeida (2012)	ADB	L:S	2.7	4.50	Uniaxial Tensile Test
Almeida <i>et al.</i> (2002)	Conventional brick	C:S	7.1 - 12.8	7.79 - 8.13	Uniaxial Tensile Test

3.1.3 Shear Characteristics of the Joint Interface

Shear strength of masonry plays an important role, especially when in-plane shear forces act upon the structure. The non-linear reaction at the joint interface usually causes this interface to be the weakest point of a masonry wall and is often the location of shear failure (Lourenço, 1998). This phenomenon, in-plane shear failure of masonry buildings, mostly occurs in earthquakes or strong winds (Schneemayer *et al.*, 2014). Therefore, to successfully model buildings, it is important to characterise the shear behaviour of the joint interface of masonry. Figure 3.7 compares the stress-displacement diagram of the behaviour of masonry under shear stress with and without a normal confining load. This defines mode II failure and represents the concept of cohesion. Shear failure at the joint interface is also characterised by the slipping of units along the interface (Lourenço, 1998).

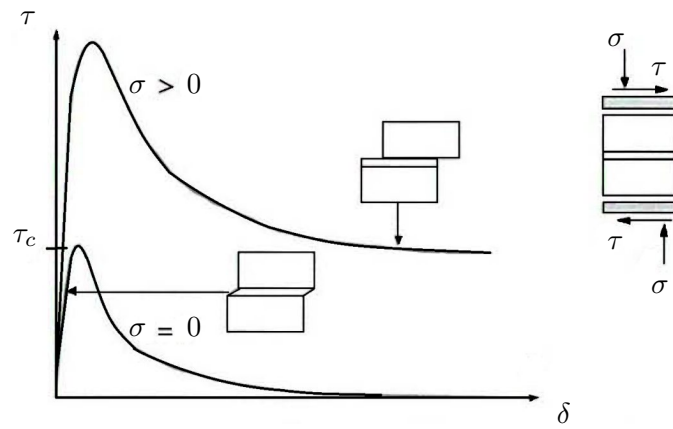


Figure 3.7: Shear behaviour of the joint interface with and without a normal confining load (Lourenço, 1998)

An important aspect in characterising the shear behaviour of masonry joints is for the test setup to ensure a uniform, normal stress distribution in the joints. Equilibrium constraints cause non-uniform normal stresses to occur in the interface joints (Van der Pluijm, 1993). According to Zeranka and Van Zijl (2018), there are two important aspects that need to be considered when performing shear tests. Firstly, little to no bending moment must be allowed to develop over the shear plane. Pure shear values become distorted when compression or tensile forces are present in the shear plane. Forces on the shear plane may allow the mode of fracture to differ. Secondly, it is important to accurately measure the post-fracture behaviour, from initial fracture until total fracture, to determine the total interfacial fracture energy.

Lourenço (1998) states that it is important to keep the normal stress applied to the test specimen constant throughout the test. Keeping the normal stress constant is the best way to obtain post-peak characteristics. Literature suggests a number of tests to characterise the shear behaviour of horizontal masonry joints, indicating the difficulty of finding consensus with regards to the best testing method. The three most general test methods are the couplet test, Van der Pluijm test and the triplet test (Lourenço *et al.*, 2004; Van der Pluijm, 1992b). Riddington *et al.* (1997) developed the following quality criteria for evaluating masonry shear test setups. This criteria has also since been used by Montazerolghaem and Jaeger (2014).

1. The shear and normal stress should be uniform over the length of the joint interface.
2. If failure occurs at one point in the interface, other parts of the joint should be close to failure.
3. Tensile and compression stresses should be avoided along the interface.
4. Failure should not be initiated at the edge.
5. The experiment should be easy to implement and execute.

Figure 3.8 displays the three test methods and their loading configurations.

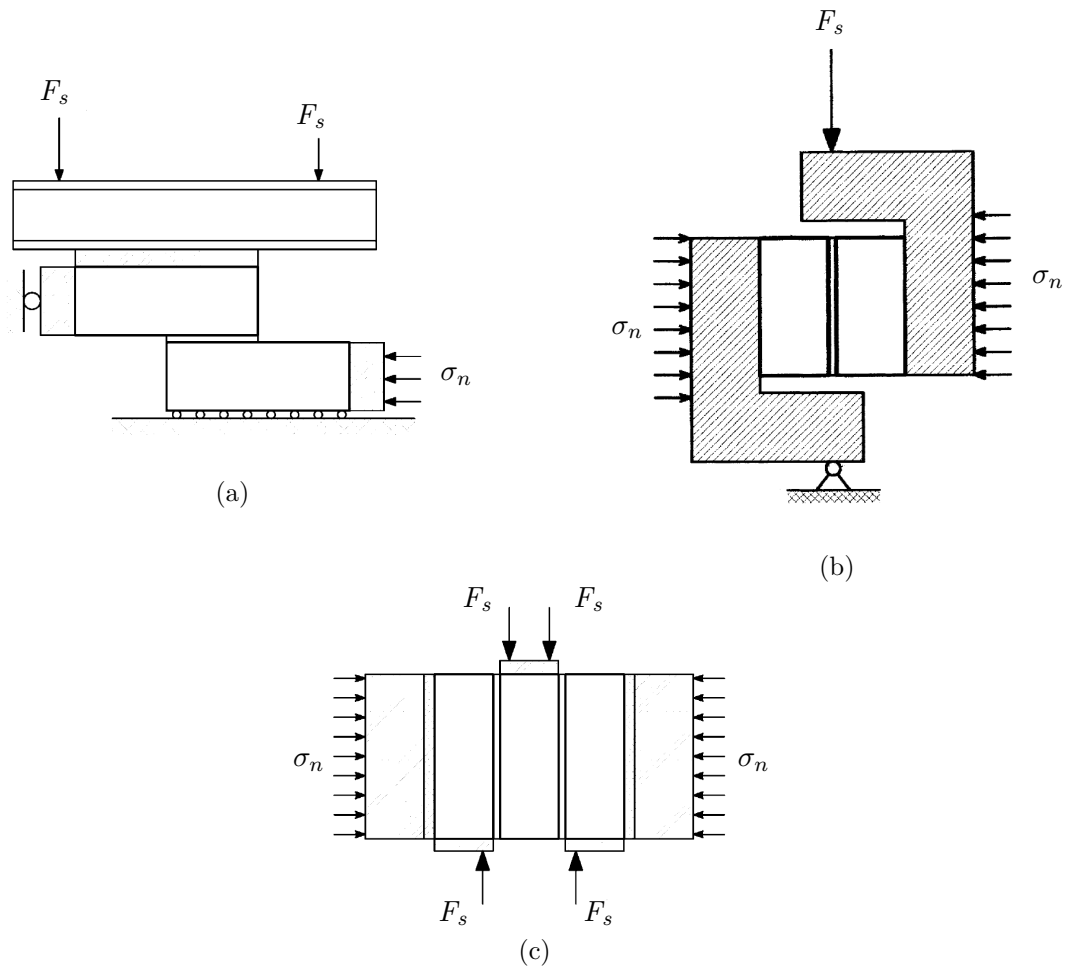


Figure 3.8: Horizontal masonry joint shear test methods: a) the couplet test, b) van der Pluijm test and c) triplet test.

The couplet test (also known as the Hoffman/Stöckl test) has the most uniform normal and shear stress data in comparison to the other two tests. However, the complexity of the geometry of the test setup keeps this test from being standardised (De Vasconcelos, 2005). After performing a numerical analysis on the Van der Pluijm test the results revealed an almost uniform shear stress over the joint interface, but an uneven normal stress distribution. Regarding the triplet test, the shear strength can be affected by the non-uniform load distribution, however, if the bending moment is minimised reliable results can be obtained. This can be achieved by reducing the eccentricities of the reactions, as close as possible to the vertical joint interface (De Vasconcelos, 2005). The triplet test presents the most straightforward test setup, and is relatively easy to implement and execute, in comparison to the other two shear tests. The study of Zhang *et al.* (2019) evaluate these three masonry shear tests through non-linear finite element analysis and justifies the use of the triplet test for the shear characterisation of the joint interface of masonry.

Due to the advantages of the triplet test, the disadvantages of the other two methods, and the fact that this test setup is available at Stellenbosch University (similar test were conducted on the same masonry materials by Fourie (2017)), the triplet test is used for shear characterisation of the joint interface in this study. The triplet test is also the only test, out of the three, that is standardised by the European testing standard, and due to South Africa adopting this code in the near future this motivates the decision of using the triplet test for this study. The European testing standard, EN 1052-3 (2002), standardised the triplet test for the determination of the initial shear strength masonry joints. The triplet test, as per EN 1052-3 (2002) is discussed in Section 5.3.2.

Shear failure of the joint interface occurs when a shear load produces a sliding failure along a specific failure plane (Lourenço, 1998). The shear bond strength (τ_a), for a pure shear test, is calculated by dividing the maximum shear force (F_{max}) by the cross sectional area of the joint interface (A_i). The shear strength of the joint interface can also be characterised by the Mohr-Coulomb friction law (Lourenço *et al.*, 2004; RILEM, 1996; ASTM C 1531-09, 2009). This law establishes a linear relationship between the shear stress and normal stress applied to a masonry joint (*adapted from* De Almeida (2012); Lumantarna *et al.* (2014)). Equation 3.1 can be used to determine the cohesion and friction angle of the interface.

$$\tau_a = \tau_c + \mu\sigma_n \quad (3.1)$$

where,

τ_a = shear stress at a certain normal stress;

τ_c = pure shear stress without normal stress, this represents the cohesion of the material;

μ = coefficient of friction (calculated as $\tan(\varphi)$, where φ is the friction angle);

σ_n = normal compression stress.

The cohesion, τ_c , and coefficient of friction, μ , can be determined from the shear stress, τ , versus normal stress, σ_n , relationship by determining best-fit linear equations. The vertical axis intercept of this equation represents, τ_c , and the slope, μ (De Almeida, 2012).

Table 3.4 presents shear bond strength results from different researchers. The masonry unit type, mortar type and mortar compressive strength are again presented. The normal compression stress levels, cohesion and coefficient of friction obtained from each study is given, with the respective test methods. An almost linear relationship was obtained between the shear stress and the normal compression stresses by De Almeida (2012), higher compression loads lead to larger values in both the shear strength and shear fracture energy (refer to Table 3.5 for shear fracture energy values). The study of De Almeida (2012) further reported that the cohesion and coefficient of friction values were much smaller for the joint interface than for individual units. This confirms the interface as being the weaker part of masonry (Lourenço, 1998).

Table 3.4: Shear bond strength results from literature

Researcher	Unit Type	Mortar Type	f_{cm} (MPa)	σ_n (MPa)	τ_c (MPa)	μ	Test Method
Lumantarna <i>et al.</i> (2014)	URM clay	L:S	1.2 - 8.6	0.02 - 0.6	0.15 - 0.39	0.83 - 0.90	Triplet Test
De Almeida (2012)	ADB units	L:S	2.7	0.1 - 0.3	0.1	1.35	Couplet Test
Van der Pluijm (1993)	Fired brick	C:L:S	3.0 - 14.4	0.1 - 1.0	0.10 - 0.85	0.83 - 1.2	Van der Pluijm
	Mud brick				0.88 - 1.85	0.72 - 0.97	
	Sand lime				0.15 - 0.28	0.75 - 1.01	
Lourenço <i>et al.</i> (2004)	Hollow brick	Micro - concrete	unk	0.2 - 1.0	1.39	1.03	Direct Tension Test
De Vasconcelos (2005)	Granitic	L:S	5.5	0.5 - 1.25	0.359	0.63	Couplet Test

Lumantarna *et al.* (2014) estimated that the cohesion of the joint interface is better characterised by the mortar compressive strength than the masonry compressive strength. Figure 3.9 represents the relationship between the joint interface cohesion and the average mortar compression strength, as well as the relationship between the joint interface cohesion and the average masonry compression strength.

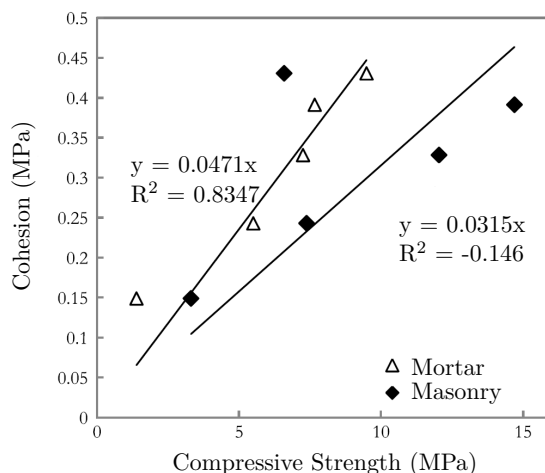


Figure 3.9: Cohesion vs compressive strength relationship (Lumantarna *et al.*, 2014)

Table 3.5 shows shear fracture energy results of the joint interface obtained from two researchers.

Table 3.5: Shear fracture energy ($G_{f,s}$) results from literature

Researcher	Unit Type	Mortar Type	f_{cm} (MPa)	σ_n (MPa)	$G_{f,s}$ (N/m)	Test Method
De Almeida (2012)	ADB units	L:S	2.7	0.1 - 0.3	400 - 625	Couplet Test
	Fired brick				71 - 188	
Van der Pluijm (1993)	Mud brick	C:L:S	3.0 - 14.4	0.1 - 1.0	36 - 126	Van der Pluijm
	Sand lime				12 - 39	

In conjunction with the cohesion and friction angle an equally important aspect of shear behaviour at the joint interface is dilatancy. Cohesion and friction angle are mechanical properties frequently investigated in literature but dilatancy less so. Dilatancy represents the difference in normal displacements of the upper and lower unit (Δv), due to shear displacement (Δu). This concept is visually represented in Figure 3.10. Figure 3.10 presents the concept of dilatancy on a individual unit and not on the joint interface, nonetheless, the same principle applies for both. The change in volume of a sample under shear loads is called the dilatancy angle. The dilatancy angle (ψ) is defined as the uplift of one unit over the other while shearing (Lourenço, 1996). This angle represents the ratio $\Delta v/\Delta u$ (De Almeida, 2012).

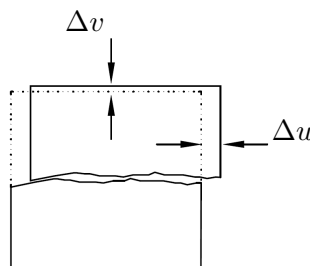


Figure 3.10: Visual interpretation of the concept of dilatancy with ratio $\Delta v/\Delta u$ (De Vasconcelos, 2005)

Some research has investigated the concept of dilatancy at the joint interface of masonry (Lourenço, 1996; Van Zijl, 2004; Burnett *et al.*, 2007; Haach *et al.*, 2011). Numerous numerical interface models have been developed in the past, but only more recently have models been

developed where dilatancy formulations successfully reproduce the volume increase of masonry under shearing. Experiments have shown that unconfined masonry undergoes significant inelastic volume increase (Δv and Δu of the same order) upon shearing and in the case of confined masonry, pressure build-up occurs. This highlights dilatancy as a possible source for volume increase, and significant strength increase, of masonry under shear (Van der Pluijm, 1992a).

Dilatancy is dependant on two factors, namely the confining pressure and shear-slipping deformation (Lourenço, 1996; Van Zijl, 2004). Firstly, considerably reduced normal displacements are experienced at increasing confining pressures and, secondly, normal displacements reach a plateau or even reduce at large shear-slip deformations. These factors often occur simultaneously in masonry, especially when confined, and lead to a fast degradation of the dilatancy. Figure 3.11 reveals the concept of dilatancy from experimental data and also confirms the influence of these two factors on dilatancy.

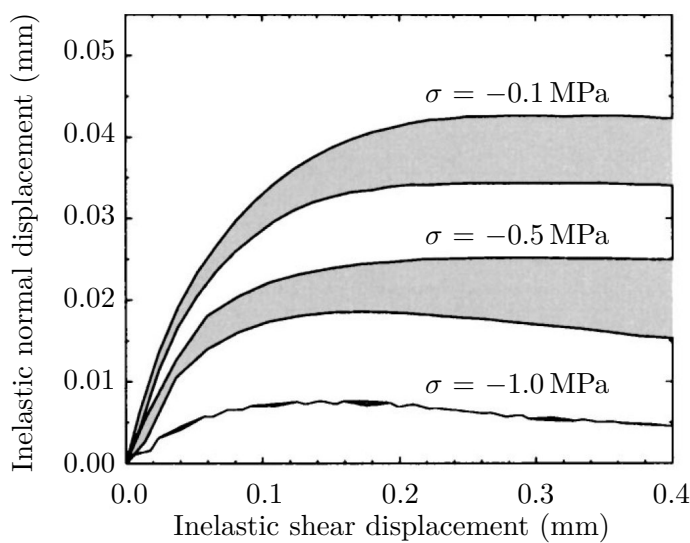


Figure 3.11: Dilatancy displacement at the joint interface upon inelastic shear of masonry (Van der Pluijm, 1992a)

Due to the fast degradation of dilatancy and to avoid adding two additional material parameters to material models (the two factors dilatancy is dependant on discussed earlier) most researchers assume the dilatancy angle as zero in numerical models (Lourenço, 1996). Van Zijl (2004) stated that a dilatancy angle of zero can be overly conservative, leading to the over designing of structures. However, a danger is to assume a constant non-zero dilatancy angle throughout the analysis. This has shown to lead to masonry of unlimited resistance under confined shear in computations, even for a small dilatancy angle.

Lourenço (1996) pointed out the large influence dilatancy has on shear wall analyses. An average dilatancy angle of 22° was assumed while all the other material properties were kept constant. This led to failure loads of between 1.5 and 2.5 times larger for shear walls with and without openings. This confirms Van Zijl's (2004) statement, taking dilatancy as zero could be overly conservative. This raises the need for more experimental data available in literature, to avoid inappropriate modelling, better validated material models and gaining a greater understanding of the dependence of dilatancy on confining pressure and shear-slipping deformations.

Up to date, no international standard has been published to determine the dilatancy of the joint interface of masonry. A possible reason for this is that not much research has been done

in this field in the past. Literature, however, has discussed methods to determine dilatancy. Lourenço (1996) developed Equation 3.2 and 3.3, for the dilatancy coefficient and dilatancy angle respectively.

$$\tan(\psi) = \Delta v / \Delta u \quad (3.2)$$

$$\psi = \arctan(\Delta v / \Delta u) \quad (3.3)$$

One of the physical characteristics of masonry that influences dilatancy the most is surface roughness. Lourenço (1996) noted for low confining pressures, that the dilatancy is dependent on the surface roughness of the units. For high confining pressures the dilatancy angle tends to zero. According to Lourenço (1996) a confining stress of between 1.0 MPa and 2.0 MPa is sufficient to reduce the normal displacement under shearing, and hence the dilatancy angle to zero. From the results of Van der Pluijm (1993), it is predicted that the confining stress level at which the dilatancy angle tends to zero are 1.37 MPa and 2.44 MPa for two types of clay bricks. While no direct relationship can be drawn between the confining stress at which the dilatancy tends to zero and the cohesion, similar cohesion values were found for both bricks, 1.33 MPa and 2.76 MPa. Table 3.6 presents dilatancy results obtained from literature.

Table 3.6: Dilatancy results from literature

Researcher	Unit Type	Mortar Type	f_{cm} (MPa)	σ_n (MPa)	ψ (°)
	Fired brick				
Van der Pluijm (1993)	Mud brick	C:L:S	3.0 - 14.4	0.1 - 1.0	35 - 11.3
	Sand lime				
Haach <i>et al.</i> (2011)	CON	unk	unk	0.56 - 1.3	27.5
Burnett <i>et al.</i> (2007)	Clay brick	unk	unk	unk	7.1
Van Zijl (2004)	Clay brick	unk	unk	0.1	33.8
	Calcium-silicate	unk	unk		36.5

3.1.4 Concluding Remarks

This section firstly discussed the need for obtaining the mechanical properties of the joint interface of masonry to successfully apply numerical models to masonry structures. The concept of fracture energy is defined, as well as the tensile and shear characteristics of the joint interface. These tensile and shear characteristics include the tensile strength, tensile fracture energy, initial shear strength, shear fracture energy, cohesion, friction angle and dilatancy, all of the joint interface of masonry. The importance of the tensile and shear strength of the joint interface of masonry are highlighted, and the fact that it cannot be ignored or taken as zero in numerical analysis.

Different test methods proposed by standards and literature are considered for characterising the tensile and shear properties of the joint interface. Advantages and disadvantages of different test methods are discussed and the thought process behind choosing test methods for further application in this study is explained. Flexural, tensile and shear bond strength results of the joint interface from literature, as well as tensile and shear fracture energy results, are presented to determine acceptable ranges of results for these mechanical properties.

The triplet test is chosen for the shear characterisation of the joint interface and three tensile tests were chosen for further investigation. Section 3.3 further investigates these tensile tests.

3.2 Factors Influencing the Bond Strength of the Joint Interface

This section considers a number of parameters and how they influence the bond strength of the joint interface. Groot (1993), Grenley (1969) and Reddy and Gupta (2006) all listed a number of masonry unit characteristics and mortar parameters responsible for bond strength development of the joint interface. The masonry unit characteristics that influence the bond development are: surface roughness or surface porosity, cement content, compressive strength, absorption characteristics and moisture content of the masonry unit at the time of casting the prisms.

A masonry prism in this study is referred to as two or more individual masonry units stacked on top of each other and joined together with mortar. Likewise, the following mortar parameters influence the bond strength: composition, clay and cement fraction, water content, flow/workability, water retentivity and compressive strength. Groot (1993) and Sugo *et al.* (2001) agree that the joint interface bond development is mainly a mechanical process influenced by hydration of the binder occurring at the brick/unit surface and in the brick/unit pores.

Sections 3.2.1 and 3.2.2 investigate, respectively, the masonry unit characteristics and mortar parameters that influence the bond development of the joint interface.

3.2.1 Masonry Unit Characteristics Affecting the Bond Development of the Joint Interface

As stated in Section 3.1.2, the research of Reddy and Gupta (2006) investigates the tensile bond strength of soil-cement block masonry using soil-cement mortars. Other mortars also investigated were cement-lime mortars and normal cement mortars. Results obtained from masonry constructed with cement mortars are most applicable to this study, and only these are discussed further.

Reddy and Gupta characterised the surface roughness of the soil-cement blocks with pore size and surface porosity. The pore size and surface porosity are determined with scanning electron microscopy (SEM) on samples cut from undisturbed block surfaces. The pore sizes varied with the cement content in the blocks. Surface porosity stayed the same for different cement contents. An increase in cement content led to a decrease in pore size and an increase in the number of pores (pore density). Blocks with higher pore densities showed higher tensile bond strengths. This encouraged better mechanical interlocking of the hydration products. Therefore, the surface roughness, for soil-cement blocks can be seen as a function of the cement content in the block.

Blocks with higher cement contents showed higher compressive strengths. This also correlates the bond strength with the compressive strength of the block for soil-cement blocks. The mean size of the pores varied between 0.08 and 0.28 mm and the surface porosity between 14-15%. Reddy and Gupta concluded that an increase in surface pore size leads to a decrease in the tensile bond strength, with a constant pore density. Tensile bond strengths varied between 0.1 and 0.18 MPa for different surface roughnesses.

Tschegg *et al.* (2008) investigated the influence of surface roughness on the fracture properties of marble-mortar compounds. The surface roughness was determined by the use of a Perthometer. The Perthometer is a surface roughness tester that measures the mean roughness value (R_a) in micrometer (μm) (Mahr, 2005). The results showed that a higher mean roughness value gen-

erated a higher resistance against crack growth in fracture mechanic tests. Schneemayer *et al.* (2014) also stated that the roughness of a materials can influence the bond strength.

Walker (1999) observed the bond characteristics of earth block masonry. Results showed that when the bond strength is limited by the block strength a strong linear correlation can be drawn between the bond strength of the joint interface and the compressive strength of the block. Selecting a mortar that resembles the block's characteristics optimises the bond strength.

Sugo *et al.* (2001) examined different factors that influence the development process of the mortar/unit bond with uniaxial tension tests. Results showed that the mortar dewatering process at the time of prism construction affects the bond strength of the interface. Dewatering of mortar at construction can be partly caused by the water absorption characteristics of the masonry unit, however, other factors also play a role like the rheology and water retentivity of the mortar. Therefore, the water absorption characteristics of the masonry unit alone cannot predict the bond strength with accuracy. Sugo *et al.* included the following masonry unit types in their research study, dry pressed clay unit, extruded clay wire cut unit, concrete unit and calcium silicate unit. The initial rates of absorption (*IRA*) for each of the units were 3.39, 1.24, 1.45 and 1.33 kg/m²/min, respectively. Results further showed that the amount of moisture removed from the mortar at construction is not completely dependent on the *IRA* of the units. However, units with high *IRA* values can cause workability problems for the mason and a lower water-cement ratio in the mortar, leading to weaker bonds. Sarangapani *et al.* (2005) agree that the rate of absorption of the brick and the water retentivity of the mortar play an important role in the bond development process. From literature it can be seen that earth block masonry has the highest *IRA*, with *IRA* values of between 6.6 and 8.9 kg/m²/min obtained for earth block masonry (Walker, 1999).

Reddy and Gupta (2006) found low tensile bond strengths when the masonry blocks were completely dry at casting. This can be caused by the block absorbing water from the freshly mixed mortar, leading to a low water-cement ratio in the mortar and improper hydration of the binder product. Freshly mixed mortar is further in this study referred to as fresh mortar. The influence of the moisture content, at the time of construction, was one of the major findings of the research done by Reddy and Gupta. The highest bond strength was obtained when the moisture content of the blocks, at the time of construction, was the optimum moisture content. The optimum moisture content is between 50% and 75% of the saturated moisture content of the block. Blocks that are completely dry or wet at time of construction gave tensile bond strengths of about 20-55% of the optimum bond strength. The results showed that the tensile bond strength increased with an increase in the moisture content of the block until the optimum moisture content is reached. Tensile bond strengths varied with 0.19 MPa for different initial moisture contents at time of construction. Walker (1999) also reported on the influence of the moisture content of the block at the time of casting prisms for compacted soil-cement blocks. Initial moisture content of 50%, of the saturated moisture content, gave the maximum bond strength.

Rao *et al.* (1996) found that the moisture content of the masonry block at the time of casting the masonry has a remarkable effect on the flexural bond strength of masonry. Optimum moisture content leading to maximum bond strength is between 75 and 80% of the saturated moisture content of the block. Sinha (1967) also examined the influence of moisture content at the time of casting masonry on the tensile bond strength. Bricks with moisture content of about 80% of the saturated moisture content showed highest bond strengths. This is seen as the optimum moisture content of the bricks. Dry or fully saturated bricks gave weaker bonds.

3.2.2 Mortar Parameters Affecting the Bond Development of the Joint Interface

Reddy and Gupta (2006) investigated the influence of the clay content and cement content in mortar, on the bond strength. Reddy and Gupta found that cement-soil mortar gives 15-50% more bond strength when compared to cement or cement-lime mortars. Results also showed that the bond strength decreases with an increase in clay content in the mortar and on the other hand increases with an increase in cement content. The bond strength is more sensitive to the cement content than the clay fraction. The highest bond strengths were obtained by cement-soil mortars, showing its higher importance above normal cement and cement-lime mortars. Numerous literature investigated and compared composite mortars (cement-soil and cement-lime mortar) to normal cement mortar and found that the cement-soil mortar outperforms the rest in terms of bond strength (Rao *et al.*, 1996; Sarangapani *et al.*, 2005; Walker, 1999). This study, however, only considers cement mortars and therefore the influence of composite mortars and clay content in mortar, on the bond strength, is not further discussed.

Reddy and Gupta further investigated the flow/workability characteristics of mortar and its influence on the bond strength. Reddy and Gupta concluded that the flow/workability of mortar can affect the characteristics of the mortar as well as the bond strength. A decrease in bond strength is observed when the flow of the mortar decreases. A reason for this can be that the mortar becomes more dry at a lower flow value which causes the mortar to be less workable and this makes it harder for the fresh mortar to effectively bond with the block surface. A bond strength decrease of about 9% is observed for a cement mortar, for a decrease of flow from 100% to 80%. Even though the mortar compressive strength increases with a decrease in flow, the bond strength increases with an increase of flow.

Grenley (1969) and Rao *et al.* (1996) studied various joint combinations and concluded that the tensile bond strength generally increased with the increase in mortar compressive strengths. Walker (1999) on the other hand stated that if the block strength governs the bond strength of the joint interface, then increasing the strength of the mortar would gain little benefit. Lumanarna *et al.* (2014) highlighted the concern of relating the masonry flexure bond strength and shear bond strength of existing buildings to other masonry properties due to the fact that performing mechanical tests on existing masonry is not always practical. Lumantarna *et al.* explored the influence of mortar compressive strength on the flexural and shear bond strength of masonry. As stated in Section 3.1, it was found that the flexural bond strength and cohesion of masonry can be better characterised using the mortar compressive strength than the masonry compressive strength.

Groot (1993) investigated the effects of water flow in the mortar immediately after brick laying. This phenomenon of the joint interface and its influence on the bond strength is not widely studied even though its effect on hydration conditions and the mortar composition at the interface are assumed significant. Two parameters that mainly influence the water flow in mortar at construction are the bricks water absorption characteristics and the water retentivity attributes of the mortar. Groot (1993) used two measuring techniques to obtain the water retentivity of a mortar. The first is a neutron transmission technique, where thermal neutron energies are utilised to obtain data, and the second a scanning technique, where the water distribution profiles of the cross-section of the interface are scanned and interpreted. Even though other researchers (Sarangapani *et al.*, 2005; Sugo *et al.*, 2001) confirm that the water retentivity of the mortar influences the bond strength, this is not further examined in this study due to time limitations.

3.2.3 Concluding Remarks

The factors suggested by literature, that influence the bond strength of the joint interface of masonry are discussed in this section. Two overarching factors are investigated, firstly, the masonry unit characteristics and secondly, the mortar parameters. Findings from literature are observed to obtain a better understanding on the bond development process and the factors that influences this process the most.

Literature agreed that one of the factors that influence the bond strength development the most is the moisture content of the masonry units at the time of construction (Reddy and Gupta, 2006; Rao *et al.*, 1996; Sinha, 1967). The optimum moisture content is between 50 and 80%. Other factors like the water absorption characteristics, surface roughness of the masonry unit also affected bond strength results, but not as much as the moisture content.

It is frequently found in literature that cement-soil mortars achieved higher bond strengths in comparison to normal cement-sand and cement-lime mortars. Other mortar parameters that also influences the bond strength are the flow value and the compressive strength.

It can be seen from this section that the bond development process of masonry is influenced by a number of different factors and that these factors are normally integrated. This concludes that the bond development process is complex and no straightforward method is available to fully understand this process.

3.3 Different Testing Procedures

This section investigates the crossed-brick couplet test, bond wrench test and wedge splitting test to characterise the tensile mechanical properties of masonry. The stability in terms of fracture mechanics and the availability of test setups or equipment, to build new test setups, are considered for each test method. After considering this in conjunction with experimental results from literature, a method is proposed for this study.

3.3.1 Direct Tensile Test

The American standard ASTM C 952-12 (2012) provides a good guideline for the determination of the bond strength of mortar to masonry units via the crossed-brick couplet test method. The crossed-brick couplet test provides a method to determine the direct tensile strength on the joint interface. It is important to note that this test method, due to the nature of the setup, could provide problems with determining the tensile fracture energy. A sudden failure is expected to occur after failure.

The crossed-brick couplet test has little equipment requirements and was proposed and included in the American standard in 1976. This test is executed without pulling the specimen, but rather by applying compression loads on upright bars until failure in the joint interface occurs (Almeida *et al.*, 2002). Figure 3.12 displays the test setup and gives an indication of where the different forces are applied onto the couplet specimen (Katiyar, 2015). Figure 3.12 refers to the crossed-brick test setup from the original American standard. Figure 3.3a refers to the newer and improved setup. The improved setup, consists of upper and lower platens with only three bars, instead of four.

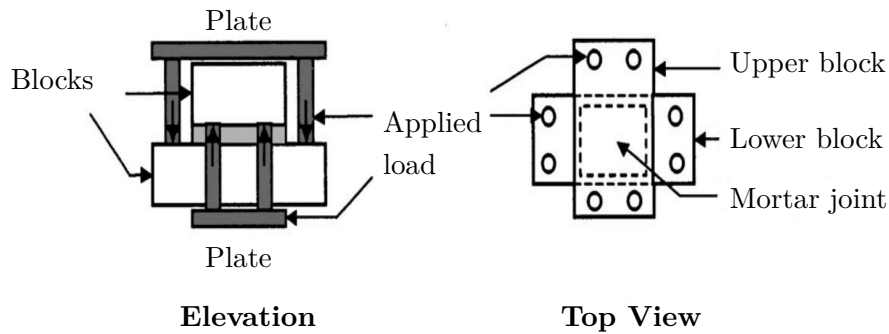


Figure 3.12: Front and top view of the crossed-brick couplet specimen in test setup configuration (*adapted from Katiyar (2015)*)

The maximum tensile bond strength (f_t) is obtained by Equation 3.4:

$$f_t = F_{\text{applied}}/A_b \quad (3.4)$$

where,

F_{applied} = the total applied load;

A_b = the cross-sectional area of the mortar bed joint.

ASTM C 952-12 (2012) specifies a certain methodology for the construction of the crossed-brick couplets, the curing process and the testing procedure, which is elaborated on in Section 5.3.1. The advantages and disadvantages of the crossed-brick couplet test are summarised as follows:

Advantages

- The direct tensile strength of the joint interface is determined
- The test setup requires little equipment and is easy to construct
- Building crossed-brick couplet specimens is quick and easy
- Test method is straightforward and quick to execute

Disadvantages

- Problems are foreseen with determining the tensile fracture energy
- Self weight can become a problem when the interface is weak

3.3.2 Bond Wrench Test

The initial bond wrench was developed in 1980 by Hughes and Zsembery (1980). This test is a variant of the bond beam test (Almeida *et al.*, 2002). The flexural bond strength of the joint interface is quite a well known topic in literature. The European testing standard EN 1052-5 (2005) and American Standard ASTM C 1072-06 (2006) provide guidelines for determining the flexural bond strength of the joint interface. The European testing standard EN 1052-5 (2005) is investigated in this section. This standard specifies a method for determining the bond strength of horizontal bed joints in masonry. The American Standard is not discussed, due to the test setup being similar to that of the European testing standard. The European testing standard will also be adopted by South Africa in the near future and this further motivates the reason for only discussing the test procedure by EN 1052-5 (2005).

EN 1052-5 (2005) tests for the bond strength of the joint interface of masonry by use of the bond wrench method. Masonry specimens are rigidly held and a clamp with a lever arm is attached onto the top unit. A bending moment is applied to the clamp until the top unit tears off. The characteristic value, determined from the average of the maximum stresses of all the samples, is considered as the bond strength of the masonry.

The standard specifies an apparatus with a support structure and clamp which holds in place the lower part of the masonry specimen without applying any substantial bending moment or force to the units under the top unit. Further is specified a lever arm with a clamp at one end which is attached to the top unit. The lever arm shall be at least 1 m in length and apply a stress of less than 0.05 N/mm^2 to the specimen, due to its own weight. Figure 3.13 displays an example of a suitable support structure and clamp.

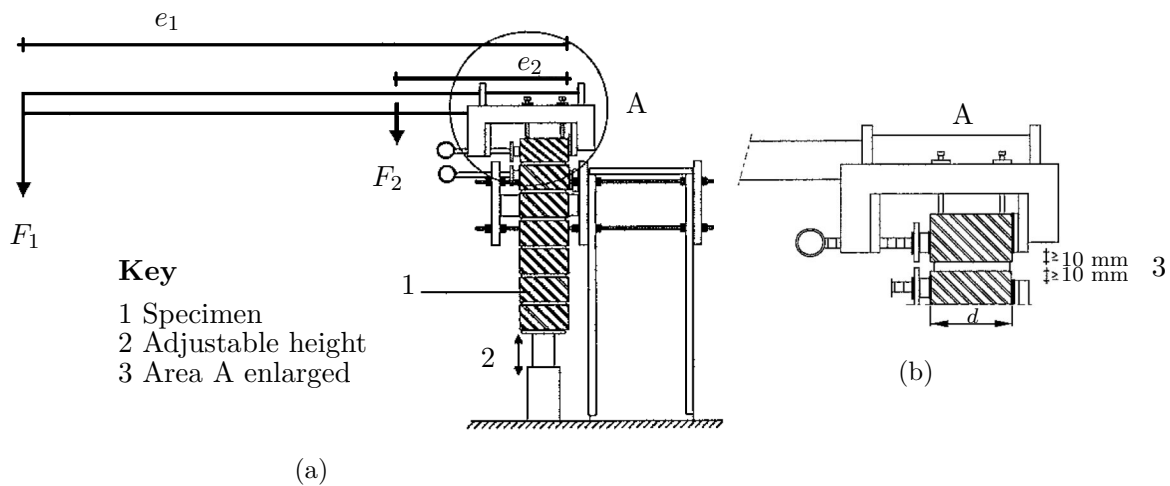


Figure 3.13: Example of a) suitable support structure and b) clamp for the bond wrench test (*adapted from EN 1052-5 (2005)*)

Applying the correct technique for the construction and preparation of the masonry specimens is important. For more details on preparing the masonry specimens and the curing and conditioning regime of the specimens prior to testing refer to EN 1052-5 (2005). For the test setup, the masonry specimen is to be clamped in the support structure in such a way that the second unit from the top has as sensible degree against rotation. The mortar joint between the top and second from the top unit should be between 10 and 15 mm clear of the support structure clamp, and the same applies for the clamp with lever arm which is attached to the top unit, refer to Figure 3.13b.

The load is applied at such a rate that failure occurs in 2 to 5 min. The bond strength is calculated with the following formula (for each valid failure type):

$$f_f = \frac{F_1 e_1 + F_2 e_2 - \frac{2}{3}(F_1 + F_2 + \frac{W}{4})}{Z} \quad (3.5)$$

where $Z = \frac{bd^2}{6}$ and,

b = mean width of mortar joint in mm;

d = mean depth of specimen;

e_1 = distance from applied load to the tension face of specimen in mm;

e_2 = distance from centre of gravity of lower and upper clamp to tension face of specimen in mm;

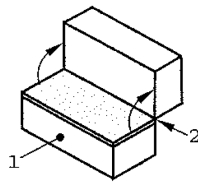
F_1 = applied load in N;

F_2 = weight of bond wrench in N;

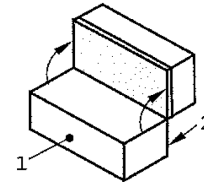
W = weight of top unit after test including the mortar on it;

f_f = flexural bond strength in MPa.

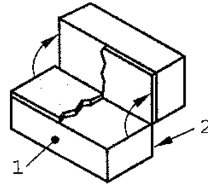
Figure 3.14 represents the different failure modes.



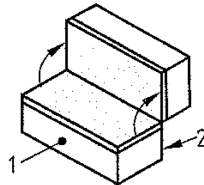
(a) At interface between upper unit and mortar



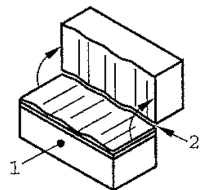
(b) At interface between lower unit and mortar



(c) At interface between both units and mortar



(d) Within mortar bed



(e) Within unit near interface

Figure 3.14: Failure modes providing valid bond strength results as per Annex A of EN 1052-5 (2005)

The advantages and disadvantages of the bond wrench test are summarised as follows:

Advantages

- Test can be conducted in-situ
- Test can be conducted manually, no testing machine required

Disadvantages

- Test provides only the indirect tensile strength
- The tensile fracture energy cannot be

- Once test setup is assembled, consecutive tests are quick to execute
- determined
- Test is seen as unstable in terms of fracture mechanics
- Test procedure cannot be force or displacement controlled

3.3.3 Wedge Splitting Test

The wedge splitting test is one of the most popular tests used in literature to determine the specific fracture energy of masonry materials (Brühwiler and Wittmann, 1990; Schneemayer *et al.*, 2014). There is no standard yet for the use of this method and the guidelines of Brühwiler and Wittmann (1990) are followed.

The wedge splitting test consists of a specimen, cubic or prismatic, placed on a support in a compression machine. A notch is cut into the specimen to control the crack location. The wedge is placed between two load transmission pieces, equipped with rollers, which are attached to either sides of the notch (Brühwiler and Wittmann, 1990). The wedge then splits the specimen in half while the horizontal force and the crack mouth opening displacement (CMOD) is measured (Schneemayer *et al.*, 2014). Essentially the fracture section is exposed to a bending moment (Brühwiler and Wittmann (1990)).

Figure 3.15 displays the wedge splitting test set-up, as illustrated by Brühwiler and Wittmann (1990). A clip gauge is used in this setup to determine the CMOD, however other researchers have used linear variable differential transducers (LVDT) successfully (Schneemayer *et al.*, 2014; Zhao *et al.*, 2008).

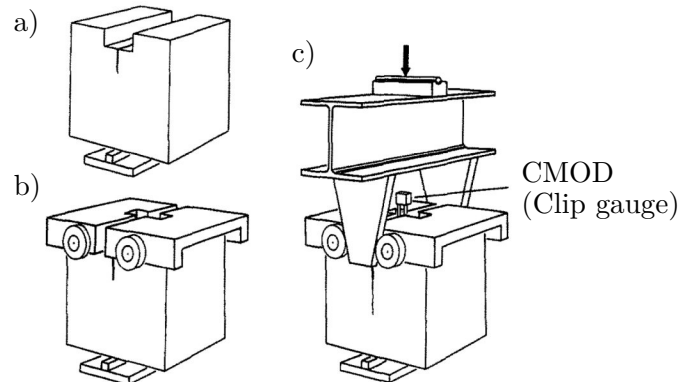


Figure 3.15: Steps of assembly for the wedge splitting test set-up (Brühwiler and Wittmann, 1990)

The horizontal force (F_h) is calculated by dividing the vertical force (F_v), applied by the compression machine, with 2 times the tangent of the wedge angle (α), see Equation 3.6. Refer to Section 3.1.1 for calculations regarding the specific fracture energy.

$$F_h = \frac{F_v}{2 \tan(\alpha)} \quad (3.6)$$

The wedge splitting test should be conducted with a closed-loop servo-hydraulic testing machine and controlled by the crack displacement (Brühwiler and Wittmann, 1990). The wedge angle

should be as small as possible but not less than 5° . Narrower wedge angles render the test impractical. The smaller the wedge angle, the more F_v is reduced relative to F_h , which is desired for a stable fracture mechanics test (Brühwiler and Wittmann, 1990).

Brühwiler and Wittmann (1990) used the test method to determine the fracture energy of masonry units, where Schneemayer *et al.* (2014) analysed the fracture mechanical properties of the mortar-brick compound. The research of Schneemayer *et al.* (2014) is more in line with the objective of this study and therefore their method is briefly discussed.

Schneemayer *et al.* (2014) created a wedge splitting test specimen which consists of mortar in the middle, with a notch milled into the mortar, and half block masonry units connected to either side of the mortar. Figure 3.16 displays the test specimen as created by Schneemayer *et al.* (2014).

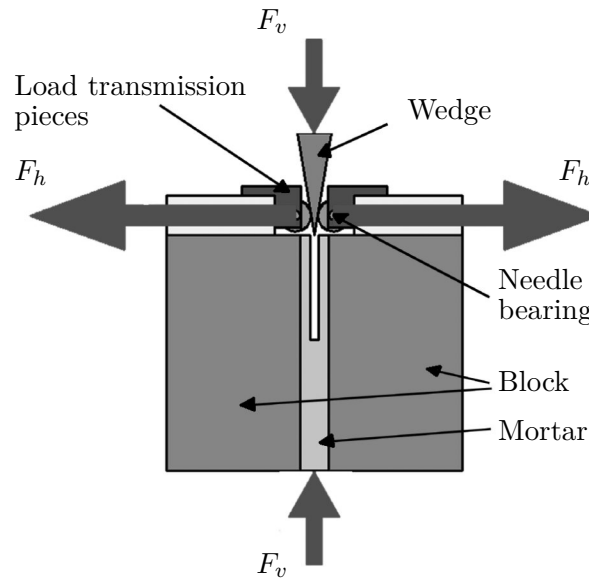


Figure 3.16: Wedge splitting test with mortar-brick interface in the middle of the specimen (Schneemayer *et al.*, 2014)

The wedge splitting test provides only an indirect method to determine the tensile strength. The following equation is used to calculate the notch tensile strength:

$$\sigma_h = \frac{F_h}{A_f} + \frac{M_b}{Z} \quad (3.7)$$

where,

F_h = horizontal splitting force;

A_f = fracture area;

M_b = bending moment acting on specimen;

Z = section modulus.

The advantages and disadvantages of the wedge splitting test are summarised as follows:

Advantages

- Outperforms other tests in terms of frac-

Disadvantages

- Test provides only the indirect tensile

- | | |
|--|--|
| <p>ture mechanics</p> <ul style="list-style-type: none"> • Compact test setup reduces negative effect of self weight • The test can be controlled and monitored very accurately with testing machine • Test provides a stable crack formation for brittle and quasi-brittle materials | <p>strength</p> <ul style="list-style-type: none"> • Most complex test setup with regards to other tests discussed in this section • Construction of test specimens can present challenges |
|--|--|

After considering Sections 3.3.1 - 3.3.3 the crossed-brick couplet test is chosen for the tensile characterisation of the joint interface. The method of determining the tensile strength of the joint interface was considered for each test method, as well as the test's stability in terms of fracture mechanics. Even though challenges are foreseen with determining the tensile fracture energy, this method is the only one providing the direct tensile strength. Challenges have also been encountered in the past by Stone (2017) to characterise the joint interface with the wedge splitting test, at Stellenbosch University.

3.3.4 Concluding Remarks

This section compares the advantages and disadvantages of the crossed-brick couplet test, the bond wrench test and the wedge splitting test. Even though the crossed-brick couplet test is considered as less stable in terms of fracture mechanics this method is chosen for further application in this study. One of the main reason for choosing this test method is its ability to determine the direct tensile strength of the joint interface. Another reason is the simplicity of the test setup and straightforward testing procedure.

The bond wrench test method posed an easy testing procedure, but is discarded due to the fact that the test procedure cannot be force or displacement controlled. The wedge splitting test presented a the most stable test procedure in terms of fracture mechanics, but has a complex test setup. Due to this and a previous study at Stellenbosch University failing to obtain acceptable results from a similar test method Stone (2017), this test is discarded.

3.4 Conclusion

This chapter discussed the tensile and shear characterisation of the joint interface of masonry.

Different available test methods, obtained either from international standards or literature, are discussed to determine the best test methods for obtaining tensile and shear properties of the joint interface of the alternative masonry types investigated in this study. The crossed-brick couplet test and triplet test were chosen as the joint interface tensile and shear tests respectively, for this study. The focus of this study is not based on optimising alternative masonry performance, but rather to obtain specific material properties through specialised testing.

The material properties under consideration in this research are not frequently studied in literature and therefore different test setups are discussed and investigated for obtaining the most accurate results. This chapter concludes which test method is used for further utilisation in this study.

Chapter 4

Materials and Masonry Unit Production

This chapter investigates the properties of the materials used for masonry unit manufacturing in this study. Four types of masonry units were produced for this study from a wide variety of materials. These masonry unit types are concrete (CON), cement stabilised earth (CSE), adobe (ADB) and geopolymer (GEO). The CSE unit, ADB unit and GEO unit are classified as alternative masonry units (AMUs), and the concrete (CON) unit as a conventional masonry unit (CMU), which is used as the benchmark material.

Firstly, the materials used for masonry unit production are characterised in Section 4.1. Secondly, the production process of each type of masonry unit is discussed in Section 4.2. The production process consists of the mix design, mixing procedure, manufacturing process and curing of each unit. Lastly, the mix design and mixing procedure of the mortar used for masonry construction are also covered.

4.1 Materials

The materials used for masonry unit manufacturing include coarse and fine aggregates, binders, an alkaline solution and water. The total amounts of materials needed for the production process were calculated based on mix designs proposed by Fourie (2017). The total amount of masonry units needed was calculated according to the number of units required for all the unit and masonry tests. The amount of materials required for the mortar, to build the masonry prisms, was determined from mortar mix proportions by Shiso (2019).

All the materials were ordered from local suppliers. An excess of approximately 10% was ordered of every material, for trial experiments and unforeseen losses. Literature has shown that different material batches of the same material can lead to different end product results, especially for aggregates (Illampas *et al.*, 2011). Therefore, all the materials were ordered simultaneously to avoid the changes of different material batches.

4.1.1 Aggregates

Seven types of aggregates were used in this study. Five of the aggregate types are known as fine aggregates (sands and clay) and two coarse aggregates (gravels). The fine aggregates consisted of four sands and one clay soil. Three of the four sands were of the same type, locally known as Malmesbury sand, and the other one is termed Phillipi sand. The clay soil is a mixture of, what is locally termed, white and yellow clay. White, yellow and red clay are locally available. The red clay is a type montmorillonite clay and the white, a type kaolinite clay, and yellow a

mixture of the two. White clay has less organic matter and metal oxides, making this clay the preferred clay for this study. However, at the time of conducting this study only a mixture of white clay and yellow clay was available. The clay was obtained from a local brick manufacturer. Two of the Malmesbury sands were used for masonry unit production (coarse Malmesbury sand #1 and fine Malmesbury sand #2) and one for mortar production (fine Malmesbury sand #3). Greywacke 13 mm stone, a type of sandstone, and crusher dust, formed by the mechanical crushing of other stones, were used as the two coarse aggregates. For the proportions of each aggregate in the respective masonry units refer to the mix designs in Section 4.2.

Figure 4.1 gives the gradings of each aggregate, except the 13 mm greywacke stone. None of the 13 mm greywacke stone particles passed the 4.75 mm sieve and, therefore, this grading was left out of Figure 4.1. The grading of the crusher dust and clay soil was accomplished with dry sieving and the others with wet sieving as per SANS 201 (2008). From Figure 4.1 it can be seen that Malmesbury sand #2 is fine (almost all the sand particles went through the 1.18 mm sieve), Malmesbury sand #3 and Phillipi sand are also relatively fine and Malmesbury sand #1 is a bit more coarse. The crusher dust shows the most coarse profile with the best grading, which was expected.

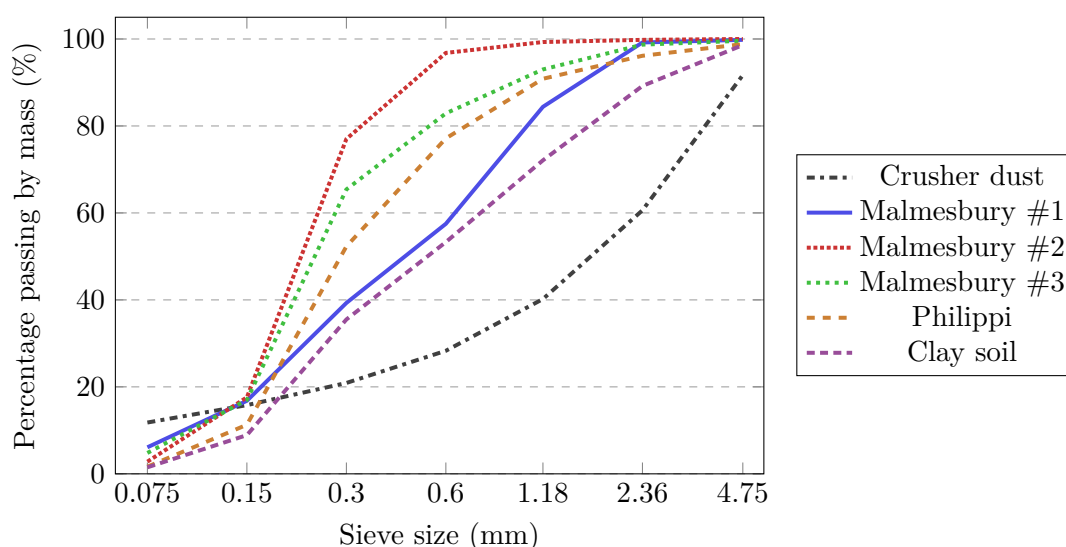


Figure 4.1: Grading of Materials

Figure 4.2 shows the respective sieves after conducting a sieve analysis on Malmesbury sand #3.



Figure 4.2: Sieve analysis of Malmesbury sand #3

The relative density (RD) of each aggregate was determined by performing the Pycnometer test according to SANS 5844 (2006). Figure 4.1 displays the fineness modulus (FM) and dust content of each aggregate obtained from the grading tests, with the respective RD's of each aggregate. The FM of an aggregate is a number that represents the mean size of particles in the aggregate, the lower the FM the finer the aggregate.

Table 4.1: Characterisation of aggregates

Aggregate	FM	Dust content (%)	RD	Particle shape
Greywacke 13 mm stone	-	-	2.74	Angular
Crusher dust	3.42	11.76	2.73	Angular
Malmesbury sand #1	2.03	6.12	2.62	Round
Malmesbury sand #2	1.09	2.78	2.61	Round
Malmesbury sand #3	1.44	4.80	2.61	Round
Phillipi sand	1.73	1.64	2.60	Round
Clay soil	2.42	1.46	2.40	Round

4.1.2 Binders

Five binders were used in this study, of which three were Portland cements and the other two Ulula fly ash (FA) and ground granulated corex slag (GGCS). The following Portland cements were used for production, CEM III 42.5 N for the CON unit, CEM II 52.5 N for the CSE unit and CEM II 42.5 N for the mortar. No additional liquid extenders were used. To ensure the same quality of masonry units in the production process it is important that the binder stays exactly the same for each type of masonry unit produced. To ensure the consistency of the binder, the same suppliers were used for each binder.

The Ulula FA was ordered from Kriel Power Station, a coal-fired power plant in Mpumalanga, South Africa, and the GGCS from Saldanha Steel in Western Cape, South Africa. Ulula FA is a by-product of burning coal and GGCS a by-product of an iron production process. Ulula FA is categorised as ASTM type F FA, due to its low calcium content. Table 4.2 displays the chemical compositions of Ulula FA and GGCS from Saldanha Steel.

Table 4.2: Chemical composition of Fly ash (FA) and Ground granulated corex slag (GGCS) (Fourie, 2017)

Content	SiO ₂	Al ₂ O ₃	CaO	Fe ₂ O ₃	MgO	K ₂ O	MnO	Cr ₂ O ₃	Na ₂ O	P ₂ O ₅	TiO ₂	L.O.I
FA	56.00	29.55	4.61	3.58	1.16	0.89	0.03	0.03	0.21	0.48	1.56	0.36
GGCS	33.27	13.90	35.57	1.19	12.07	0.68	0.07	0.00	0.19	0.01	0.48	-1.48

4.1.3 Alkaline Solution

The alkaline solution used as part of the GEO unit mix consists of sodium hydroxide (SH) and sodium silicate (SS). The SH is originally in pellet form, which is mixed with water in a certain ratio to ensure a specified concentration. When the pellets and water are combined the mixture must be stirred repeatedly until all the pellets have dissolved. This concentration, expressed in Molar, is measured as the amount of SH pellets per litre of water. An exothermic reaction

occurs as the pellets dissolve in water and must be left to cool down before mixing for approximately one to two hours depending on the amount of solution. If the SH solution is still warm at mixing this accelerates the reaction process and decreases the setting time of the mix which can complicate the casting process. The SS is in a thick turbid liquid form and is added in its original state to the mix design.

The SH pellets was ordered from Sigma-Aldrich and the SS from Kimix Chemicals, both companies in the Western Cape, South Africa. The chemical composition of the SH pellets and SS are NaOH and $\text{Na}_2\text{Si}_3\text{O}_7$, respectively. It is important that the needed safety equipment is worn when working with these chemicals, it can be harmful when coming into contact with the skin or eyes.

4.1.4 Water

Water plays a pivotal role in the construction industry around the world. Water is mainly responsible for the hydration process of cement, giving concrete its strength. It is used in all the mixes done in this study, for all the masonry units and mortar. The water content, in most cases, has a direct influence on the unit strength and workability of the mixes in their fresh state.

The GEO unit is the only mix where the amount of water has no real effect on the unit strength, here it only affects the workability of the mix. Local municipal tap water was used for this study and is classified as potable.

4.2 Masonry Unit Production

This section explains the production process of each type of masonry unit. The production process consists of the mix design, mixing procedure, manufacturing process and curing. As stated earlier in Section 4.1, the mix designs adapted in this study were proposed by Fourie (2017). The aim of this study is not to improve the mix designs of Fourie (2017), but rather to produce masonry units with more or less the same properties as those of Fourie, to compare results and further the knowledge on these types of alternative masonry. The gradings of the materials used in this study were compared to the gradings of the materials used by Fourie, to adjust the mix designs and to obtain masonry units of more or less the same overall gradings and mechanical properties as Fourie.

All the aggregates were air dried in open laboratory space until they were completely air dried before being used for production. After mixing the respective materials for each type of masonry unit a manual block press was used for unit manufacturing. All the units were manufactured in the block press except the GEO units. Figure 4.3 displays the block press, this specific block press is manufactured by Hydraform. Hydraform states that the press can deliver pressures of up to 2.9 MPa. The same press used in this study is commercially used for the production of conventional masonry units, therefore, the pressure capacity of this press is a good representative of the compaction energy used in industry.

Figure 4.3 also shows wooden boards used for removing units from the block press that were still soft after extrusion. The block press manufactures masonry units with dimensions, 116 mm high, 140 mm wide and 290 mm long. These dimensions could not be changed and, therefore, the GEO units, which are not produced in the block press, also need to be of the same dimensions. The different experimental setups were constructed in such a manner that they complied to the unit dimensions.



Figure 4.3: Manual block press, from Hydraform, with wooden boards

Reddy (2012) refers to two techniques when considering stabilisation of soil by compaction, which are static and dynamic compaction. The block press in this study uses the static compaction technique. Compaction is one of the most widely known techniques to increase strength and reduce porosity of masonry units (Reddy, 2012). The density of the masonry unit can be directly correlated to the compaction energy, the higher the compaction energy the denser the unit. The compaction energy required was controlled by the weight and volume of the masonry unit in its fresh state before compaction.

Walker (1999) studied the bond characteristics of earth block masonry, but got a wide scatter of results. One of the possible reasons for this scatter in results was varying dry densities of the blocks used in his study. The densities of his blocks varied from 1584 to 1775 kg/m³. Therefore, weight batching was adopted in this study to keep the density of the units constant. Sections 4.2.1 - 4.2.2 refer to the respective production processes of each type of masonry unit produced in this study.

4.2.1 Concrete (CON) Units

The aim of this study is to characterise the tensile and shear properties of the joint interface of alternative masonry. However, it was decided that a benchmark material is needed to which the results of the alternative materials could be compared. The CON unit was chosen to act as the benchmark material in this study. The CON unit is seen as one of the most popular conventional masonry units used for low income housing (LIH) construction in South Africa. Comparing the results from the CON masonry to the alternative masonry, therefore, shows how viable the alternative masonry are as replacement for the CON masonry. Another reason for proposing a benchmark material was to determine if the experimental test setups created for this study functioned correctly and gave acceptable results. Therefore, all experiments were first conducted on the CON masonry to see if the tests functioned properly, and thereafter on the alternative masonry. This would also indicate if standard tests or tests from literature that are conducted on conventional masonry, can be applied to alternative masonry used in this study.

Mix Design

The mix design for the CON unit was adopted from the study of Fourie (2017). The aim of Fourie was to design a CON unit that resemble those used in practice. However, certain changes needed to be made due to the size of the unit and the method of manufacturing. Therefore, Fourie employed the method of Jablonski (1996) to do the mix design of the CON unit. Jablonski uses the FM method to proportion the mix. The mix design of Fourie was taken as the original

mix design for the CON unit, but was thereafter changed by considering the method of Jablonski to obtain a unit with similar material and mechanical properties as obtained by Fourie. The reason for changing the mix proportions of Fourie was due to different gradings of materials. Table 4.3 shows the different FMs of the materials used in this study to those used by Fourie.

Table 4.3: Comparison of aggregate materials in CON Unit

CON Unit Aggregates	FM	
	Fourie	This study
Crusher dust	3.51	3.42
Malmesbury sand	2.33	2.03

Jablonski proposes that the aggregates are blended in certain proportions to obtain a desired FM for a specific class CON unit. Jablonski stated that the industry recommends FMs of 3.70 for normal-weight CON units, 3.67 for medium-weight CON units and 3.84 for light-weight CON units. From the recommended FM values it can be seen from Table 4.3 that the FM values from Fourie and those from this study are too fine to obtain these recommended values. Due to the FM values of this study being less than those of Fourie the proportion of crusher dust in the mix design was increased in an attempt to increase the blended FM. This, however, led to a mix with too little cohesiveness and the CON unit would fall apart after manufacturing. Fourie also experienced problems with the cohesiveness of the mix and this occurred due to the method of forming the units (explained in Section 4.2). He, therefore, replaced 25% of the cement with FA. Materials with high fineness increase the cohesiveness of a mix. If the amount of FA in the CON unit mix was to be increased this could lead to a weaker unit, and therefore the original mix of Fourie was again adapted.

Jablonski proposes a cement to aggregate ratio method rather than a cement to water ratio for determining the cement content of the mix. It is recommended that a ratio of cement to aggregate of between 1:8 and 1:12. A ratio of 1:10 was chosen by Fourie and also for this study. The final step in the Jablonski method is to choose the water content of the mix. Jablonski recommends that the water content is determined through trial batches. The amount of water needed to deliver a good product will vary according to the aggregate type used, the cement content, desired appearance and method of construction.

The same amount of water used by Fourie led to a unit that was too wet and difficult to extrude and remove from the block press. The wet mix also caused the unit to deform when removing the unit from the block press after manufacturing, and some of the mix would stick to the sides of the block press upon demoulding. This was unexpected as finer materials usually need more water to reach the same level of workability. Less water added to the mix produced a workable mix with a desired appearance after manufacturing. This mix still allowed the unit to be compacted with relative ease, which is usually where problems occur with drier mixes.

A possible reason why less water was needed for the CON unit mix was due to the change in cement. A CEM II 42.5 N cement was used by Fourie and a CEM III 42.5 N was used in this study. CEM III cement has more extenders than CEM II cement, and CEM III is a blast furnace cement meaning that the main extender replacing cement is ground granulated blast-furnace slag (GGBS). One of the technical advantages of extenders is that the mix design requires less water (Concrete Society of Southern Africa, 2019). Similar to FA, less water is required when GGBS is added to a mix. Generally approximately 3% less water is required in comparison to ordinary

portland cement (OPC) for an equal slump and workability of the wet mix (Khan *et al.*, 2014). Owens (2009) suggests that the water content for a CON masonry unit is generally between 6 and 9% of the mass of the unit. The optimum water content for this study was determined as 8.4%. Table 4.4 shows the mix proportions used for the CON unit in this study.

Table 4.4: Mix design of CON unit

Constituents	kg/m ³
Crusher dust	607
Malmesbury sand #1	1316
CEM III 42.5 N	144
FA	48
Water	193
Total	2308

Mixing and Manufacturing Procedure

The materials for the CON units were mixed in a 50 L pan mixer. The dry materials and water were weighed off in such proportions that the wet mix would result in a 32 L mix. First, the aggregates and binders (dry materials) were mixed until a homogeneous mix was obtained, this took approximately 2 minutes. Then the water was added to the mixture and mixed until the water was evenly distributed, which took another 2 to 3 minutes.

The units were then weight batched from the wet mix into small steel bowls and taken to the block press. The wet 32 L mix allowed for eight units to be weighed off from one mix. Figure 4.4 displays the CON material after being weight batched from the wet mix. A weight of 10.5 kg was adapted from the study of Fourie (2017) for a single CON unit. This amount of CON could be compressed in the block press with relative ease and delivers a unit with satisfactory appearance. The material in each steel bowl was placed in the block press mould layer by layer with a scoop and levelled with a trowel (see both in Figure 4.4), to ensure a uniform distribution of CON in the block press, especially in the mould corners where voids tend to occur if this process is not followed.



Figure 4.4: CON units weight batched into steel bowels on a trolley

Problems were encountered with moving the units from the block press to a storing location. An advantage of compressed earth is the clay content of the earth mix which helps to hold the shape of the unit after being compressed. The CON unit does not have any clay in its mix and therefore the mix is quite brittle after compaction and, if not handled with extreme care, can be damaged easily. Two wooden boards were developed to enlarge the contact area when handling the units. These wooden boards, see Figure 4.3, allowed handling of the units with enough care to move them from the block press without breaking. Two wooden moulds, also shown in Figure 4.3, were developed to ensure the units were in their original shape after the moving process.

Curing

After the CON units were removed from the block press they were stored on tables in open laboratory space for one day, whereafter they were moved into curing tanks filled with water. The water in the curing tanks was kept at a constant temperature of 25 °C. The CON units were left to cure in the curing tanks for 28 days, then they were moved and stored in open laboratory space until testing or masonry construction. Figure 4.5a and 4.5b shows stored CON units directly after manufacturing, and a CON unit after being cured for 28 days in the curing tanks and dried in the laboratory air.



(a) CON units stored in laboratory air



(b) CON unit after curing

Figure 4.5: Curing process of CON unit

It can be seen from Figure 4.5b, that the CON unit looks similar to the "maxi-block" from Figure 2.1a. The CON unit has larger voids than the "maxi-block" and this can be attributed to the method of manufacturing the units with the block press.

4.2.2 Geopolymer (GEO) Units

GEO differs greatly from any conventional building material. Where the strength of conventional concrete is dependent on the water:cement ratio, the strength of GEO concrete is dependent on a lot of different factors. These factors are elaborated on in Table 2.2 of Section 2.3.3. Due to the complex nature of the GEO material a lot of time can be spent on optimising the mix design. This, however, was not the focus of this study and a mix design was rather adopted from previous studies conducted at Stellenbosch University that produced a GEO masonry unit with a strength close to that of the CON unit. The mix design procedure of Fourie (2017) was considered for this study.

Mix Design

Due to numerous factors influencing the strength of GEO concrete, a straight forward mix design procedure is not available, as in the case of conventional concrete. The mix design of Fourie (2017) is obtained from a study conducted on alkali-activated concrete (AAC) at Stellenbosch University by Barnard (2014). Fourie modified one of the mixes proposed for AAC by Barnard to obtain his final mix design. An overview of the mix design procedure of Barnard is discussed in Section 2.3.3. Fourie (2017) aimed at designing a GEO unit that could be cured at ambient temperatures and is cost-effective. These attributes were also aimed for in obtaining the mix design for this study.

The constituents of the GEO unit included aggregates, binders, an alkaline solution and water. The mix design used by Fourie produced a mix with no workability in trial mixes. Therefore, a trial and error technique was adopted until a mix of adequate workability and strength was obtained. The factors influencing the strength of AAC proposed by Barnard and the available materials in the laboratory were taken into account while designing the new mix. After a number of trial mixes an acceptable mix was obtained that was workable enough for six units to be cast before the mixture was too dry to use. The aim of the GEO mix design was not to obtain the optimum GEO unit, but due to the time sensitivity of the fresh mix while casting, the aim was rather to find a mix design with adequate workability.

Key findings from the trial mixes included that an increase in the sodium hydroxide solution (SHS) to SS ratio gave a more workable mix with an acceptable setting time. It was also concluded that an increase in SS initially also increases the workability of the mix but decreased the setting time. Less water was needed for this mix to still produce a workable mix. This could be attributed to less binder materials (FA and slag) used in this mix than in the mix of Fourie (2017). Literature states that the only reason for adding water to the mix is to ensure the workability of the fresh mix (Davidovits, 1994; Hardjito *et al.*, 2005).

Fourie also encountered workability issues, therefore, it is proposed that further research is conducted to develop mix designs that stay workable longer. Table 4.5 compares the desired factors of constituent proportions proposed by Barnard to the factors obtained from the final mix of Fourie to the final mix used in this study.

Table 4.5: Factors that influence AAC strength of the mix used in this study

Factors that influence the strength of AAC	Barnard (2014)	Fourie (2017)	This study
Sodium silicate to sodium hydroxide ratio	0.6 to 2.5	1.8	0.78
Fine aggregate to total aggregate ratio	0.50	0.4	0.41
Alkaline to binder ratio	0.55	0.22	0.36
Binder to sand ratio	0.85 to 1.10	1.14	0.64
Slag content	20%	23.10%	4%
Aggregate content	60%	62%	42%
Sodium hydroxide solution	3 - 6M	4M	6.4M
Percentage alkaline liquid replaced by water	25%	30%	40%

Table 4.6 gives the final mix proportions used for the GEO units in this study. Malmesbury sand #1 was used as the fine aggregate, and even though considerably less slag was used, the stronger concentration of SHS still allowed the mix to set at ambient temperatures.

Table 4.6: Mix design of GEO unit

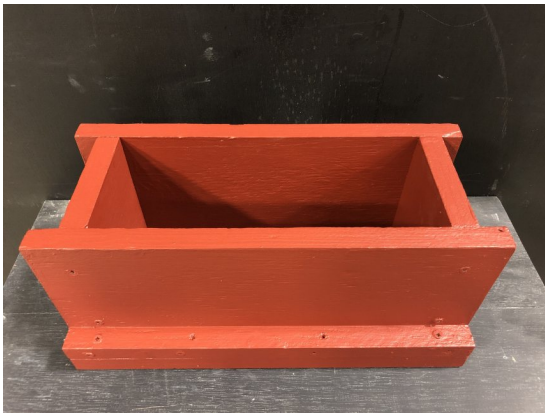
Constituents	kg/m ³
Greywacke 13 mm stone	1000
Malmesbury sand #1	700
FA	350
Slag	100
SS	70
SHS	90
Water	88
Total	2398

Mixing and Manufacturing Procedure

The GEO mix was conducted in a 50 L pan mixer. Each mix consisted of a 30 L GEO material mixture. The mixing procedure of the different GEO materials is important and this is mainly due to the reaction characteristics of the alkaline solution. It is important that the materials are added in a specific order, otherwise the reaction of the alkaline solution with the binders could cause the mix to set too rapidly. First the SHS solution is prepared and left to cool for between 1 and 2 hours, depending on the size of the mix. Once water is added to the SH pellets, an exothermic reaction takes place, which heats up the solution. If this solution does not cool down for at least an hour and a half before adding it to the rest of the GEO mixture, its reaction with the SS causes the hardening reaction of the mix to happen more rapidly, not leaving enough time to cast the fresh GEO material. Once the SHS has cooled down the dry material was added to the pan mixer and mixed for approximately 2 minutes. The alkaline solution was then added in a specific order. First the SHS was added slowly over a period of 2 minutes, thereafter the SS was added for approximately the same period of time. Lastly, the water was added and mixed until a homogeneous mix was reached.

The GEO material was found to set quickly, so as soon as the mix reach homogeneity the material was immediately cast into the wooden moulds. Each wooden mould was designed to deliver a masonry unit of dimensions 116 mm high, 140 mm wide and 290 mm long, the same dimensions as the units extracted from the block press. Refer to Figure 4.6 to see (a) the wooden moulds used for casting the GEO units and (b) six wooden moulds and a cylinder filled with GEO material on the vibration table.

After casting, the GEO units were vibrated on a vibration table to remove all the air bubbles from the mix. Care was taken not to over vibrate the units, as this caused the greywacke stones to segregate from the mix. The cylinders were cast for the modulus of elasticity test, normal conventional cylinder moulds were used for this. Cylinders were only cast for the GEO units and not for the other alternative masonry units (AMUs) and CON units. This is further elaborated on in Section 5.1.2.



(a) Wooden mould for casting GEO unit



(b) Six GEO units and cylinder on vibration table

Figure 4.6: Mixing procedure of GEO unit

Care was taken throughout the whole process of working with the alkaline solution, from mixing the SHS to casting the GEO units into the wooden moulds, due to the corrosive and irritant nature of the SHS and SS. Appropriate safety equipment was worn at all times to avoid contact of the mix with the skin or eyes. The health concerns associated with the GEO material can cause problems if this material is to be introduced on the housing market. More research would need to be done in this area on how this could be dealt with.

Curing

Usually FA is the only binder included in a GEO material mix and heat curing is required for the material to set (Davidovits, 2008). This, however, would defeat the purpose of obtaining the AMUs with a low embodied energy. Therefore, slag was introduced in the mix, allowing the mix to cure at ambient temperatures.

After casting the mix the wooden moulds and cylinders were stored in open laboratory space for the mixture to dry in the moulds for one day. Thereafter the units and cylinders were demoulded and moved to a curing room with a constant temperature of $24 \pm 2^\circ\text{C}$ and $65 \pm 5\%$ relative humidity. The units and cylinders were left in the curing room until used for testing or masonry construction. Figure 4.7 shows a GEO unit after curing for 28 days.

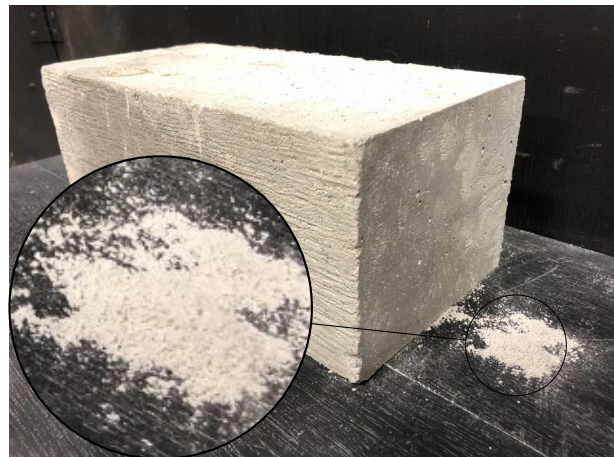


Figure 4.7: GEO unit after curing

Efflorescence was noticed on the surface of the GEO units while curing. Efflorescence is the formation of white salt deposits on the surface of concrete and is generally harmless (Pachecotorgal *et al.*, 2012). However, for GEOs, as they contain a much higher soluble alkali content than conventional concretes, this can be a significant issue. Especially when the GEO is exposed to humid air conditions or water. Ways to mitigate or reduce efflorescence are to cure GEOs at elevated temperatures or to add slag to the mix design. The first suggestion would, however, defeat the purpose of low embodied energy AMUs. It is also stated that adding slag to the mix design only reduces the initial formation of efflorescence, but over the long term efflorescence potential could be equivalent to a 100% fly ash activated geopolymer (Zhang *et al.*, 2013). This phenomenon was also observed by Shiso (2019). The units in this study, however, showed less of the substance than in the study of Shiso. The reason for this can be attributed to the differences in the mix design. A different batch of Malmesbury sand and amount of water content was used for this study, than by Shiso. Figure 4.8 displays (a) the efflorescence on the surface of the unit and (b) the unit after being brushed by a hand brush. All the units were cleaned with a hand brush before testing and construction.



(a) Crystal-like substance on surface of GEO unit



(b) Cleaned GEO unit

Figure 4.8: Crystal-like substance brushed of GEO unit

4.2.3 Cement Stabilised Earth (CSE) Units

The mix design of Fourie (2017) was also adopted for the CSE units. Fourie (2017) followed the mix design procedure from a previous study conducted at Stellenbosch University by Malherbe (2016). The aim of the mix design by Malherbe (2016) was to manufacture a block that is similar to blocks used in the housing construction industry in South Africa.

Mix Design

The mix design of Fourie (2017) included two type of aggregates, sand and a clay soil. The same aggregates were used for this study which consisted of Phillipi sand and a white-yellow mixed clay soil. The Phillipi sand is a bit coarser than the one used by Fourie, the FM of the Phillipi sand used in this study is 1.73 and the one used by Fourie (2017) 1.17, even though both sands came from the same quarry and local supplier. This confirms the finding of Illampas *et al.* (2011), showing that different material batches of the same material can lead to different end product results. Reddy and Gupta (2006) proposed that sandy soils is best suited for earth-cement blocks, Reddy and Gupta proposed a clay soil to sand mixture of ratio 1:2. This supports the mixing proportions of the clay soil and Phillipi sand used by Fourie.

The clay soil was obtained from a local brick manufacturer. The clay was already crushed by the local supplier, but still contained a number of clumps in and was still moist. The clay was spread out on the laboratory floor and left to dry for a few days. After the clay was air dried, a mechanical roller was used to crush the small lumps that was still in the clay. The clay was seen as air dry when no moist patches could be seen on the laboratory floor after the clay was removed. The clay was then sieved through a 2.36 mm sieve to ensure the clay is fine enough to provide an acceptable mix.

The same binder used by Fourie was also used in this study, CEM II 52.5 N cement. Reddy and Gupta indicate that a cement content in the range of 6-10% is generally used to manufacture earth-cement blocks for use in load bearing buildings of up to three stories. A cement content of 8.4% by mass of the total mix was used as the binder. To obtain the water content of the mix design, the optimum moisture content (OMC) of the dry materials was determined by a method proposed in SANS 3001-GR30 (2015). The maximum dry density and OMC can be obtained from this method.

Figure 4.9 shows the results of this method in graph format. From Figure 4.9 it can be seen that the maximum dry density of the CSE unit is 2050 kg/m³ and the OMC 8.4%. It should be noted that this method of determining the OMC uses dynamic compaction, where the method of manufacturing the units in this study uses static compaction. This caused the mix with OMC to be too dry when compacted in the block press. A water content of 9% of the mass of the dry materials gave an acceptable unit after compaction.

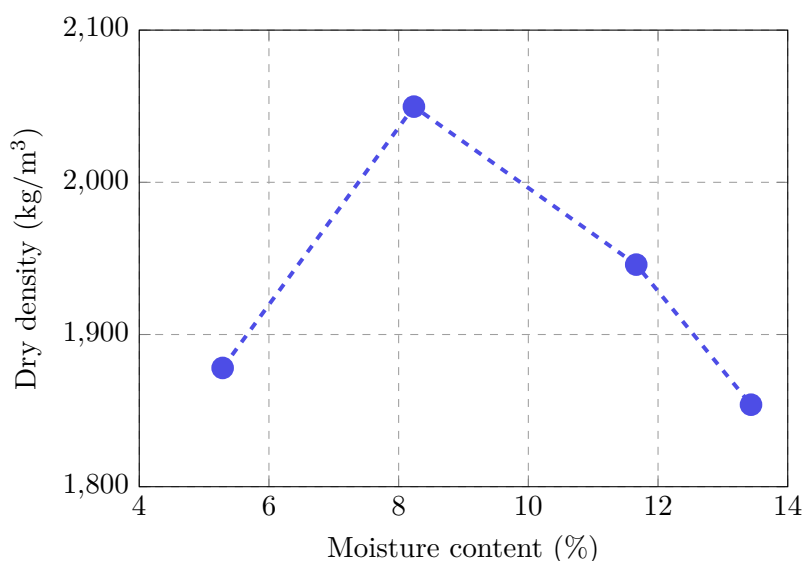


Figure 4.9: The maximum dry density and OMC of the CSE unit as per SANS 3001-GR30 (2015)

Even though the Phillippi sand is finer than the one used by Fourie, the proportion of Phillippi sand proposed by Fourie was still kept the same for this study. The end product showed a masonry unit that held its shape well, was demoulded easily from the block press and was well compacted. Table 4.7 shows the mix proportions used for the CSE unit.

Table 4.7: Mix design of CSE unit

Constituents	kg/m ³
Phillipi sand	1198
Clay soil (2.36 mm)	798
CEM II 52.5 N	200
Water	198
Total	2394

Mixing and Manufacturing Procedure

The production process of the CSE unit was nearly the same as the CON unit. First the dry materials were mixed in the 50 L pan mixer for around 2 minutes and then the water was added and mixed for another 2 to 3 minutes. The dry materials and water were again weighed off in such proportions that the wet mix resulted in a 32 L mix, allowing eight units to be weighed off from the mix.

A 32 L mix was the largest mix that could be made, of the CSE material, in the 50 L pan mixer. The clay started to swell upon adding the water causing the mixture to fill the whole 50 L pan. A problem that occurred while mixing was that clumps formed when the water was added, due to the clay content in the mix. After mixing, most of the clumps were broken up by hand and then the mixture was mixed again for one minute to ensure an even distribution of the broken clumps.

The units were weight batched from the moist mix in quantities of 9.4 kg. This amount was adopted from the study of Fourie and gave a unit that could be compressed in the block press with ease and produced a unit with satisfactory appearance. The CSE material was placed in the block press layer by layer with a scoop and after each layer the mixture was levelled with a trowel. The CSE unit held its shape well and could be moved from the block press to the storing location by hand. Figure 4.10 shows the CSE unit in the block press after demoulding.



Figure 4.10: CSE unit after demoulding

Curing

After moving the CSE units from the block press, they were stored on tables in open laboratory space. Immediately after storing, the units were covered with polythene sheets. The polythene sheets were held in place with small weights which prohibited air movement over the units and sealed the units off preventing the units from drying out quickly.

As part of the curing process the units were sprayed with a water spray bottle every 24 hours, until each unit was completely covered with a layer of moisture. This continued for 7 days, each time again covering the units with the polythene sheets after spraying (this process is also explained in Section 2.3.2). This allowed for proper hydration of the cement particles in the mix. After 7 days the units were moved to a curing room with a constant temperature of $24 \pm 2^\circ\text{C}$ and $65 \pm 5\%$ relative humidity. The units were left in the curing room until used for testing or masonry construction. Figure 4.11 displays (a) the CSE units after storing them in open laboratory space, (b) the CSE units after covered with polythene sheets and (c) a CSE unit after curing for 28 days after manufacturing.



(a) CSE units stored in laboratory air



(b) CSE units covered with polythene sheets



(c) CSE unit after curing

Figure 4.11: Curing process of CSE unit

4.2.4 Adobe (ADB) Units

The aim of the ADB unit was to create a unit that somewhat replicates the type of mud-brick sometimes used to build houses in more rural parts of South Africa. The ADB unit does not have a specific type of mix design and the materials used for ADB unit construction in industry, or in local communities, varies a lot.

Usually natural soils that are available near the build site are selected and used for manufacturing the unit. Also explained in Section 2.3.1, ADB units are generally produced through filling "ladder-like" wooden moulds with ADB material by hand until the mould is full. Immediately after filling the moulds, the units are demoulded and left in the sun to dry. This method of manufacturing ADB units leads to units with varying densities, due to the compaction pressures not being kept constant. Available natural soil was not used in this study for ADB unit manufacturing, an ADB unit with constant mix proportions and density was rather developed for the reason of obtaining more reliable results that can be used for comparison against the other AMUs. The mix proportions were kept constant by choosing aggregates available from the laboratory to develop a replicate type of ADB unit. The mix was weight batched and compressed with the block press to keep the density of the units constant.

Mix Design

The mix design of Fourie (2017) was adopted for the ADB mix. However, this exact mix gave an ADB unit with a large number of voids. Voids usually indicate that the mixture is too wet. Even though the units were exactly the same weight, coarser materials can cause the mix to be more wet. The more fine material there is in a mixture the more water is needed to produce a mix with the same workability. Therefore, coarser materials need less water to produce a mix with the same workability. The exact same mix showed a higher combined FM than the one from Fourie.

Table 4.8 shows the combined FM for the ADB unit for Fourie and this study for the original mixing proportions of the mix design of Fourie. It can be seen from Table 4.8 that the mix from this study has less fines than the one by Fourie. This would predict a wetter mix if the same mix proportions are used.

Table 4.8: Combined FM of ADB Unit

CSE Unit Aggregates	FM	
	Fourie	This study
Malmesbury sand	2.33	2.03
Phillipi sand	1.17	1.73
Combined	1.75	1.88

A finer sand, Malmesbury sand #2, was introduced into the mix. This sand made provision for the coarser aggregates and brought the combined FM down to an acceptable value. Malmesbury sand #1, Malmesbury sand #2 and the Phillipi sand each contributed to a third of the sand aggregates in the mixture. Figure 4.12 compares the combined gradings of the first ADB mix design (without Malmesbury sand #2) and the final ADB mix design (with Malmesbury sand #2). It should be noted that the clay soil is not included in these mixes. From Figure 4.12 it can be seen the the new ADB mix showed more fine aggregates, this caused the FM of the mix to be lower.

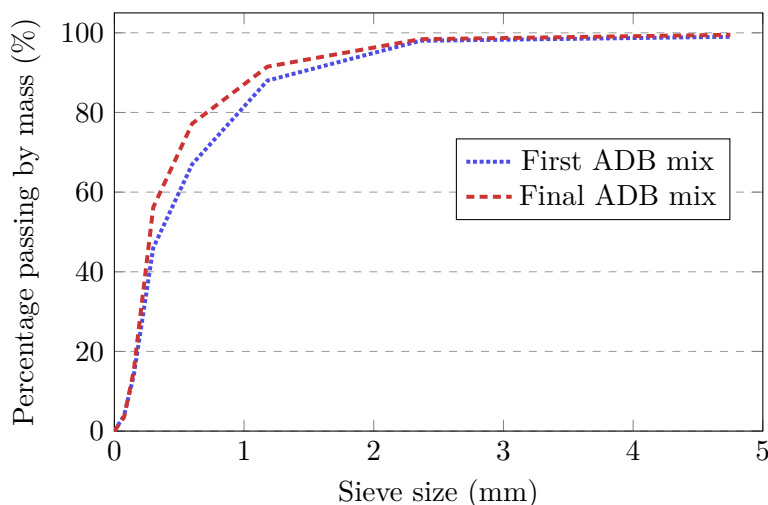


Figure 4.12: Combined gradings of first ADB mix design vs new ADB mix design

The clay soil acted as the binder in the ADB mix and, therefore, the strength of the unit is greatly dependent on how well the clay binds with the other aggregates. For this reason the clay was sieved through a 1.18 mm sieve, to ensure a fine clay soil of good quality. The water content of the mix was obtained through trial and error. A water content producing a well compacted unit that held its shape was desired. The optimum water content was found to be approximately 6% of the mass of the unit. Table 4.9 shows the mix proportions used for the ADB unit.

Table 4.9: Mix design of ADB unit

Constituents	kg/m ³
Malmesbury sand #1	539
Malmesbury sand #2	539
Phillipi sand	540
Clay soil (1.18 mm)	534
Water	145
Total	2412

Mixing and Manufacturing Procedure

The production process of the ADB unit was also similar to the CON and CSE units. A 32 L mix, consisting of dry materials and water, was weighed off and mixed in the 50 L pan mixer. The dry materials were first mixed in the 50 L pan mixer for approximately 2 minutes. Thereafter, water was added and the mixture was further mixed for another 2 to 3 minutes. The ADB mix gave the same problem as the CSE mix, the clay content caused clumps to form in the mix. The clumps, however, showed a similar mixture inside the clumps as in the rest of the mixture as they were broken. Therefore, time was only spent on breaking the large clumps.

After mixing, eight units were again weight batched from the moist mixture. A total of 9.4 kg was weighed of for each unit, this amount was adopted from Fourie (2017), and showed an acceptable unit after compaction. Figure 4.13(a) and 4.13(b) shows the process of placing the mix into the block press mould with the scoop and trowel and the unit after extraction from the block press.



(a) Manufacturing process of the ADB unit



(b) ADB unit after extraction from the block press

Figure 4.13: Manufacturing procedure of ADB unit

Curing

The curing process of the ADB is the simplest of all the AMUs in this study. The ADB units held their shape well and were, therefore, moved by hand from the block press to a storing area. Once the units were moved to a storing area, they were left there to cure until used for testing or masonry construction. The storing area was located inside the laboratory.

Some literature suggests that after manufacturing, the units should be cured outside in the sun (Pacheco-Torgal and Jalali, 2012). However, to avoid the inconsistent weather conditions in the winter in the Western Cape area, the units were cured inside the laboratory. Figure 4.14 shows (a) ADB units while being cured in open laboratory space and (b) one ADB unit after being cured for 28 days.



(a) ADB units left to dry in the laboratory



(b) ADB unit after curing

Figure 4.14: Curing process of ADB unit

4.3 Mortar Design

Mortar plays an important role in the bond strength of the joint interface of masonry. The bond strength of the joint interface of masonry usually governs the strength of the masonry in tensile and shear (Lourenço, 1998). The focus of this study is to characterise the tensile and shear properties of the joint interface of alternative masonry. The crossed-brick couplet test and triplet test were conducted on small masonry prisms with different geometries to characterise the interface.

Mortar was used to build the masonry prisms for both tests. Two mortars are compared in this study, a weaker and a stronger mortar of approximately 7 MPa and 20 MPa. The 7 MPa and 20 MPa mortar are further referred to as 7M and 20M in this study. These strengths are the 7-day characteristic strength of the mortar. All of the masonry tests were conducted on 7 days \pm 1 day from construction.

Even though a number of researchers have concluded that cement-soil and cement-lime mortars outperform normal cement-sand mortar in terms of bond strength (Reddy and Gupta, 2006; Rao *et al.*, 1996; Sarangapani *et al.*, 2005; Walker, 1999), both 7M and 20M are cement-sand mortars. The reason for selecting cement mortars was fourfold. Firstly, the aim of this study is not to design a mortar that gives the highest bond strength, but rather to compare the characteristics of the joint interface of different alternative masonry. Secondly, for comparison purposes (all previous studies in this specific field of alternative masonry conducted at Stellenbosch University used cement mortars). Thirdly, due to availability of materials at the time of the study. Lastly, cement-sand mortars are typically used in the LIH industry in South Africa.

It should be noted that mortars with compressive strengths as high as that of 20M is not commonly used in industry and 7M presents a better and more common replica of what is used in industry. The reasons for selecting these two mortars are as follows. The South African standard, SANS 10145 (2011), proposes a Class II mortar for normal load bearing applications for walls exposed to severe dampness. The strength of this mortar is 5 MPa. This mortar was first adopted for this study and due to a better workability in its fresh state a 7 MPa mix design was adopted. The Eurocode, EN 1996-1 (2005), allows mortars between 2 and 20 MPa. A mortar was desired with a similar strength than that of the strongest masonry unit from this study and to compare the difference in results from the joint interface tests for mortars with different compressive strengths. Therefore, the second mortar that was adopted for this study has a 20 MPa mix design.

Table 4.10 shows the mix proportions of 7M and 20M. A fine sand, Malmesbury sand #3, was used as the aggregate in the mix, providing structural stability to the mix, and the binder that was used is CEM III 45.5 N cement. The reason for selecting Malmesbury sand for the mortars in this study and not Phillipi as in the study of Fourie (2017) and Shiso (2019) was due to Malmesbury sand being the preferred sand used by masons for masonry construction in the Western Cape area. Phillipi sand is more popular for use in plaster mortars, for plastering masonry structures. A parameter that was kept constant throughout the study was the flow value of both mortars. A constant flow value of 100% was adopted for 7M and 20M for all the tests conducted in this study. Refer to Section 5.2.1 for the definition of the flow value as a percentage.

Table 4.10: Mortar mix proportions

Constituents	Proportions	
	7 M	20 M
CEM III 42.5 N	1	1
Malmesbury sand #3	5.08	2.77
Water	1	0.61

4.4 Conclusion

This chapter investigated the properties of the materials, namely grading, FM, dust content and RD, used for masonry unit manufacturing in this study. The production process of each type of AMU and CON unit is discussed which consists of the mix design, mixing procedure and curing.

The respective AMUs that are covered are the CSE unit, ADB unit and GEO unit. The benchmark CMU discussed is the CON unit. Mix designs were adopted from previous research at Stellenbosch University and adapted to available materials to replicate the four masonry unit types and mortar. The focus of the study is investigating test setups for the tensile and shear characterisation of the joint interface for these four AMUs. Chapter 5 discusses the experimental design adopted for this study.

Chapter 5

Experimental Procedure

To further the field of knowledge of alternative masonry, the characterisation of the masonry mechanical properties is necessary. Certain properties, namely the tensile and shear properties of the masonry joint interface, are focused on to avoid duplication of previous research. Therefore, tensile and shear tests on the joint interface, as well as companion tests on individual masonry units and the mortar are conducted. The aim and second objective of this study is to characterise the tensile and shear properties of the joint interface of masonry. Therefore, tensile and shear tests are conducted on the joint interface of masonry, as well as, companion tests on the individual masonry units and mortar for quality control.

Before discussing the experimental procedure, this chapter considers relevant literature and international standards and how they recommend these tests are carried out. Tests from both the South African National Standard (SANS) and European Norm (EN) are mainly considered in this study. Tests from the American Section of the International Association for Testing Materials (ASTM) are considered if the previous standards do not provide a suitable test. The EN, however, is mostly considered for this study since South Africa is in the process of adopting Eurocode 6, SANS is then considered and then the ASTM. If none of these standards provide a suitable test method, tests from literature are considered.

The experimental setup and testing procedure adopted in this study, to characterise the masonry units, mortar used for masonry construction and the tensile and shear properties of the joint interface, are covered in this chapter. The compressive strength, modulus of elasticity, dry density, water absorption, surface roughness, direct tensile and triplet tests are detailed in this chapter, as well as the flow value, dry density, flexural and compressive strength tests conducted on the two mortar types. The testing schedule of this study was conducted as follows. First, each test was applied on the concrete (CON) material which acted as the benchmark material in this study. Thereafter, on the geopolymer (GEO), the compressed stabilised earth (CSE) and lastly the adobe (ADB) material.

5.1 Masonry Unit Tests

This section details the experimental procedure for characterising the mechanical properties of each type of masonry unit used in this study. The tests considered are referred to as companion tests, which are used to ensure that the masonry units used throughout this study stay consistent (of the same quality) and for comparison (in following chapters) against research studies previously conducted at Stellenbosch University and in literature.

The test specifications proposed by international standards, or literature, are first considered for each test, after which the experimental procedure followed for each test is discussed. The

tests investigated are the compressive strength, modulus of elasticity, dry density and water absorption tests. A technique for determining the surface roughness of the respective masonry units is also discussed.

5.1.1 Compressive Strength Test Specifications

The European testing standard, EN 772-1 (2011), specifies a method for determining the compressive strength (f_c) of masonry units.

According to the code, the specimens are tested in the orientation specified. Two orientations are usually specified and these are, bedface and headface. Surface preparation is also important. Grinding and capping are two proposed methods for the surface preparation regime specified in EN 772-1 (2011). According to the surface preparation regime specifications of EN 772-1 (2011), a tolerance of 0.1 mm in any 100 mm are accepted, where the top and bottom planes of the unit are parallel to each other. The standard specifies that a minimum of six specimens should be tested, and the average of these tests are the compressive strength of the unit.

The specimen is conditioned to a specified regime of moisture condition. Four types of conditioning regimes are defined by the standard. These are, conditioning to the air dry condition, to the oven dry condition, to a 6% moisture content and by immersion. For all these conditioning regimes, except conditioning by immersion, free air circulation around each specimen is ensured. The gross area of the surface loaded during testing is determined in square millimetres. The length and width of the loaded area is multiplied to obtain the gross area. The standard also presents a method for calculating the net loaded area, but this is disregarded in this study due to all the units tested being solid units.

The testing procedure specified by the standard is as follows. Wipe the bearing surfaces of the testing machine and the bed face of the specimens, removing any loose particles from the specimens and grit from the testing machine. The loading rate specified is in $\text{N}/\text{mm}^2/\text{s}$, so that failure of the specimen occurs in not less than approximately 1 min. The maximum load achieved must be recorded and this load is used to calculate the strength.

The standard specifies that the strength of each specimen is calculated by dividing the maximum load with the gross loaded area and expressed to the nearest $0.1 \text{ N}/\text{mm}^2$. The compressive strength is calculated as the mean value of the strengths of all the individual specimens tested, also to the nearest $0.1 \text{ N}/\text{mm}^2$. The coefficient of variation (COV) is also determined and presented.

EN 772-1 (2011) also presents an informative Annex A, for determining the normalised compressive strength (f_{nc}) of masonry units for design application. To obtain the normalised compressive strength, the air-dry compressive strength is multiplied by a shape factor (d). The shape factor allows for dimensions altered by surface preparation and accounts for the aspect ratio effect, this removes the restraint factor and converts results to unconfined strengths (Morel and Walker, 2007). Table A.1 in EN 772-1 (2011) represents a method for determining the shape factors for different size masonry units. The width and height (after surface preparation) of the specimens should be known to calculate the shape factor.

Compressive Strength Test

The procedure presented by EN 772-1 (2011) was followed to determine the compressive strength of individual masonry units in this study and was also used by Fourie (2017) and Shiso (2019) in their respective studies, of which this study is an extension. The units were tested in bedface

orientation at a curing age of 28 days. A total of ten units were tested of each masonry unit type to represent an average of the particular masonry group created. These units were taken from the group in such a manner that they represent the whole group well, a unit was taken from every second batch of eight units that was manufactured. For the GEO units a unit was taken from every third batch of six units manufactured.

The masonry units were ground with an industrial grinder produced by MATEST on the top bedface surface of the units. Figure 5.1 shows a GEO unit placed inside the grinder before starting the grinding process. All the alternative masonry units (AMUs) and CON units tested were ground, except for the ADB unit. The ADB units were so soft that grinding led to large voids forming on the surface of the unit. A large ball joint was rather used for testing, to account for any inequalities of the top bedface surface of the ADB units.

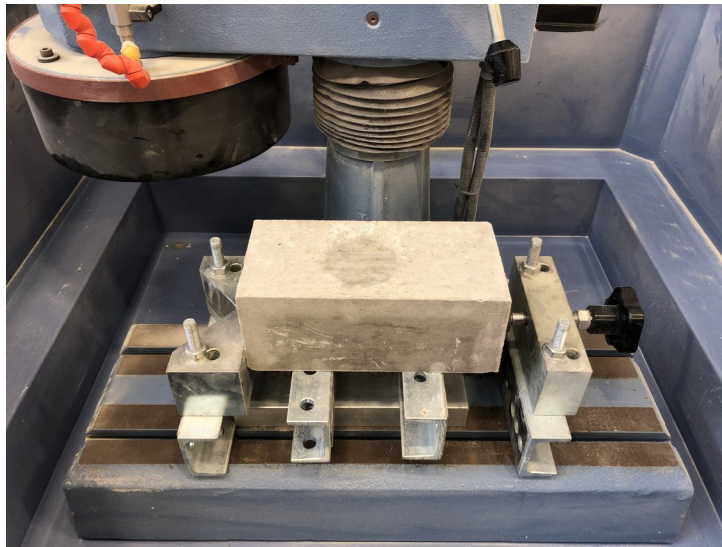


Figure 5.1: GEO unit in industrial grinder from MATEST

All the masonry units were conditioned to the air dry condition prior to testing. The reason for adopting this conditioning regime was twofold. Firstly, the ADB units could not be immersed or wetted. Upon immersion the ADB unit completely dissolves due to the absence of cement binder in the mix design, refer to Figure 5.9 to see an example of this. Secondly, to ensure that the different type units are all tested under exactly the same conditions. This would allow for easier comparisons between the materials.

The loaded area was calculated by measuring the width and length of the units after surface preparation. This area stayed constant for most units created by the block press. Some GEO units, however, had varying lengths due to the ageing of the wooden moulds. The testing machine used for this test is a 2 MN Instron Materials Testing Machine (IMTM). The tests were conducted with displacement controlled loading and not force controlled loading as indicated by EN 772-1 (2011). A loading rate of 0.75 mm/min was chosen for all the tests. Such a slow loading rate was chosen due to the weak nature of the ADB unit. This loading rate led to failure of the ADB unit after a minimum of 1 min, as required per EN 772-1 (2011). To stay consistent and allow comparable results this loading rate was used for all the masonry units. The test was stopped when the applied load decreased by 25% of the maximum load.

Figure 5.2 shows a CSE unit placed in the centre of the test setup prior to testing. Steel plates were used to ensure an even distribution of load unto the unit while testing.



Figure 5.2: CSE unit in compressive strength test setup

For each test the maximum load from the 2 MN Instron and the loaded area of the unit were recorded. The maximum loads with the shape factor were used in the next chapter to determine the normalised compressive strength of each type of masonry unit.

5.1.2 Modulus of Elasticity Test Specifications

The modulus of elasticity, also known as Young's modulus (E), is a value that gives an indication of the stiffness of a material. If the stiffness is known the stresses developing inside a material, when it experiences strain, can easily be calculated by using the well-known stiffness-displacement relationship. Hereby, material failure can be predicted under strains. A method of successive loading cycles is normally used to determine the stress-strain relationship of materials (Domone and Illstone, 2001).

Masonry is not an ideal elastic material. The non-homogeneous nature of masonry and the varying stiffness's at the joint interface results in a non-linear stress-strain curve. Two different types of elastic modulus values can be defined from the non-linear stress-strain curve. One, the tangent modulus measured as the slope of the tangent to the stress-strain curve. Two, the secant modulus measured as the slope of a line between the origin and a point on the stress-strain curve, normally between 33 to 40% of the ultimate strength of the material (Domone and Illstone, 2001). Most international standards provide a method for determining the secant modulus of elasticity, and therefore only this method is considered for this study.

The European testing standard EN 12390-13 (2013) specifies a method for determining the secant modulus of elasticity on test specimens that are cast or taken from a structure. The test method allows the determination of two secant moduli of elasticity, the initial modulus of elasticity ($E_{C,0}$) and the stabilised modulus of elasticity ($E_{C,S}$). EN 12390-13 (2013) provides two methods to determine these moduli of elasticity of a specimens, Method A and Method B. Method A determines both the $E_{C,0}$ and $E_{C,S}$, where Method B only determines the $E_{C,S}$. Method B determines the secant slope of the stress strain curve after three loading cycles. Method A determines the same secant slope as Method B and also the secant slope after the first loading cycle. The secant slope is termed by EN 12390-13 (2013) as the secant modulus of elasticity in compression.

According to the code, for this test a specimen is centred in a testing machine and loaded under axial compression. The stresses and strains are recorded and the slope of the secant to the stress-strain curve is determined after three loading cycles. Apparatus that complies with EN 12390-13 (2013) must be used for this test. The measuring instrumentation is able to measure the strain directly or use the strain (ε) formula to calculate the average strain. The base or gauge length of the measuring equipment is between two-thirds of the specimen diameter or width and one-half of the specimen length. The gauge length is not less than $3D_{max}$, where D_{max} is the upper sieve size of the coarsest fraction of aggregate in the specimen.

Test specimens are cast in cylinders or prisms or sampled from existing structures according to the sampling requirements of the code. The dimension d , diameter or width of a specimen, is at least 3,5 times D_{max} . The ratio between the specimen length (L) and the dimensions (d) is in the range $2 \leq L/d \leq 4$. The compressive strength (f_c), used to define the stress levels of the loading cycles, of a companion specimen is determined and preferably this specimen is of the same shape and dimensions as the specimens used for the secant modulus of elasticity test. If the companion specimen is not of the same shape and size the shape factor (d) can be used to relate these strengths.

For testing, the test specimen is placed centrally inside the testing machine (with the measuring equipment already attached to the specimen). Three loading cycles are carried out as part of the test. Apply a pre-load stress (σ_p) and hold the pre-load stress for a period not exceeding 20 s. After this period increase the stress applied to the specimen at a rate of 0.6 ± 0.2 MPa/s from the pre-load stress to the upper stress (σ_a). Hold the upper stress for a period not exceeding 20 s. While holding the stress the nominal value can vary within $\pm 5\%$. Reduce the stress at a rate of 0.6 ± 0.2 MPa/s until the pre-load stress is reached, and hold the pre-load stress for a period not exceeding 20 s. This process is repeated three times. Record the strain and calculate the average strain (ε_p) after completion of the second loading cycle. Record the strain and calculate the average strain (ε_a) in the third loading cycle after holding the upper stress for a period not exceeding 20 s and before reducing the stress to the pre-load stress. Two checks are conducted as the test is carried out, refer to EN 12390-13 (2013) for guidelines on these. Figure 5.3 shows the loading cycles for determining the secant modulus of elasticity of a material.

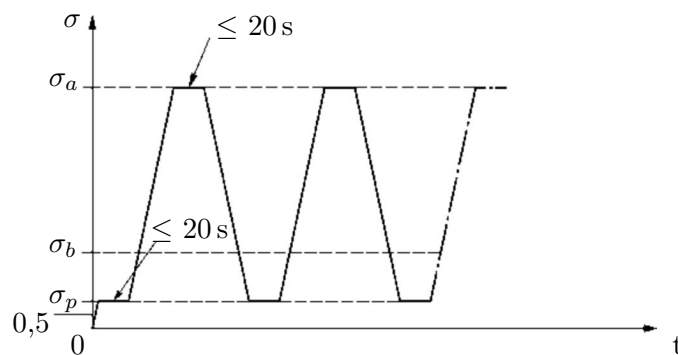


Figure 5.3: Loading cycles for the determination of the secant modulus of elasticity (*adopted from EN 12390-13 (2013)*)

σ applied stress in MPa

σ_a upper stress - $f_c/3$

σ_b lower stress - $0.1 \times f_c \leq \sigma_b \leq 0.15 \times f_c$

σ_p preload stress - $0.5 \text{ MPa} \leq \sigma_p \leq \sigma_b$

t time in s

The stabilised secant modulus of elasticity ($E_{C,S}$) is defined in Equation 5.1. The results are expressed to the nearest 0.1 GPa and the COV is also determined and presented.

$$E_{C,S} = \frac{\Delta\sigma}{\Delta\varepsilon_S} = \frac{\sigma_a - \sigma_p}{\varepsilon_a - \varepsilon_p} \quad (5.1)$$

Modulus of Elasticity Test

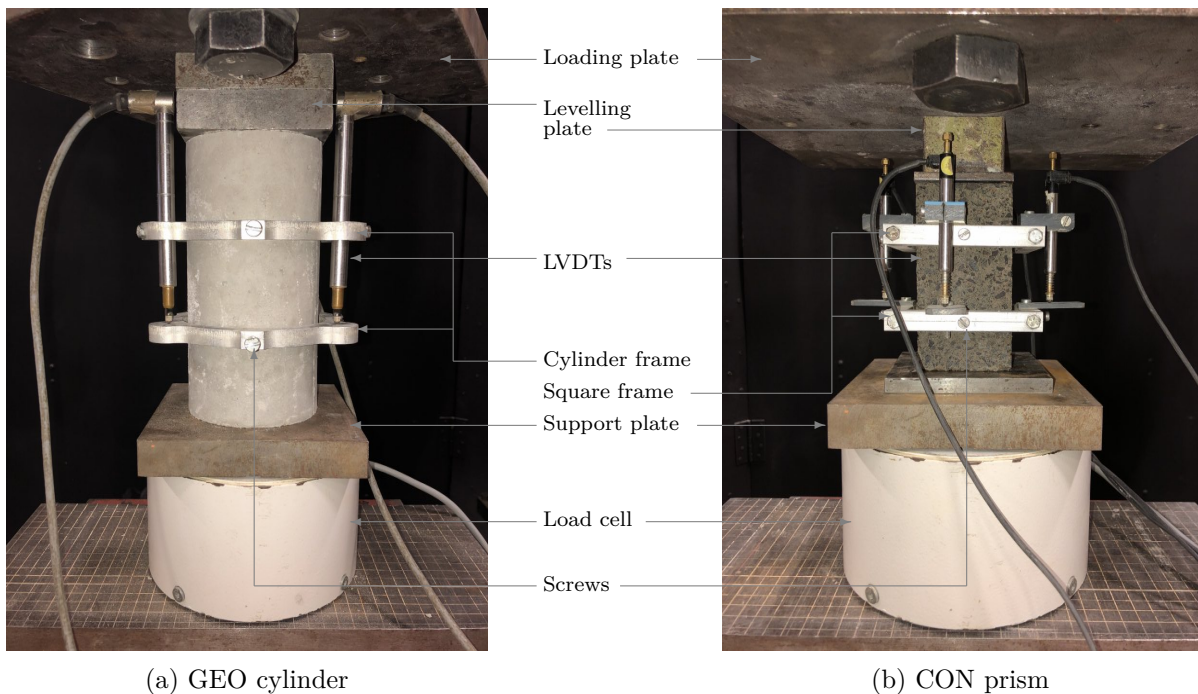
Method B presented by EN 12390-13 (2013) was followed to determine the stabilised secant modulus of elasticity ($E_{C,S}$) of each type of masonry unit and mortar used in this study. A total of ten specimens were tested for each masonry material after curing for 28 days. The CON, CSE and ADB specimens were cut from their respective masonry units according to the sampling requirements of the code. The reason for cutting smaller specimens from the masonry units was twofold. One, the modulus of elasticity of the smaller cut specimens can be tested in the same direction as the compaction pressure applied by the block press at manufacturing of the unit, and in the same orientation under which masonry units experience predominant loading in masonry walls. Two, previous research at Stellenbosch University used the same experimental setup to conduct modulus of elasticity tests on small specimens cut from masonry units.

Specimens with a prism shape, having a length and width of 58 mm and height of 116 mm, were cut from the respective AMUs and CON units with an industrial asphalt sawing machine. These dimensions gave an L/d ratio of 2, which falls within the acceptable range of specimen geometry specified by EN 12390-13 (2013). Figure 5.4 shows the CON, CSE and ADB specimens after being cut for the modulus of elasticity test.



Figure 5.4: The CON, CSE and ADB prism for the modulus of elasticity test

Cylinder specimens were created for testing the elastic modulus of the GEO material and mortar. Due to the fresh properties of the GEO material and mortars, they were cast in normal conventional cylinder moulds with a height of 200 mm and diameter of 100 mm. A 2 MN IMTM was used for testing both the cylinder and prism shaped specimens. Before testing, each specimen were ground on the loading face with an industrial grinder to ensure the surface is plumb and parallel with the bottom. Grinding was done to remove any inequalities in the specimen geometry and ensure accurate readings from the measuring instrumentation. A CATMAN data logger was used to capture data from the measuring instrumentation. Figure 5.5 shows the elastic modulus test setup for (a) the cylinder specimens and (b) the prism shaped specimens.



(a) GEO cylinder

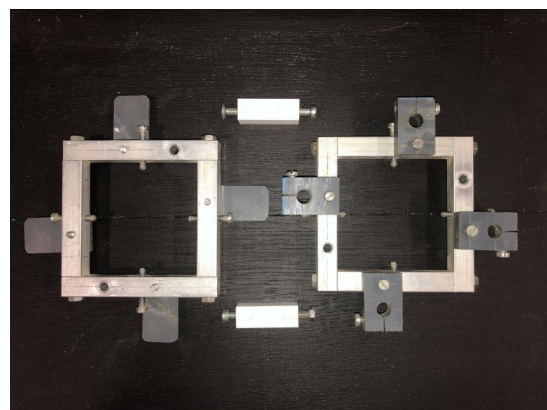
(b) CON prism

Figure 5.5: Elastic modulus test setup

The measuring equipment consisted of a 2 MN load cell, a cylinder and square frame designed for the specimen geometry and linear variable differential transducers (LVDTs). The load cell was used to verify the load applied during testing by the 2 MN IMTM. The cylinder frame was made out of aluminium and consisted of two rings with blunt screws (screws with flat header point). The square frame was also made of aluminium and like the cylinder frame has two rings (square rings) with screws in. The cylinder frame has a gauge length of 112 mm and the square frame one of 58 mm, both comply to the gauge length requirements of EN 12390-13 (2013). The purpose of the screws in both frames is to attach the top and bottom parts of the frame to the specimen to follow the movement (strain) of the specimen under loading. The LVDTs were attached to the top part of the frame and centred onto the bottom part to measure the change in length of the specimen, over the gauge length, under loading. A total of three 10 mm LVDTs were used in the cylinder frame and a total of four 10 mm LVDTs were used in the square frame. Figure 5.6 shows (a) the cylinder elastic modulus test frame and (b) the square elastic modulus test frame.



(a) Cylinder frame



(b) Square frame

Figure 5.6: Elastic Modulus testing frames

A companion specimen was created for each elastic modulus test of the same geometry, from which the maximum compressive strength was determined. The pre-load and upper load was calculated from this strength according to EN 12390-13 (2013). A step-wise loading function from the 2MN IMTM was used to apply the three loading cycles to the specimens. The stabilised secant modulus of elasticity was then calculated by using the load and displacement data, according to Equation 5.1.

A loading rate of 0.6 ± 0.2 MPa/s, as proposed by EN 12390-13 (2013) for the loading cycles, showed erroneous results for the prism shaped specimens. A reason for this is the size of the specimens, these specimens are smaller than the cylinder specimens and have a much lower compressive strength before the shape factor (d) is taken into account. A loading rate of 0.04 MPa/s resulted in a test that could be completed without further issues for the CON and CSE specimens. This loading rate, however, resulted in difficulties with the weaker ADB units and a lower loading rate was again required. For the 2MN IMTM to maintain such small margins of control it was required that the test is done displacement controlled. The same principles applied and instead of using the pre-load and upper load the displacements at these locations were used. This technique provided a way to successfully determine the elastic modulus of the ADB material. A loading rate of 0.0056 mm/s was used for the ADB specimen. A loading rate of 0.6 ± 0.2 MPa/s was successfully used for the GEO and mortar cylinder specimens.

The change in loading rates for the CON, CSE and ADB specimens could influence the results and, therefore, the modulus of elasticity results cannot be compared directly to each other. However, higher loading rates were not possible for any of the materials as they would give erroneous results.

5.1.3 Dry Density Test Specifications

The European testing standard EN 772-13 (2013) specifies a method for the determination of the net and gross dry density of masonry units. EN 772-13 (2013) presents a method for determining the dry density of masonry units by drying a unit to a constant mass and then calculating the volume of that unit. The apparatus required for this test is a ventilated oven capable of maintaining temperatures of up to $105^\circ\text{C} \pm 5^\circ\text{C}$ and a weighing instrument capable of weighing to an accuracy of 0.1% of their mass.

According to the code, to reach constant mass (m_d) the specimens are dried in the oven until two subsequent weighings over a 24 h period have a loss in mass of less than 0.2% of the total mass of the specimen. Two different temperatures are specified by the standard at which the units are dried, $70^\circ\text{C} \pm 5^\circ\text{C}$ for aggregate concrete and manufactured stone masonry units and $105^\circ\text{C} \pm 5^\circ\text{C}$ for clay, calcium silicate and autoclaved aerated concrete masonry units.

Once constant mass is reached the mass of the specimen is divided by its volume (V) to obtain the dry density (ρ_d) of that specimen. Equation 5.2 shows the formula to calculate the dry density. Results are expressed to the nearest 5 kg/m^3 for specimens with densities up to 1000 kg/m^3 and to the nearest 10 kg/m^3 for specimens with densities over 1000 kg/m^3 . The COV is also determined and presented.

$$\rho_d = \frac{m_d}{V} \quad (5.2)$$

The masonry units are not completely dry once they have been air dried in the laboratory and the initial moisture content ($w_{initial}$) of the masonry units can be determined by dividing the difference in weight after the unit were dried to constant mass by the dry mass of the unit, see Equation 5.3.

$$w_{initial} = \frac{m - m_d}{m_d} \quad (5.3)$$

Dry Density Test

The dry density of the masonry units is used for quality control and comparison to previous research in this study. As stated in Chapter 4 the material used for CON, CSE and ADB unit manufacturing was weight batched to ensure a constant density. The density of the GEO units should also stay constant as the fresh GEO material is compacted under self weight.

The European testing standard EN 772-13 (2013) was adopted for determining the dry density of each type of masonry unit in this study. Ten units of each material were used to conduct this test. The units were dried in a ventilated oven that is available in the laboratory. All the units were dried at $70\text{ }^{\circ}\text{C} \pm 5\text{ }^{\circ}\text{C}$.

The units were removed from the oven every 24 h and left to cool down for about half an hour before weighing. The units were termed oven dry when a constant mass was reached and the difference in weight between two subsequent weighings was less than 0.2% of the total mass of the unit. The dry density was then calculated by dividing the oven dry mass by the unit's volume.

5.1.4 Water Absorption Test Specifications

The European testing standard EN 772-11 (2011) specifies a method for determining the water absorption characteristics of masonry units. This standard presents a method for determining the water absorption of aggregate concrete, autoclaved aerated concrete, manufactured stone and natural stone masonry units due to capillary action, and the initial rate of water absorption of clay masonry units.

In principle the procedure of determining the water absorption of masonry units consists of drying the unit to a constant mass (m_d) (the same as specified in the dry density test from EN 772-13 (2013)) and then immersing a face of the masonry unit in water for a specific period of time. The increase in mass is used to determine the absorption characteristics. The standard specifies a minimum of six specimens should be tested and the average of these tests is the water absorption of the masonry unit.

A large tray is used to immerse the units, the tray must be larger than the face of a masonry unit, deeper than 20 mm and have a means of maintaining a constant water level. A supporting frame is used to keep the units off the bottom of the tray and not cover more than 400 mm^2 of the face of a unit. The specimens are immersed in water to a depth of $5\text{ mm} \pm 1\text{ mm}$ for the duration of the test, this water level should be kept constant. The units are immersed for a specific time period and then removed and weighed. Upon removing the units the immersed surface is wiped clean with a cloth before weighing.

European testing standards EN 771-1 (2011) and EN 771-3 specify the immersion time (t_s) for clay masonry units and aggregate masonry units. The time specified for clay units is 1 min and the time for the aggregate units, 10 min. EN 772-11 (2011) provides two methods for determining the coefficient of water absorption due to capillary action, one for aggregate concrete and manufactured stone and the other for autoclaved aerated concrete and natural stone. These methods do not apply to clay units and a method for calculating the initial rate of water absorption (IRA) is proposed for clay units.

Equations 5.4 and 5.5 present first, the equation for determining the coefficient of water absorption due to capillary action of aggregate concrete and second, the initial rate of water absorption for clay units. Results are expressed to the nearest 0.1 g/(m² s) for the coefficient of water absorption due to capillary action, and 0.1 kg/(m² min) for the IRA. The COV is also determined and presented.

$$c_s = \frac{m_s - m_d}{A_s \times t_s} \times 10^6 \quad (5.4)$$

$$c_s = \frac{m_s - m_d}{A_s \times t_s} \times 10^3 \quad (5.5)$$

c_s coefficient of water absorption for Equation 5.4 [g/(m².s)] and IRA for Equation 5.5 [kg/(m².min)]

m_s mass of masonry unit after being immersed

m_d mass of masonry unit after being oven dried

A_s area of immersed surface of masonry unit

t immersion time

Water Absorption Test

Water absorption tests were conducted according to EN 772-11 (2011) on all the different types of masonry units investigated in this study. Ten units from each masonry material were tested after curing for 28 days. All water absorption tests were conducted on masonry units that were oven dried to a constant mass at 70 °C.

White rectangular plastic containers were used to immerse the units for the test. The supporting device consisted of painted steel angle irons, which kept the units clear from the container floor, and immersed at a depth of 5 mm in water. Lines inside the containers indicated the water level and depth of immersion of the unit. Throughout the test the water level was constantly checked with a ruler and adjusted accordingly by hand with a smaller water bucket, to maintain a constant water level. Figure 5.7 shows (a) one of the plastic containers filled with water and (b) GEO units placed inside the container during the water absorption test.



(a) Container with angle irons filled with water (b) Water absorption test conducted on GEO units

Figure 5.7: Water absorption test procedure

EN 772-11 (2011) does not specify a method for obtaining the water absorption of the alternative masonry materials investigated in this study. Therefore, well known methods from literature and methods presented by EN 772-11 (2011) that are most applicable to the AMUs of this

study were adopted. A popular water absorption characterisation method for masonry units in literature is the IRA, numerous studies investigate this material property and use this method for comparing a number of different types of masonry units Grenley (1969); Sugo *et al.* (2001); Katiyar (2015); Sarangapani *et al.* (2005); Lawrence and Page (1994). Therefore, the IRA is also investigated in this study on the CON units and all the other AMUs. Due to the CON unit being similar to the aggregate CON unit, the method proposed by EN 772-11 (2011) to determine the coefficient of water absorption due to capillary action of aggregate concrete was also adopted for all the units in this study.

Data that was recorded from each test was the mass of the unit after being immersed, area of the immersed surface of the unit and immersion time. This with the mass of the masonry unit after being oven dried was used to determine the respective types of water absorption characteristics of each unit. Lawrence and Page (1994) studied absorption rates for different masonry units over a 24 h period. The results showed that absorption still continued at significant rates after the usual studied 1 min time period (used for calculating the IRA). Different rates were observed for different materials, but these results show that absorption still continues after the first few minutes which is usually the only time period studied in absorption tests. This will also effect the bond development and hydration rate of cement particles at the joint interface.

Therefore, for a better understanding of the unit absorption, and movement of fluids at the interface upon construction, the water absorption by mass of the different units was investigated over a 24 h period. To understand the absorption over time, readings were taken at 1 min, 10 min, 1 h, 4 h, 8 h and , 24 h intervals. If the absorption still continued after 24 h, the test continued until the absorption stopped completely. Figure 5.8(a) to 5.8(e) shows the water absorption of a CSE unit at different time periods during the water absorption test.

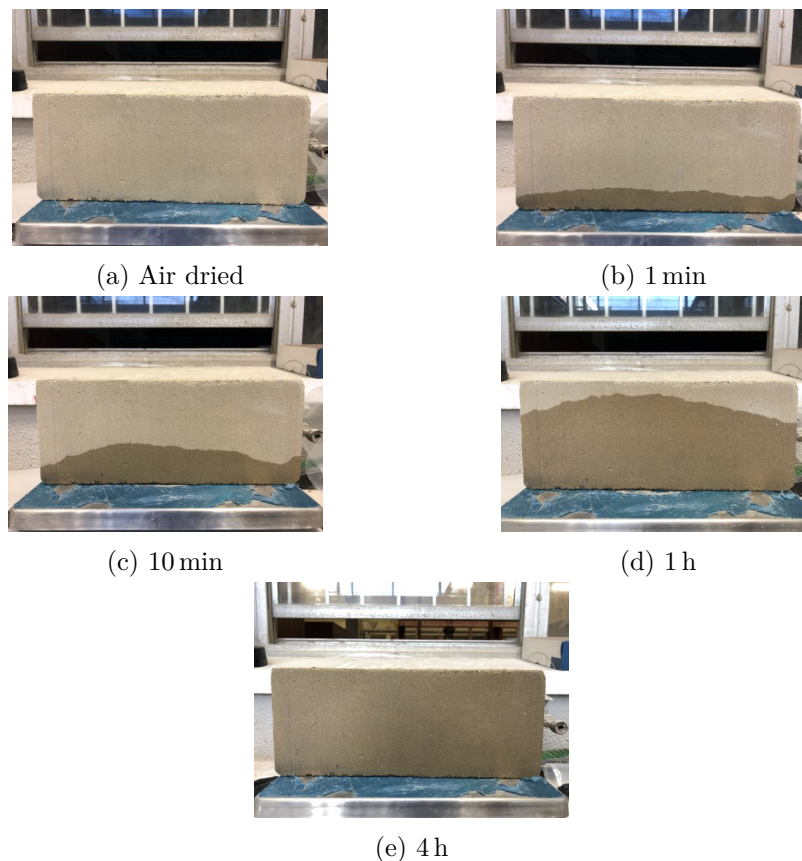


Figure 5.8: Water absorption of CSE unit at different time periods

Problems were encountered with the absorption test on the ADB unit. Due to the absence of a cement binder the unit disintegrated when coming into contact with water. The clay content in the ADB unit acted as the binder, but upon contact with water the bonds between the clay and sand particles weaken until failure. Figure 5.9 shows an ADB unit after being immersed in a depth of 5 mm water for 1 min.



Figure 5.9: ADB unit surface after immersion

5.1.5 Determination of Surface Roughness

There are currently no standards available for determining the surface roughness of masonry units. A parameter has also not yet been defined by which the surface roughness can be quantified. The surface roughness is a surface characteristic of masonry units not regularly studied. However, literature that did investigate this phenomenon concluded that the bond strength of the joint interface increased with an increase in surface roughness (Reddy and Gupta, 2006; Tschegg *et al.*, 2008; Schneemayer *et al.*, 2014).

Reddy and Gupta (2006) quantified the surface roughness of soil-cement blocks by determining the pore size and surface porosity of the block surface with scanning electron microscopy (SEM). Samples were cut from the undisturbed block surfaces and used in scanning electron microscopy SEM analyses. As stated in Section 3.2.1, other research that investigated the surface roughness is Tschegg *et al.* (2008). Tschegg *et al.* investigated the surface roughness with a perthometer and measured the mean roughness value (R_a). A method used by Reddy and Gupta was adopted in this study.

Surface Roughness Procedure

To determine the surface roughness's of the different masonry units investigated in this study, samples were cut from the undisturbed bedface surfaces. The samples were cut to the following dimensions, 40 mm × 30 mm × 10 mm (length × width × height) to fit the apparatus used for quantifying the surface roughness. An Axiocam microscope camera from ZEISS was used to investigate the surfaces with different magnifications. The pore size and surface porosity was then quantified with free ImageJ software. Figure 5.10 shows specimens cut from masonry units for the surface roughness procedure.

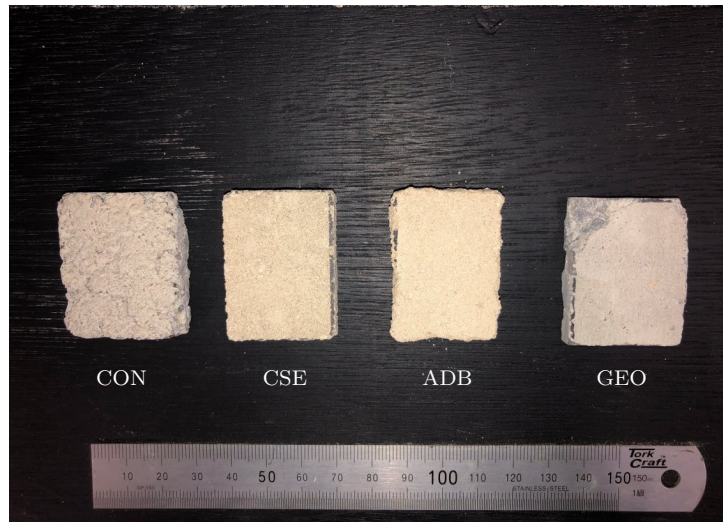


Figure 5.10: Surface roughness specimens

5.2 Mortar Tests

This section presents the experimental procedure followed for characterising the two different mortars (7M and 20M) used throughout this study. The test specifications proposed by international standards are again firstly considered and, thereafter, the experimental procedure for each experiment.

The tests conducted on the mortar are flow, dry density, flexural and compressive strength tests. The flow value is a fresh mortar property and is therefore tested directly after casting while the mortar is still fresh. The other tests indicate material and mechanical properties of mortar in its hardened state and was tested for on 7 days after casting.

5.2.1 Consistence (Flow value) Test Specifications

The European testing standard EN 1015-3 (1999) specifies a method for determining the flowability (consistence) of fresh mortar by means of determining the flow value from the flow table test. The apparatus required for this test consist of a flow table (which conforms to the requirements of EN 1015-3 (1999)), a conical mould, tamper device and a measuring tool able to measure with an accuracy of 1 mm.

According to the standard a sample of fresh mortar is placed onto a flow table inside a cone-like mould. The mortar is placed in the mould in two layers, each layer being compacted 10 times by the tamper device. The excess mortar must be removed after the second tamper and the area around the mould cleaned from any mortar or water. Thereafter, the mould is removed slowly and the flow table jolted fifteen times, by turning the small lever arm, to spread out the mortar on the flow table disc. The rate at which the flow table is jolted is approximately one jolt per second.

The flow value of a sample of mortar is calculated as the mean of two measurements. The diameter of the mortar in two directions at right angles to one another is measured. This process is repeated twice and the mean of the flow value of each process is the final flow value of the mortar. If one of the two flow values from the individual test differ by more than 10% from the final mean flow value the test must be repeated and if not the test is valid. The results are expressed as a percentage to the nearest 1%. For example, if the diameter of the spread out

mortar after the test is complete is 200 mm and the internal diameter of the conical mould is 100 mm the flow value would be 100%. The COV is also determined and presented.

Flow Table Test

The flow table test was conducted according to EN 1015-3 (1999) in this study. Figure 5.11 shows certain parts of the flow table test procedure.



(a) Flow table test apparatus



(b) Mould filled with mortar and excess removed



(c) Flow table disc after 15 jolts

Figure 5.11: Flow table test procedure

The flow table test was used as a quality control test throughout the masonry construction phase of this study. Literature found that a flow value of below 100% gave a dry mortar with low workability and a fresh mortar that will not effectively penetrate pores on the surface of the masonry unit, which reduces the bond strength (Reddy and Gupta, 2006). Walker (1999) found that varying flow values gave a scatter in results. Therefore, a constant flow value of 100% was adopted for 20M and 7M, in their fresh mortar state, throughout this study.

5.2.2 Dry Density Test Specifications

The European testing standard EN 1015-10 (1999) specifies a method for determining the dry density of hardened mortars and is almost identical to method proposed by EN 772-13 (2013) for determining the dry density of masonry units. The volume of the mortar specimen is not

less than 50 times the maximum aggregate particle size and not less than 50 ml or 1.5 times the quantity needed to perform the test, whichever is greatest.

The mortar is dried in a ventilated oven at $105\text{ }^{\circ}\text{C} \pm 5\text{ }^{\circ}\text{C}$ until constant mass ($m_{d,m}$) is reached. Constant mass is reached if two consecutive weighings 2 h apart during the drying process do not vary by more than 0.2% of the mass of the mortar specimen. The dry density of the mortar specimens can be calculated as the dry mass ($m_{d,m}$) of each specimen divided by the volume of that specimen. The result is expressed to the nearest 10 kg/m^3 and the COV is also determined and presented.

Dry Density Test

The European testing standard EN 1015-10 (1999) was adopted for determining the dry density of both mortars in this study. Six cubes of each mortar were used to complete the test. The mortar cubes were cast in conventional concrete cube moulds of dimensions, $100 \times 100\text{ mm}$.

The same process followed for obtaining the dry density of the masonry units in Section 5.1.3 was followed here. The mortar cubes were dried in a ventilated oven at $105\text{ }^{\circ}\text{C} \pm 5\text{ }^{\circ}\text{C}$ until constant mass was reached. The dry density of each mortar cube is calculated by dividing the dry mass ($m_{d,m}$) of the cube by its volume. The final dry density of each mortar is calculated as the mean of the six dry densities of the individual mortar specimens.

5.2.3 Flexural and Compressive Strength Test Specifications

The European testing standard EN 1015-11 (1999) specifies a method for determining the flexural and compressive strength of moulded mortar specimens. A method to determine the flexural strength by a three point loading test on a moulded mortar prism until failure is proposed. The compressive strength of the mortar is determined from two half prisms resulting from the flexure test. The moulds deliver a test specimen of dimensions, $160 \times 40 \times 40\text{ mm}$. A minimum of three prisms are cast for one flexural test, and six half prisms is required for a compressive strength test. This standard is adopted in this study.

According to EN 1015-11 (1999) the flexural and compressive strength tests are carried out on mortar at an age of 28 days, or more if a retarding agent is incorporated in the mix. For full preparation and conditioning guidelines, for mortars of different compositions, refer to EN 1015-11 (1999).

The three point bending test setup has two supporting steel rollers of between 45 and 50 mm in length and a $10 \pm 0.5\text{ mm}$ diameter, at a distance of $100 \pm 0.5\text{ mm}$ apart (centre to centre) and a third steel roller of the same size located centrally between the two supporting rollers. The loading roller and one of the supporting rollers are able to tilt slightly to allow for any inequalities and avoid torsional forces in prism.

The machine conforms to requirements presented in EN 1015-11 (1999) and apply a loading rate of between 10 and 50 N/s, to reach failure within a period of 30 to 60 s. The flexural strength is calculated with Equation 5.6. Results of each specimen is expressed to the nearest 0.05 N/mm^2 , and the mean of all the results to the nearest 0.1 N/mm^2 . The COV is also determined and presented.

$$f_{fm} = \frac{3}{2} \times \frac{F_f l}{bd^2} \quad (5.6)$$

f_{fm} maximum flexural strength [MPa]

F_f maximum load applied to middle of prism [N]

l support span [mm]

b width of prism [mm]

d depth of prism [mm]

The compressive strength testing procedure of EN 1015-11 (1999) is not discussed here, due to this test not being part of this study. Normal cube compressive strength tests were conducted to determine the compressive strength of the respective mortars.

Flexural and Compressive Strength Test

The guidelines presented by the European testing standard EN 1015-11 (1999) were adopted for determining the flexural strength of both mortars in this study. Nine prisms of each mortar were cast for testing. Metal moulds conforming to Annex A of EN 1015-11 (1999) were used for prism creation. Each prism, after demoulding, had dimensions, 160 mm long, 40 mm wide and 40 mm high.

After casting the mortar specimens were left in the moulds to dry for one day in the laboratory. Thereafter, the prisms were demoulded and cured in curing tanks that were kept at a constant temperature of 25 °C. The prisms were left in the curing tanks until testing. The flexural strength tests were conducted on 7 days after casting, due to the masonry tests (crossed-brick couplet test and triplet test) also being conducted on 7 days after construction.

A four point bending test was used to determine the flexural strength of mortar, and not a three point bending test as specified in EN 1015-11 (1999). Statistically the four point bending test should produce lower average flexural strengths than that of the three point bending test, due to the stress concentration over a larger area, allowing a better chance for imperfections to occur within this area. Figure 5.12 shows the four point bending test on one of the mortar prisms.

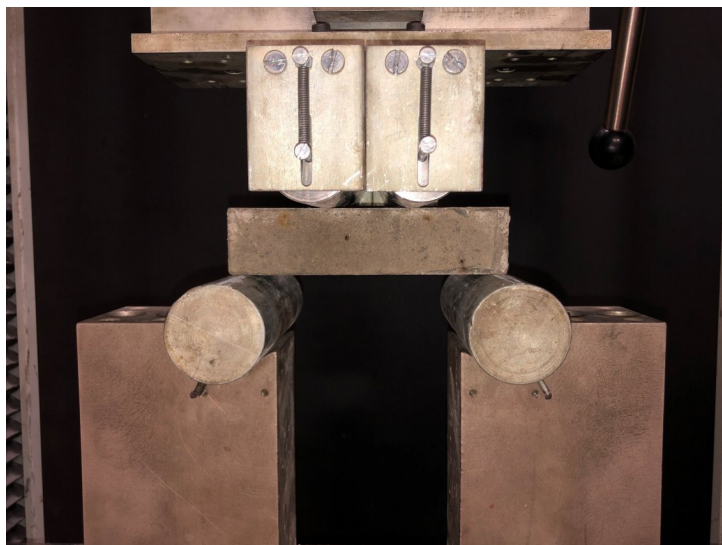


Figure 5.12: Four point bending test

A loading rate of 25 mm/min was applied by the testing machine for the four point bending test. This loading rate resulted in prism failure between 1 and 2 min. The displacement controlled test produced a more consistent and stable test than force controlled on the testing machine.

The flexural strength for the four point bending test is calculated with Equation 5.7. Equation 5.7 is for calculating the flexural stress for a four point bending test where the loading span is one third of the support span of the test setup. These parameters were recorded during the test and used to determine the flexure strength of each individual prism.

$$f_{fm} = \frac{F_f l}{bd^2} \quad (5.7)$$

F_f maximum load applied to prism [N]

the remaining parameters are defined as in Equation 5.6

Normal 100 mm cubes were tested to obtain the compressive strength (f_{cm}) of the respective mortars and not the halved prisms resulting from the four point bending tests. A Zwick Z250 Material Testing Machine and Contest 2 MN Press were used to determine the flexural strength of the mortar prisms and the compressive strength of the mortar cubes, respectively. A loading rate of 90 kN/min was applied on the 100 mm cubes for the compressive strength test.

5.3 Joint Interface Tests

This section presents the experimental procedure used to characterise the tensile and shear properties of the joint interface of the three different alternative materials investigated in this study. The tensile and shear tests consisted of two tests, the crossed-brick couplet test (a direct tensile test) and the triplet test (a shear test). For each of the two tests different types of masonry prism specimens were constructed.

A crossed-brick couplet is cast by laying one unit on top of another, with mortar in between, in a crosswise direction with the centres of both units aligning. A triplet prism consists of three units laid on top of each other, separated by two layers of mortar. Figure 5.13 shows the couplet and shear specimens after construction. Both types of masonry prisms were constructed by experienced masons using conventional tools. Two masons built all the prisms constructed in this study to ensure consistency in the construction technique.



Figure 5.13: The (a) CSE crossed-brick couplet specimen and the (b) CON triplet specimen after curing for 7 days

One of the major findings of the study of Reddy and Gupta (2006) was the effect of the initial moisture content of the blocks at the time of construction on the bond strength. Reddy and

Gupta concluded that the use of partially saturated blocks gave better bond strengths than completely dry or fully saturated blocks. For this study, however, units were all dried to an air dry state before construction. The reason for this was two fold. Firstly, the ADB unit cannot be immersed in water. Once the ADB unit is immersed it starts to disintegrate, refer to Figure 5.9. Secondly, experimental consistency is more important than stronger bond developments, therefore, all the units were tested in the same air dried condition. This also allows better comparison of results.

All the masonry tests were conducted at 7 ± 1 day after construction. In a research study on the bond strength of earth block masonry, Walker (1999) concluded that little bond strength, at the joint interface, is gained after one day. This shows that the initial bond development is the most significant and not the development over time. Therefore, most of the bond development would already have taken place at 7 days.

Sections 5.3.1 and 5.3.2 explain the testing specifications of standards used for both the tensile and shear testing procedures, as well as how the respective tests were applied to the alternative materials and where they differed from the standards.

5.3.1 Direct Tensile Strength Test Specifications

The American standard, ASTM C 952-12 (2012), specifies a test method for determining the tensile strength of the joint interface of masonry. This test is a direct tensile test (unlike the bond wrench or the wedge splitting test) and, therefore, the direct tensile strength of the joint interface can be calculated from the test results. Currently there is no EN or SANS standard for determining the direct tensile strength of the joint interface of masonry.

The standard specifies a certain methodology is followed for the construction of the test specimens. A square steel mould is centered on the lower brick and filled with mortar for a one minute interval. The steel mould is between 8 and 15 mm thick. At the end of the one minute interval the upper brick is placed on the mortar bed in a crosswise direction and hit into place with a drop hammer. The drop hammer should have a weight of 2 kg and be dropped a distance of 38 mm inside the drop hammer frame, whereafter the excess mortar is cut away from the mortar joint. For a detailed description refer to ASTM C 952-12 (2012).

The curing method proposed is to enclose the test specimen with an airtight covering for 7 days. After 7 days the cover is removed and the specimens, unless specified otherwise, stored in laboratory air with a relative humidity of at least 50% until testing.

For testing, the specimen is centred between the two tripods, refer to Figure 3.3a in Section 3.1.2. Then the specimen is loaded at a rate of 2.7 kN/min or a rate leading to failure between 1 and 2 minutes. The maximum load and type of failure is recorded. Failure types are discussed in Section 3.3.2 and these failure types are also applied to the crossed-brick couplet test in this study. The cross-sectional area is calculated in millimetres using the width squared of the mortar bed. Refer to Equation 3.4 in Section 3.3.1 for the equation to calculate the maximum tensile bond strength (f_t).

Direct Tensile Test

The method proposed by, ASTM C 952-12 (2012), was adopted in this study to determine the tensile strength of the joint interface. The direct tensile strength was obtained by testing crossed-brick couplet until failure. The tensile fracture energy of the joint interface cannot be determined using this test results, due to the sudden brittle failure of the interface. Therefore, this mechanical property of the interface was not further investigated in this study.

The crossed-brick couplets were constructed according to ASTM C 952-12 (2012). Figure 5.14 shows parts of the construction process of a CSE couplet, (a) the square mould filled with mortar and centred on the bottom masonry unit and (b) the drop hammer used for subsiding the top unit. The square plastic mould ensured that the mortar layer between the two units was between 8 and 15 mm thick, depending on how much the top unit subsided after being hit by the drop hammer.

A problem was encountered with the construction process of the ADB couplet, upon hitting the top unit with the drop hammer the top unit would split in half. Therefore, the drop hammer was not used for constructing the ADB couplets and these were rather constructed only by hand.



(a) Plastic mould 10 mm thick

(b) Drop hammer

Figure 5.14: Crossed-brick couplet construction procedure of CSE material

Due to the geometry of the test setup it is important that the surfaces onto which the tripods apply loads are level. To ensure this the bottom units were placed on wooden planks. Sand was used to level the wooden plank in such a manner that the top bedface surface of the bottom unit on top of the wooden plank is levelled.

Due to the method of manufacturing the units (with the block press) the top bedface surface of units was not always level and parallel to the bottom bedface surface. To get these surfaces parallel the top bedface surfaces of all the top units of the crossed-brick couplets were ground with an industrial grinder (see Figure 5.1). The two surfaces that were tested for each crossed-brick couplet were not ground. This ensured that the mason only needed to level the top bedface surface of the top unit to obtain the correct geometry of a couplet for testing. A spirit level was used to ensure the surfaces were level and parallel to each other.

During construction a mortar sample was taken from each mortar batch created. The flow table test was conducted on each mortar sample before and after construction to observe the change in the flow value of the mortar over the construction period. The flow value was also used for quality control and to ensure a mortar with consistent workability throughout the study. Compressive strength tests were also conducted on the mortar samples at the time of testing the couplets, to know the mortar strength at the time of testing the couplets. Figure 5.15 shows constructed crossed-brick couplets of each masonry material investigated in this study.

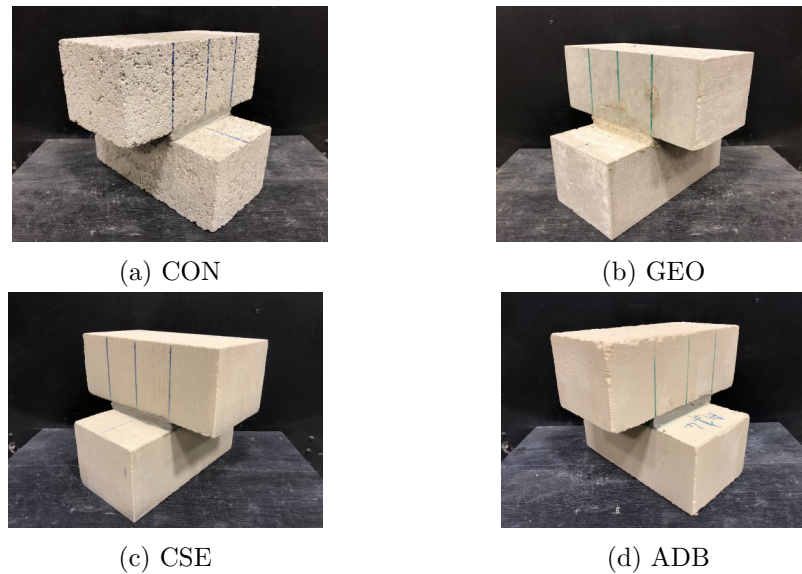


Figure 5.15: Crossed-brick couplet of each material investigated in this study

The crossed-brick couplets were covered with polythene sheets directly after construction until they were tested. The number of specimens that needs to be tested is not specified by ASTM C 952-12 (2012). Therefore, the number of specimens usually required for testing in the European testing standard are adapted for this test ranges between 6 and 10 specimens, depending on the type of test. Eight specimens per masonry material type were tested for this test. The 2 MN IMTM was used to conduct the tensile test on the masonry couplets. Figure 5.16 shows the test setup of the crossed-brick couplet test.

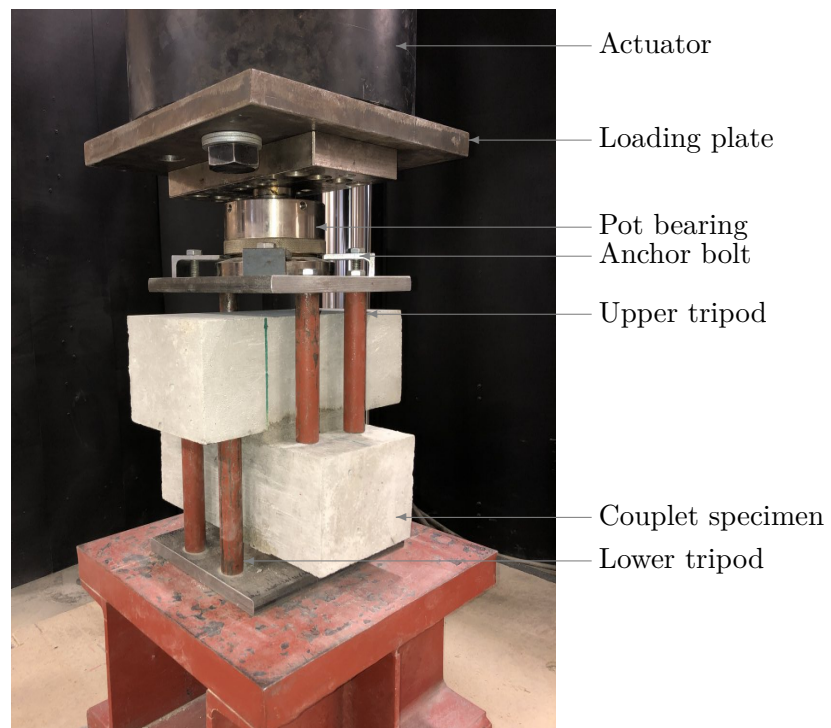


Figure 5.16: Crossed-brick couplet test setup with GEO couplet

The test setup consists of a lower and upper tripod between which the couplet specimen is centred. The upper tripod was in this case attached to a pot bearing and the pot bearing attached to the loading plate of the 2 MN IMTM. The upper tripod gripped onto the pot bearing with four bolts anchoring small angle irons onto the pot bearing. The tripods and the pot bearing ensured that everything was level in the setup and that the load was applied equally to each leg of the tripods. The testing machine applied a load at a rate of 0.25 mm/min onto the couplet specimen until tension failure occurred.

The code specifies that the failure mode of each test is recorded. The standard EN 1052-5 (2005) specifies five different valid failure modes for the bond wrench test. These same failure modes were adapted for this study and failures as in Figure 3.14(a) to 3.14(e) is further referred to as failure Type B1 to B5. If any other failure type is observed during tests the result is not considered as valid and the test is then discarded. Most tensile failures occurred at the joint interface between the mortar and the upper unit (failure Type B1).

Data that was recorded from each test was the maximum vertical force applied and the area of the mortar bed. From this data the maximum tensile bond strength of the joint interface could be determined. No additional measuring equipment was used to record data, only the data captured by the 2 MN IMTM was used. This test was successfully conducted on the CON and all the alternative masonry couplets. The only adjustment that was made to the testing procedure of ASTM C 952-12 (2012) was the loading rate. The loading rate was changed from force-controlled loading to displacement-controlled loading. Nonetheless, this still concludes that the standard ASTM C 952-12 (2012) can be successfully used on the three types of alternative masonry materials investigated in this study.

5.3.2 Shear Strength Test Specifications

The European testing standard EN 1052-3 (2002) specifies a method for determining the initial shear strength of horizontal joint interfaces by testing a prism specimen in shear. For this test a masonry prism consists of three masonry units joined together with mortar in-between the units. The final thickness of the mortar joint is between 8 and 15 mm. Immediately after construction, the prism is pre-compressed with a distributed vertical stress of between 2.0×10^{-3} N/mm² and 5.0×10^{-3} N/mm², and cured until testing. The specimen is also covered with polyethylene sheets to prevent them from drying out. Specimens are tested at 28 days \pm 1 day.

Two testing procedures are specified by the standard, Procedures A and B. Procedure A involves testing specimens at different pre-compression level, where Procedure B involves testing specimens at zero pre-compression. The cohesion and coefficient of friction can only be determined with Procedure A, therefore this procedure is adopted in this study. Procedure A uses a linear progression curve to determine the initial shear strength of the joint interface.

At least three specimens are tested at three different pre-compression loads. The average of these three tests is then used to determine the result at each pre-compression level. Pre-compression loads (also referred to as normal loads) of 0.2 N/mm², 0.6 N/mm² and 1.0 N/mm² are used for units with compressive strengths greater than 10 MPa. For weaker units pre-compression loads of 0.1 N/mm², 0.3 N/mm² and 0.5 N/mm² are used. All pre-compression loads should be kept within \pm 2% of the original pre-compression load for the duration of the test. A vertical loading rate is applied to the specimen which increases the shear stress between 0.1 N/(mm²/min) and 0.4 N/(mm²/min).

Figure 5.17 displays the triplet test setup, adapted from EN 1052-3 (2002), with vertical and pre-stress loading conditions applied to the specimen. Equations 5.8 and 5.9 determine the shear

strength and pre-compression stress applied in the test. These parameters, of both equations, should be recorded from each test. Results are expressed to the nearest 0.1 N/mm^2 . The COV is also represented.

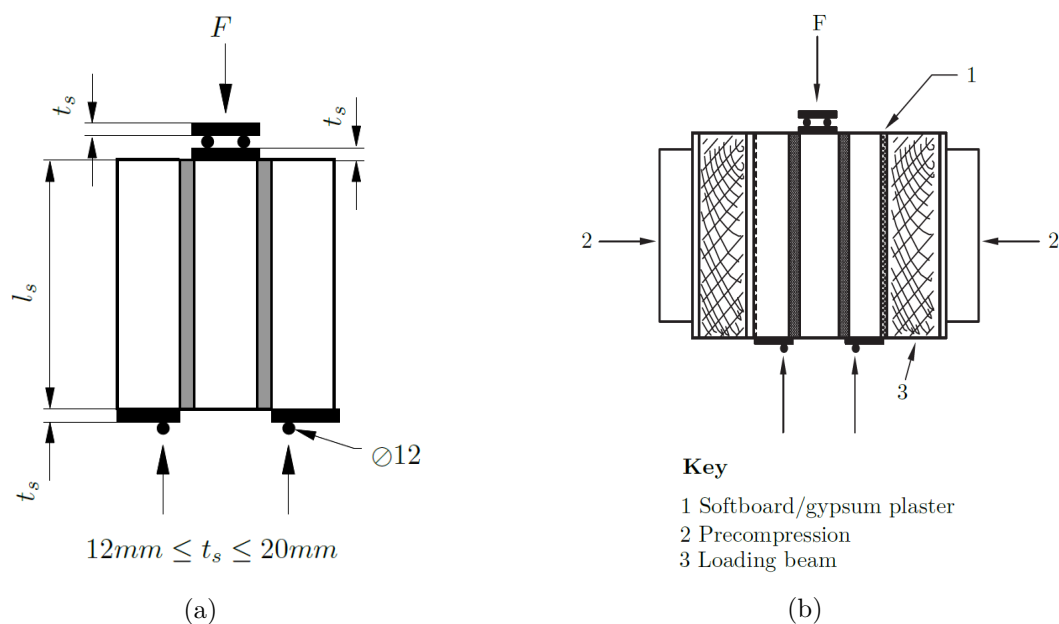


Figure 5.17: Triplet test loading and pre-compression configuration (*adapted from EN 1052-3 (2002)*)

$$\tau_a = \frac{F_{max}}{2A_i} \quad (5.8)$$

$$\sigma_n = \frac{F_p}{A_i} \quad (5.9)$$

where,

τ_a shear strength of an individual sample;

σ_n pre-compression stress of an individual sample;

F_{max} maximum shear force;

F_p pre-compression force;

A_i cross sectional area of specimen parallel to joint interface.

The standard EN 1052-3 (2002) considers four different failure modes to give valid results in an informative Annex A. If any other failure mode is obtained the results is seen as erroneous and the test is repeated.

Figure 5.18 displays these failure types and gives an explanation for each shear failure type. If failure is by shear in the unit parallel with the bed joint or crushing/splitting of the unit, like in Figure 5.18(c) and 5.18(d), further specimens must be tested until shear failure of types shown in Figure 5.18(a) and 5.18(b), occurs for each pre-compression level. For further use in

this study the failure types in Figure 5.18(a) are referred to as A1/1 and A1/2, and in Figure 5.18(b), 5.18(c) and 5.18(d) as A2, A3 and A4, respectively. Coulomb friction law provides a method for calculating the cohesion and coefficient of friction of masonry, refer to Section 3.1.3 and Equation 3.1.

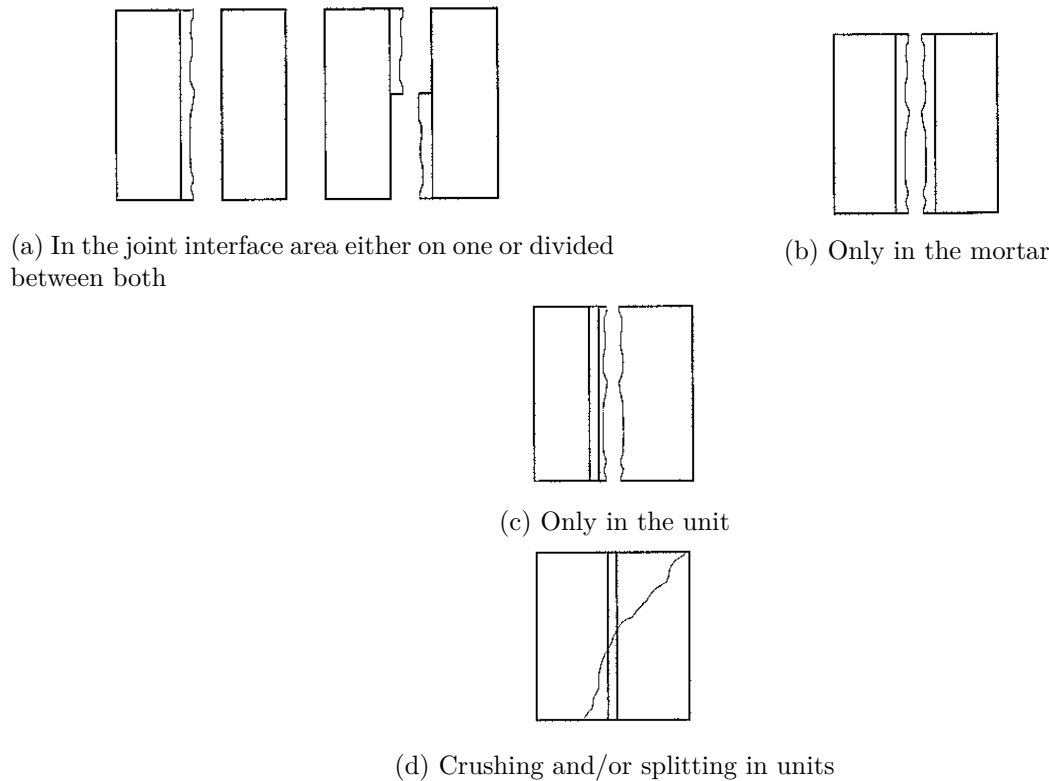


Figure 5.18: Failure modes providing a valid bond strength results as per Annex A of EN 1052-5 (2005)

As stated in Section 3.1.3 and shown in Figure 3.10, the dilatancy angle is determined by the change of volume of a sample under shear load. The ratio $\Delta v/\Delta u$ is required from the test specimen. There is no standardised method to determine the dilatancy of the joint interface of masonry. Therefore methods from literature have been implemented in this study. Equations 3.2 and 3.3, in Section 3.1.3, present methods to determine the dilatancy coefficient and dilatancy angle, respectively. These two equations are used to characterise dilatancy in this study.

Triplet Test

Triplet tests were conducted according to EN 1052-3 (2002) on the different masonry materials investigated in this study, to examine the shear behaviour of the joint interface of masonry. The standard presents a method for determining the initial shear strength of masonry by testing triplet masonry prisms to destruction. Procedure A of the standard was implemented in this study, where different pre-compression loads are applied to the specimens.

The triplet prisms were constructed on a clean surface in open laboratory space. Before construction the bearing surfaces of each unit were wiped clean with a hand brush. The lower unit was laid onto a wooden plank that was levelled beforehand with a spirit level and sand. The next unit was laid on top of the bottom unit with mortar in between, with the mortar layer having a thickness of between 8 and 15 mm. The top unit was laid onto the middle unit in the same manner. After this construction the linear alignment and level was inspected with a spirit

level by the mason. Immediately after constructing the prisms they were covered with polythene sheets and pre-compressed with a load of $2.4 \times 10^{-3} \text{ N/mm}^2$, by adding weights to the top of the prisms. The polythene sheets were kept in place by small weights, which ensured limited air movement over the prism allowing better curing and bond development of the mortar. All prisms were tested at $7 \text{ days} \pm 1 \text{ day}$ after construction.

A mortar sample was again taken from each mortar batch created to ensure the consistency of the mortar. The same tests conducted on the mortar samples taken from the construction process of the crossed-brick couplets were again conducted on these mortar samples. Figure 5.19 shows one of the ADB triplet prisms after curing for 7 days.



Figure 5.19: ADB triplet specimen

Twelve triplet specimens were constructed and tested for each masonry material. Procedure A, from the standard specifies that pre-compression loads of 0.1 N/mm^2 , 0.3 N/mm^2 and 0.5 N/mm^2 are used for units with compressive strengths below 10 MPa , and pre-compression loads of 0.2 N/mm^2 , 0.6 N/mm^2 and 1.0 N/mm^2 for units stronger than 10 MPa . The code specifies that three triplet specimens are tested at each pre-compression level. However, the pre-compression loads used in this study were adjusted from those specified by the code due to material and test setup limitations. The test setup used in this study was adopted from the study of Fourie (2017). This test setup is limited to a pre-compression load of 0.5 N/mm^2 .

The adjustments made to pre-compression loads specified by the code is as follows. Instead of applying the first pre-compression load of 0.1 N/mm^2 , zero pre-compression was applied. This allowed for obtaining a more pure cohesion value (τ_c) and not an estimation through linear regression. Fourie (2017) also did the same in his research study. Due to this study also focusing on determining the dilatancy of the joint interface at different pre-compression loads, higher pre-compression loads were desired to determine at which pre-compression load the dilatancy tends to zero. Therefore, the test setup of Fourie (2017) was adjusted to apply higher pre-compression loads. Four pre-compression levels were applied to the triplet specimens and these were, 0 N/mm^2 , 0.3 N/mm^2 , 0.5 N/mm^2 and 2 N/mm^2 . A pre-compression load of

2 N/mm^2 is not realistic for the typical compression stress state found in masonry walls of low income housing (LIH) in South Africa. However, a high pre-compression load was desired that is not usually studied in literature and presents a means to investigate the influence of such high pre-compression stress on the different shear properties of the joint interface.

Due to the weak ADB unit, pre-compression loads of 0.3 N/mm^2 and higher crushed the ADB triplets. Therefore, only three pre-compression levels were chosen for the ADB specimens and these were, 0 N/mm^2 , 0.05 N/mm^2 and 0.1 N/mm^2 . The test setup can, therefore, be seen as consisting of three parts. The first setup is for testing specimens at 0 N/mm^2 pre-compression, the second for testing specimens above 0 N/mm^2 and up to 0.5 N/mm^2 . Both these setups were also used by Fourie (2017). Lastly, to test specimens at pre-compression loads above 0.5 N/mm^2 .

The zero pre-compression test setup used the 2 MN IMTM for conducting the triplet test. Figure 5.20 shows the triplet test setup for zero pre-compression inside the testing machine.



Figure 5.20: Triplet test setup at zero pre-compression

The test setup consists of four support plates, six steel rollers and a pot bearing. The only function of the steel rod and support channels in this setup is to ensure that parts of the specimen does not fall out of the testing machine upon failure. This is not clear on the figure, but there is open space between the support channels and the specimen on either side.

The bottom support plates and rollers were first put in place, and then the specimen was lowered carefully into the test setup on top of the support plates. Thereafter, both top support plates, the rollers and the pot bearing were added to the setup. Each support plate has the same dimensions as the headface of a masonry unit, which is 116 mm by 140 mm . The support plates have a thickness of 12 mm and the steel rollers a diameter of also 12 mm . The pot bearing ensured that everything is level.

The setup was modified to test specimens with pre-compression. The modification allowed for a horizontal force to be applied to the specimen by use of a hydraulic jack and a 50 tonne load-cell. The 50 tonne load-cell has a resolution of 29.4 N which is 1.45% of the lowest pre-compression load, 0.05 N/mm^2 , applied to the ADB triplet specimen. Therefore, this resolution is deemed satisfactory for all pre-compression levels. Figure 5.21 shows the test setup for applying pre-compression loads of up to 0.5 N/mm^2 to a specimen. Figure 5.21 shows the whole setup with labels defining the different parts of the setup. Four steel channels connected with two steel rods keep the whole setup together.



Figure 5.21: Triplet test setup for applying pre-compression

The fourth channel anchors the steel rods and supports the hydraulic jack. The hydraulic jack applies a force onto the third channel which pushes against the steel spring. As the steel spring is compressed it pushes against the second channel which applies the pre-compression force to the specimen. The first channel supports the 50 tonne load-cell and anchors the steel rods on the other side. Anchor bolts are used on either side of the steel rods to anchor the first and fourth channel to the steel rods. Two vertical support plates are attached to either side of the specimen to distribute the pre-compression load over the bedface area of the specimen. These plates are not supported but are kept in place by the horizontal force of the pre-compression. Both vertical support plates have a thickness of 20 mm. The second channel and the 50 tonne load-cell push against the support plates and hold them in place. Each vertical support plate has the same dimensions as the bedface surface of a masonry unit, which is 140 mm by 290 mm. The load-cell measures the level of pre-compression applied by the hydraulic jack. This allows for adjusting the pre-compression during a test if it is required.

The code specifies that the pre-compression load should stay within $\pm 2\%$ of the initial pre-compression load during the test. However, when the masonry prism fails in shear at one of the joint interfaces there is not only vertical displacement at the interface, but horizontal displacement as well (this is termed as dilatancy), when the specimen is confined this horizontal displacement causes the pre-compression load on the specimen to increase. The steel spring was added to the setup to counteract this phenomenon and keep the pre-compression load as close as possible to the initial value. The steel spring, however, is fully compressed at a force of 0.5 N/mm^2 and, therefore, is of no use for pre-compression stresses higher than this.

To reach pre-compression stresses higher than 0.5 N/mm^2 the spring was removed from the setup. This resulted in a setup similar to the one in Figure 5.21 but without the third channel and the steel spring. The pre-compression load was adjusted by hand to ensure that the pre-compression load stay within $\pm 2\%$ of the initial value during tests. The pressure release on the jack was adjusted during tests to avoid pre-compression loads increasing to a value above the 2% threshold. Figure 5.22 shows the third triplet test setup used for testing specimens at a pre-compression level of 2 N/mm^2 . For each of the three triplet test setups the testing machine applied a vertical load onto the specimens at a rate of 0.5 mm/min until failure.

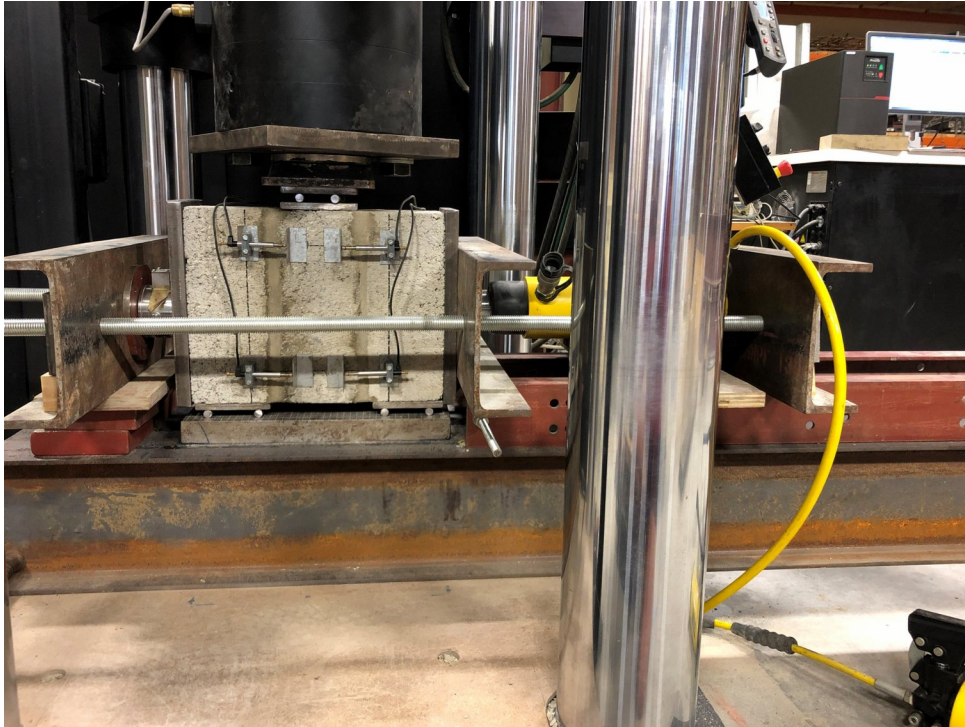


Figure 5.22: Triplet test setup for levels of high pre-compression

As stated in Section 5.3.2, the code requires that the failure mode is recorded for each test and that these failure modes comply with specific failure modes from the code. These failure modes include shear failure in the joint interface or only in the mortar. If any other failure mechanism was obtained the test was discarded. Most failures occurred at the joint interface at all the pre-compression levels. Failure occurred usually only at one of the interfaces of the specimens with zero pre-compression, where both interfaces mostly failed for specimens with pre-compression.

To obtain the dilatancy of the masonry specimens a total of six LVDTs were attached to each specimen. The six LVDTs consisted of four small 10 mm LVDTs (refer to Figure 5.20) that measure the horizontal displacement at shear failure over each interface, and two long 10 mm LVDTs (refer to Figure 5.23) that measure the vertical displacement at shear failure over each interface. Two horizontal and one vertical LVDT were attached over each interface of the masonry specimen. The average of the two horizontal LVDTs was used for a better representation of the horizontal displacement of the whole interface upon shear failure. Measurements of one vertical LVDT were considered sufficient to obtain the vertical displacement at the interface at shear failure. Figure 5.23 shows the two vertical LVDTs that are attached to the back of each masonry prism. LVDT holders held the LVDTs in the correct place and orientation during testing. The LVDT holders were glued onto the masonry prisms with Pratley steel glue, a glue usually used for steel but showed good adhesion to masonry materials.

It is important that the LVDTs and the steel measuring plates, from which the LVDTs take measurements, are leveled horizontally and vertically with respect to the masonry specimen. If this is not the case and some of the LVDTs or steel measuring plates are misaligned, it can corrupt the displacement data from the LVDTs. It is important that the steel measuring plates are perpendicular to the LVDTs. The purpose of the steel measuring plates is to provide a measurable surface for the LVDTs to determine relative displacements of both side units relative to the middle unit of the specimen. Figure 5.20 shows the four small 10 mm LVDTs with their respective steel measuring plates and Figure 5.23 the two long 10 mm LVDTs with their steel measuring plates.



Figure 5.23: Back view of triplet test setup

Data recorded from each test include the pre-compression and vertical loads applied during the test, as well as the displacement data from the LVDTs. The maximum vertical load and the area of the joint interface is used to determine the initial shear strength of the specimens. The shear fracture energy of the joint interface is calculated as the area under the load-displacement graph, after the peak load is reached. Linear regression of points was used with the shear strengths at different pre-compression loads to determine the friction angle of each type of masonry material investigated in this study. The dilatancy of each interface was calculated from the vertical and horizontal displacement data (change in volume) obtained from the LVDTs.

Due to the confined nature of the third test setup (Figure 5.22) it could affect the dilatancy. It was predicted that shear-slipping would likely occur, rather than horizontal displacement at the interface upon shear failure. Results, however, showed that horizontal displacement still occurred under these higher pre-compression loads even with the more confined test setup, but of a lesser extent than when the steel spring was included in the test setup.

This study deviated from the experimental setup proposed by EN 1052-3 (2002) by adding another steel roller to each of the two bottom support plates, see Figure 5.20. Problems were encountered with placing the masonry specimens into the test setup with only one steel roller at each bottom support plate, especially with the weak ADB prisms where failure sometimes occurred under its own weight. The addition of a second steel roller causes internal moments on the joint interface, but due to the setup challenges with only one steel roller, the effect of two steel rollers on the test setup was accepted. For comparison, this method was kept the same for all the alternative materials investigated in this study.

Another problem encountered at higher pre-compression loads was in-plane moments occurring over the joint interface of specimens, due to the point load of the load-cell onto the vertical support plate. The vertical support plate was unable to fully distribute the horizontal load over the side of the triplet specimen.

5.4 Conclusion

This chapter discussed the experimental procedure followed to characterise the mechanical properties of the different types of masonry materials and mortar investigated in this study. Experimental tests that were conducted can be divided into three categories, tests on individual masonry units, mortar tests and joint interface tests on masonry. The individual masonry unit tests included compression tests, modulus of elasticity tests, water absorption tests and dry density tests. The mortar tests that were investigated included flow table tests, modulus of elasticity tests, dry density tests, compressive tests and flexural tests. The joint interface tests included the crossed-brick couplet test and the triplet test. Both of the latter tests were conducted on masonry specimens. The four masonry materials included in the study are CON, CSE, ADB and GEO.

The following was discussed for each test in this chapter. The preparation of the test specimen, the test setup configuration, the data recording equipment used to capture results and where the test setup deviated from the standard used as reference for the test. All of the tests seemed to comply to the standard and not much deviation was required. One material, however, that presented problems with some of the test was the ADB material. Testing specifications are adjusted for the modulus of elasticity and triplet test for the ADB material.

Chapter 6

Results, Comparisons and Discussion

A number of experimental tests were conducted on masonry units, mortar and masonry specimens. Each masonry test was conducted on four different masonry materials namely, concrete (CON), geopolymer (GEO), compressed stabilised earth (CSE) and adobe (ADB). Results are also presented in this sequence since it follows the strength and stiffness trends of the different materials and makes relative comparison of results easier. The experimental procedure of each test is discussed in detail in Chapter 5.

Past research has been conducted on the four masonry materials investigated in this study at Stellenbosch University (Barnard, 2014; Malherbe, 2016; Fourie, 2017; Shiso, 2019). Therefore, this study aims at widening the knowledge of the mechanical properties of these materials and not to repeat tests that have already been done. One of the main objectives of this study is to characterise the tensile and shear properties of the joint interface of alternative masonry. Meagre research is available on these material properties and especially on alternative masonry materials. A reason for this can be attributed to the complex test setups needed to obtain these properties. This study presents an experimental procedure to characterise the joint interface of alternative masonry. A further aim of this study is to add reliable data to literature, of the mechanical properties of alternative masonry and the reason for this is twofold. Firstly, to complement further studies in developing a finite element model (FEM) to analyse structures with different geometries constructed out of alternative masonry units (AMUs) in a performance-based manner. Secondly, to contribute towards the regulation of construction with AMUs in South Africa. Both these motivations originate from seeking a sustainable solution to the backlog of low income housing (LIH) construction in South Africa.

This chapter discusses the mechanical properties that are determined from the tests discussed in Chapter 5. These tests include masonry unit, mortar and joint interface masonry tests. Compressive strength tests, modulus of elasticity tests and dry density tests are conducted on the masonry units and mortar. Further masonry unit tests include, water absorption and surface roughness tests. Additional tests conducted on the mortar include, flow table and flexural strength tests. The main tests of this study, the joint interface masonry tests, include the crossed-brick couplet test and the triplet test. The results obtained from each test are compared to literature to determine if they fall within a range of acceptable results for the mechanical property under investigation. The suitability of the test setups on the different masonry materials is discussed for each test on each material. Each test is first conducted on the CON material which acts as the benchmark material in this study to determine if the test functions properly and produces satisfactory results. Thereafter is discussed if the same setup can be successfully applied on the different AMUs.

6.1 Masonry Unit Test Results

The focus of this study is on the joint interface of masonry, therefore, different properties of the masonry units and mortars used are investigated to determine its affect on the joint interface. Two overarching factors play a role in the bond development process of the joint interface of masonry. Firstly, the unit characteristics and, secondly, the mortar characteristics. Mechanical properties such as the compressive strength, modulus of elasticity and dry density of masonry units do not have a large affect on the bond development, but, are important properties in terms of quality control of the unit itself and comparison to previous research. These tests acts as benchmark tests throughout literature. The results of these masonry unit tests are presented and discussed in this section.

Water absorption and surface roughness are seen as material properties that have a larger influence on the bond development process of the joint interface than the benchmark tests discussed earlier. Results from these tests, on the four masonry materials, are presented in this section.

6.1.1 Compressive Strength

The compressive strength of masonry units is one of the most common mechanical properties studied. This usually determines the possibilities of the geometry of a structure and aids most in the design process. The reason for determining the compressive strength of the masonry units in this study is for quality control and comparison to results obtained from literature. The results are compared to literature not to ensure that they are the same, but to determine if the masonry unit strengths fall in a range of acceptable results for each material type.

Compressive strength tests were conducted at 28 days on the CON, GEO, CSE and ADB units. The 28 day strength was specifically chosen due to this being the most common used age for compressive strength testing under conventional masonry units (CMUs). For each test 10 masonry units of the same material were used to obtain reliable results. The aim of using 10 units per materials is to present a good representation of the compressive strength of the material as a whole. All the masonry units were of the same size which meant that no aspect ratios where needed to compare results between the different materials.

As stated, this mechanical property does not have such a big influence on the joint interface properties of masonry and, therefore, compressive strength tests were not conducted on masonry units of the same age as the age of masonry units used for the joint interface tests, discussed in Section 6.3. The test procedure by the European testing standard, EN 772-1 (2011), was followed to determine the compressive strength of the masonry units and is discussed in Section 5.1.1. Compressive strength tests on masonry units are usually conducted in one of two orientations, either in bedface or headface orientation, with bedface being the more popular one. All compressive strength tests conducted in this study were on masonry units in bedface orientation.

Figure 6.1 represents the compressive strength results of the four masonry materials at an age of 28 days. The dots represent the average compressive strength measured for each material type and the variability of compressive strengths is represented by standard deviation error bars at each dot. The average compressive strength of each material, as shown in Figure 6.1, is also displayed in Table 6.1 with its respective COV percentage.

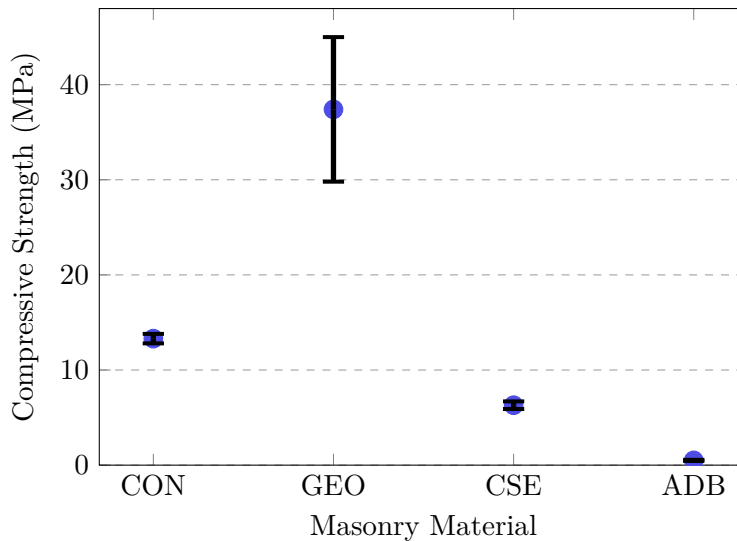


Figure 6.1: Average compressive strengths measured at 28 days for CON, GEO, CSE and ADB units

Table 6.1: Average compressive strengths (f_c) values presented in Figure 6.1 and the coefficient of variation (COV)

Material	CON		GEO		CSE		ADB	
	f_c (MPa)	COV (%)	f_c (MPa)	COV (%)	f_c (MPa)	COV (%)	f_c (MPa)	COV (%)
28 days	13.3	3.9	37.4	20.4	6.3	6.0	0.5	11.7

The differences in the average compressive strength between the different materials can clearly be seen in Figure 6.1. The GEO unit has the largest average compressive strength, almost three times the strength of the CON unit which has the second highest strength. The CSE unit has the third highest strength, almost exactly half the strength of the CON unit. The ADB unit is the weakest of all the materials reaching only 0.5 MPa.

The compressive strengths of the CON, CSE and ADB units were in line with expectations. However, the GEO unit showed much greater compressive strengths than expected and also the largest variation in results in terms of standard deviation. It was expected that the variation in compressive strength results would be the highest in the group, due to the number of factors in its mix design that have an influence on the compressive strength (refer to Table 2.2). It should be noted that larger average values are expected to have higher standard deviations than lower average values due to the nature of how the standard deviation is calculated and is, therefore, not the best value to use for comparing the variation in results from different result groups.

A value used to better understand the extent of variation of data is the coefficient of variation (COV). The COV shows the extent of dispersion of values in a group relative to the average value of that specific group and is usually expressed as a percentage. The COV presents a percentage that can be used to compare the variation of values in different result groups relative to each other, even if the average values of each group differ by a large amount.

It can be seen from the COV results that the GEO unit shows the largest variation in results, with the highest COV percentage almost double that of the material with the second highest

COV, the ADB unit. For masonry units a COV of 10% is usually acceptable and almost all of the units comply to this except the GEO unit.

It is important to note that the aim of the GEO unit mix design was not to optimise the mix in terms of strength of the end product but rather to obtain a unit with similar attributes to that of units produced in previous studies at Stellenbosch University. As stated in Section 4.2.2, the mix design of Fourie (2017) which was first adopted in this study, gave a mix with no workability. Therefore, a trial and error technique was adopted until a mix with satisfactory workability was obtained. Even though this mix produced an end unit with higher compressive strengths than the GEO unit of Fourie, the compressive strength of a unit does not affect the joint interface tests which are the main focus of this study and therefore it was accepted. The mix designs of Fourie were adopted for the CON, CSE and ADB unit and similar compressive strengths were obtained.

These strengths are compared to masonry unit strengths from literature and standards to determine if the different materials in this study fall within an range of acceptable results for the material type. As discussed in Section 2.2 the national buildings regulations (NBR) in a revised standard, SANS 10400-K (2015), states that the average compressive strength of a solid CMU shall not be less than 4 MPa and all the units, except the ADB unit, of this study exceeds this. Fourie did research on a range of acceptable results from literature for the CSE and ADB units and found that both materials complied to these ranges. Due to the results from this study being so similar to those of Fourie the compressive strengths of these material can be deemed acceptable. Again, in terms of masonry unit characteristics the aim of this study is to investigate those characteristics that influence the joint interface bond strength of masonry. Characteristics that influence the bond strength of the joint interface less were not investigated in depth.

As discussed in Section 5.1.1 the European testing standard, EN 772-1 (2011), presents a method to determine the normalised compressive strength of CMU units by the use of a shape factor. The shape factor of the units used in this study was calculated according to the size of the units and the method proposed by EN 772-1 (2011) as 0.984 for a unit in bedface orientation. Table 6.2 shows the normalised compressive strengths after the shape factor is taken into account.

Table 6.2: Normalised average compressive strength (f_{nc}) values

Material	CON	GEO	CSE	ADB
f_{nc} (MPa)	13.1	36.8	6.2	0.5

The test procedure in EN 772-1 (2011), which was adopted in this study, presents a method to determine the compressive strength of clay, calcium silicate, aggregate concrete, autoclaved aerated concrete, manufactured stone and natural stone masonry units. These units are considered as standard CMUs investigated by the European testing standard. The AMUs from this study vary from these materials to different degrees and, therefore, it is important to determine if this test procedure can be successfully applied to the different AMUs in this study.

The test procedure of EN 772-1 (2011) presents a simple and straight forward method for determining the compressive strength of masonry units. Due to this the test could be executed on all the different type masonry units without any major issues. The fact that all the masonry units had the same size meant the results were also easy to compare. From the results it can be seen that the test procedure was successfully applied on the benchmark CON material. The test produced consistent results for most materials and this can be concluded from the small COV percentages. The only material that showed high COV percentages was the GEO unit,

but this was attributed to the number of factors influencing the strength of these units and not due to inconsistencies from the test setup. Therefore, this test procedure and test setup is seen as suitable for this study.

6.1.2 Modulus of Elasticity

The modulus of elasticity of a material, also known as the "stiffness" of that material, is also a common mechanical property studied for masonry materials. If the stiffness of a material is known, the deformations under certain loads of that material can be calculated. Therefore, this mechanical property is important when load bearing structures are designed. The modulus of elasticity of the different materials in this study is determined to conclude if these materials fall within an acceptable range from literature or standards.

The test procedure in the European testing standard, EN 12390-13 (2013), was followed to determine the modulus of elasticity of the different masonry units investigated in this study. This test procedure and, how it was executed, are discussed in Section 5.1.2. The modulus of elasticity tests were conducted at 28 days on all four material types. A total of 10 specimens were tested for each material to again, such as with the compressive strength tests, obtain results that represent an acceptable average of the material as a whole. The tests were conducted on 28 days to compare, if possible, these results to the compressive strength results. The age, 28 days, is normally also the standard age for testing the modulus of elasticity for conventional masonry materials. Figure 6.2 represents the modulus of elasticity results of the four masonry materials at an age of 28 days.

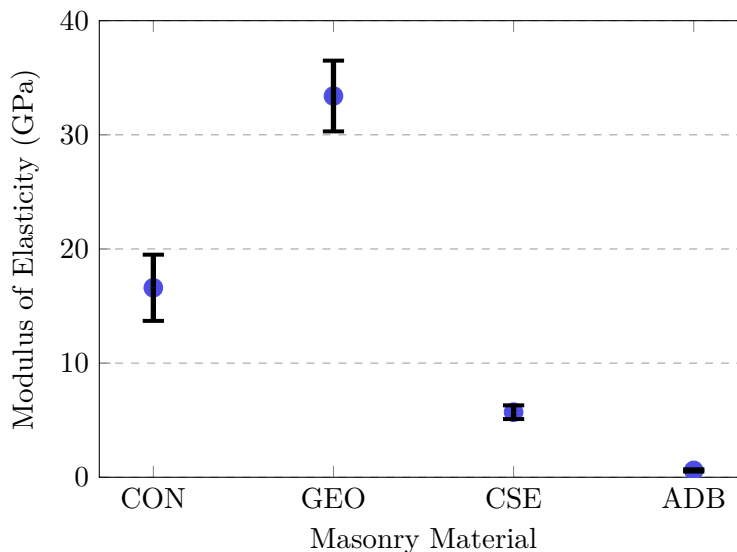


Figure 6.2: Average modulus of elasticity measured at 28 days for CON, GEO, CSE and ADB units

It can be seen that a similar trend in results is obtained as with the compressive strength results. The GEO material has the highest modulus of elasticity, then the CON material and thereafter the CSE material. The ADB material again showed the lowest value, and in this case the lowest modulus of elasticity by a relatively large amount. These results were however expected, and the low modulus of elasticity of the ADB unit was no surprise due to the weak nature of its material.

Table 6.3 shows the average modulus of elasticity results of Figure 6.2 with the corresponding COV values of the results. The modulus of elasticity test is a much more complex test than the compressive strength test and, therefore, there is larger opportunity for variations to occur in the results. This is confirmed by the COV values in Table 6.3. The slenderness of the elastic modulus specimens also likely play a role in the variability in results. The Eurocode presented a standard for design of masonry structures, EN 1996-1 (2005), where in the absence of a modulus of elastic value determined by testing, the modulus of elasticity of a material can be determined by $K_E f_{ck}$. The recommended value for K_E is 1000 (this is a conservative value) and f_{ck} is the characteristic compressive strength of masonry. Even though this method is applicable to masonry and not masonry units, it should give similar results when applied to masonry units.

Table 6.3: Average modulus of elasticity values presented in Figure 6.2 and the coefficient of variation (COV)

Material	CON		GEO		CSE		ADB	
	E (GPa)	COV (%)	E (GPa)	COV (%)	E (GPa)	COV (%)	E (GPa)	COV (%)
Age								
28 days	16.6	17.4	33.4	9.4	5.7	9.6	0.6	20.6
$K_E f_{ck}$	13.1	-	36.8	-	6.2	-	0.5	-

This would mean that the compressive strength (in MPa) and the elastic modulus (in GPa) should be of the same numeric value, and this a conservative value. For this study this was nearly the case for all of the masonry materials. If the normalised compressive strengths is multiplied by K_E , values are obtained that differ from the elastic modulus results with 21%, 10%, 9% and 20% for the CON, GEO, CSE and ADB materials respectively, see Table 6.3 for these values. Conservative elastic modulus values are obtained for the CON and ADB material while non-conservative values are obtained for the GEO and CSE materials. Nonetheless, the elastic modulus values obtained from the tests in this study are still close to the predicted modulus of elastic values from the method proposed by EN 1996-1 (2005). Interesting to note is that the method by EN 1996-1 (2005) is applicable to CMUs, but the AMUs showed less variation.

Even though higher COV values were expected for this test in comparison to the compressive strength tests, the CON material produced higher COV values than expected. This can be attributed to the method of creating the elastic modulus specimens. As explained in Section 5.1.2 the CON, CSE and ADB specimens were cut with an industrial asphalt saw from existing masonry units. This method allowed testing of each material in the same direction as the compaction pressure applied upon block manufacturing. These specimens are, however, small (refer to Figure 5.4) and this, with the technique of sawing the specimens from bigger units, can lead to various inconsistencies. This could be a possible reason for the variation in results for the CON material. The variation for the ADB specimens was expected due to the weak nature of the material, and problems were also encountered with the testing machine, for testing under such sensitive loads and displacements.

The Eurocode, EN 1996-1 (2005), presents a method to determine the modulus of elasticity of conventional hardened concrete of either cylindrical or prismatic specimens. Cylindrical specimens are more popular and the testing equipment is more widely available. Due to the fact that the cylindrical specimens were casted and the prismatic specimens cut with a saw, there is a larger chance of inequalities existing in the prismatic specimens. This could mean that the cylindrical test setup is more stable than the prismatic test setup. If possible, all the materials would be cast in cylindrical specimens, but due to the method of manufacturing the masonry units only the GEO material could be cast in cylindrical specimens without altering the material

properties. This could possibly explain why the COV value for the GEO material is lower than the other materials, due to the cylindrical test setup producing more consistent results.

Even though challenges were encountered with the modulus of elasticity tests in this study, the results obtained are deemed to acceptable and the test method suitable for AMUs. Results obtained from this study were similar to those obtained by previous researchers at Stellenbosch University (Fourie, 2017; Shiso, 2019).

6.1.3 Dry Density

Dry density tests were conducted at 28 days on the CON, GEO, CSE and ADB units as discussed in Section 5.1.3. The density of a material gives an indication of the mass of that material per unit volume. The density of each material was determined to use as a measure of quality control throughout the manufacturing process. This could present a method of determining the consistency of the mix design for different masonry unit batches in the manufacturing process.

The method proposed by the European testing standard, EN 772-13 (2013), was used to determine the dry density of the four different types of masonry units investigated in this study. A total of 10 units were tested to obtain the dry density of the material as a whole. These 10 units were taken throughout the manufacturing process of each material from different batches.

Figure 6.3 displays the dry densities of each material with standard deviation error bars. From Figure 6.3 it can be seen that the GEO material has the largest dry density with the CON material having the second highest dry density. The CSE and ADB material have similar dry densities with the CSE being a bit more dense than the ADB material, this can be attributed to the larger water content in the CSE mix design. These densities were expected, larger aggregates such as stone usually have higher densities than smaller aggregates such as sand and clay. The GEO material contains the largest aggregates (13 mm stone) in its mix design and the CON material consists of quite a large proportion of crusher dust (a mixture of small stones and dust), and both these materials have higher densities than the CSE and ADB units which consist of only sand and clay aggregates. Another reason for the high density of the GEO unit could be attributed to the self compacting nature of the fresh GEO material, which ensured less voids than the CON unit which has a dry mix in its fresh state.

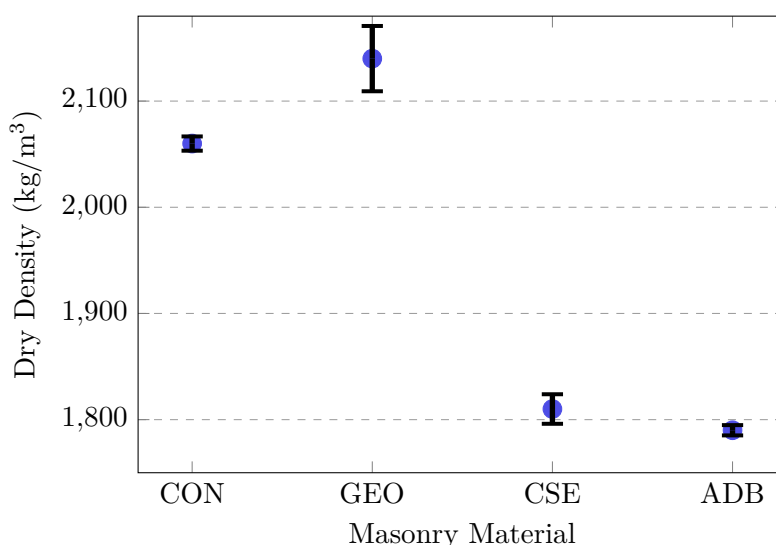


Figure 6.3: Average dry density measured at 28 days for CON, GEO, CSE and ADB units

Table 6.4 shows the dry density values of each material presented in Figure 6.3 with their respective COV values. It can be seen from Table 6.4 that the COV values for the four different materials are all low. The GEO unit shows the highest COV value, and this can again be attributed to the number of different factors that have an influence on the end product. Due to the fast setting time of the GEO material, challenges sometimes occurred with the casting process of the GEO material into the wooden moulds (this procedure is explained in Section 4.2.2). When the material set too quickly voids in the unit could not be removed with vibration and this resulted in an end product with a lower density, which could lead to a variation in results.

Table 6.4: Average dry density values presented in Figure 6.3 and the coefficient of variation (COV)

Material	CON	GEO	CSE	ADB
Dry Density (kg/m ³)	2060	2140	1810	1790
COV (%)	0.3	1.4	0.8	0.3

Another aspect that could influence the consistency of the end product of the different materials is varying curing conditions. Different materials spent different amounts of time in the laboratory air while curing, where the temperature and humidity varied. The laboratory was not enclosed at all times and, therefore, the laboratory air was sometimes subject to the outside weather conditions. Even though the total amount of each type of masonry unit was produced as quickly as possible, each material still took between two and three weeks to manufacture and the bulk of the masonry units were produced in the early winter season where weather conditions could vary enormously from day to day in the southern parts of the Western Cape in South Africa. Refer to Section 4.2 to find the curing conditions of each material.

The method proposed by EN 772-13 (2013) to determine the dry density of masonry units is straightforward and produced suitable and consistent results when applied to the AMUs of this study even though this standard was developed for the standard CMUs investigated by the European testing standard (these standard units are discussed in Section 6.1.1).

6.1.4 Water Absorption

The water absorption characteristics of a masonry unit play an important role in the bond development process of the joint interface (Sugo *et al.*, 2001; Sarangapani *et al.*, 2005; Walker, 1999). Masonry units with high water absorption rates can cause dewatering of the mortar at construction, this could lead to workability issues and cause weak bonds to form at the joint interface due to insufficient hydration of the cement particles. The reason for determining the water absorption characteristics of the four different masonry units in this study is to determine to what extent this has an effect on the bond development process.

The test proposed by the European testing standard, EN 772-11 (2011), was followed to determine the water absorption characteristics of the four different type materials investigated in this study, and how it was implemented is discussed in Section 5.1.4. The test method requires that the units be oven dried before the test, therefore the same 10 units used for the dry density test were used for the water absorption tests directly after the dry density tests were complete. The units were, therefore, just over an age of 28 days when they were tested.

The most popular water absorption parameter found in literature is the IRA and, therefore, this value was also investigated in this study for all the four materials. Table 6.5 represents the water absorption results for each material. The IRA and the coefficient of water absorption (a value caused by the capillary suction of a material) are both presented for each material in Table 6.5, each with their respective COV value.

Table 6.5: Average water absorption results and the coefficient of variation (COV)

Material	CON	GEO	CSE	ADB
IRA kg/(m ² ×min)	1.2	0.5	3.5	-
COV (%)	15.7	19.7	5.6	-
Coefficient of water absorption g/(m ² ×s)	4.2	1.9	12.9	-
COV (%)	16.5	21.2	6.4	-

It can be seen from Table 6.5 that the CSE unit has the highest IRA value. The CON unit has just more than a third of the IRA of the CSE unit, and lastly the GEO unit has an IRA value of slightly less than half the CON unit. No water absorption characteristics were recorded for the ADB unit due to the ADB unit completely dissolving upon coming into contact with water, see Figure 5.9 in Section 5.1.4. Literature suggests that earth block masonry has the highest IRA values of any masonry unit, however, a binder is required to be present in this type masonry unit otherwise the unit will likely dissolve like the ADB unit in this study.

The capillary suction is an important process in the cohesive strength of the mortar and adhesive strength between the masonry unit and mortar (Sugo *et al.*, 2001). Sugo *et al.* define the capillary suction in masonry as the process that results in the dewatering of mortar and the transport of mortar fines to the joint interface. It can be seen from Table 6.5 that the coefficient of water absorption due to capillary action follows a similar trend to that of the IRA values.

Values for the IRA of the CON and CSE unit are close to that found in literature. Sugo *et al.* did research on dry pressed clay units and concrete units and found values of 3.39 and 1.45 kg/(m²/min) respectively. The IRA values of the CON and CSE unit varied with only 0.11 and 0.25 kg/(m²/min) to the values of Sugo *et al.* IRA values of a GEO material are scarce in literature and no water absorption characteristics could be sourced for this material. Lawrence and Page (1994), however, state that an optimal IRA would be between 0.5 and 1.5 kg/(m²/min) and the IRA of the GEO unit falls within this range. It should be noted that the rate of absorption at the state of the masonry units when laying the masonry units, for constructing masonry, influences the bond strength and not the rate of absorption of units in the oven dry condition, like required by EN 772-11 (2011).

Lawrence and Page also suggest that the absorption rate of masonry units, and the effect of this brick suction on the bond strength, is not finished after the first minute (which is the time period considered for the determining the IRA), but continues for different periods of time depending on the material type. Therefore, the water absorption by weight (expressed as a percentage) of the CON, GEO and CSE units was determined over a period of 3 days or until the unit was fully saturated. Figure 6.4 shows the water absorption of the different masonry units by weight over a 24 hour period.

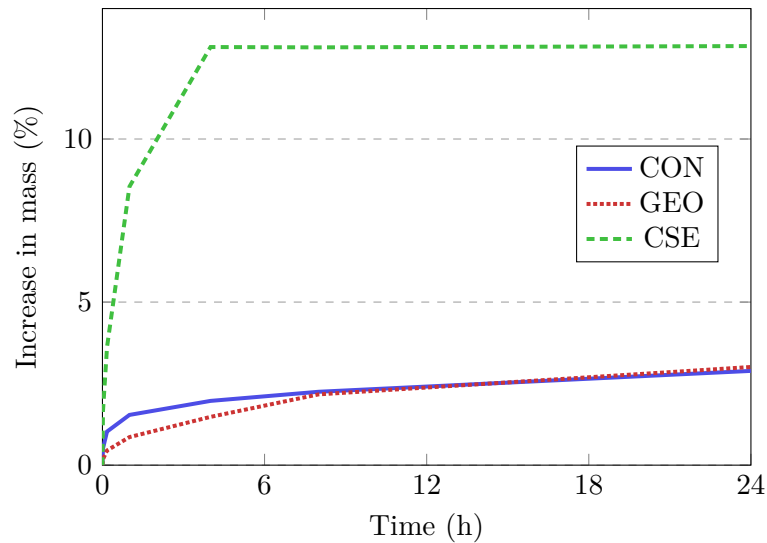


Figure 6.4: Water absorption of different masonry units by weight

It can be seen from Figure 6.4 that the CSE unit is fully saturated after 4 hours, which is confirmed by Figure 5.8 in Section 5.1.4. The CON and GEO units follow approximately the same water absorption rate after 8 hours, where the CON unit has a higher initial water absorption rate than the GEO unit. It is not displayed in Figure 6.4, but the CON and GEO units still increased with 1% and 1.5% in weight, respectively, over the next 48 hours. This shows that the GEO unit has a higher water absorption rate after 24 hours. The CON and GEO units were not fully saturated after 3 days, but the rate of absorption decreases significantly and, therefore, it was accepted that both units were nearly saturated.

It is possible that the density of a masonry unit can have an effect on the water absorption characteristics. The less dense a material, the more voids are present and the larger the capacity to absorb water into those voids. This is seen as the GEO has the largest dry density, but the smallest IRA. The CSE is again the least dense materials but has the highest IRA. Another parameter that could have an effect on the water absorption rate of a masonry unit is the clay content of that unit. Clay has a high suction characteristic upon contact with water. Both these factors could explain the high initial absorption rates of the CSE unit and the lower absorption rates of the CON and GEO material.

Even though Figure 6.4 shows that water absorption continues at different rates for different masonry units after the first minute, Sugo *et al.* (2001) suggest that this is not the case along the joint interface of masonry upon construction. Sugo *et al.* suggest that for low IRA units the end of water absorption from the mortar to the masonry unit will occur after a few minutes and for high IRA units after a few seconds. This is due to the mortar's own water absorption characteristics, which allows transportation of fluids from the saturated mortar to the relatively dry porous unit until an equilibrium is reached between the two materials where the suction potential of each material is equal to one another. This suggests that not only the water absorption characteristics influence the bond strength but also the rheology and water retentivity of the mortar.

Sugo *et al.* found that for units with a high IRA, the mortar stiffened in a few seconds at construction, causing the mortar to become unsaturated, leading to workability problems for the mason. This same problem was encountered with the CSE and ADB units in this study. This confirms that, even though the water absorption test could not be successfully conducted on the ADB units, the ADB units contained a high water absorption rate.

The test procedure of EN 772-11 (2011) presents a simple test method to determine the water absorption characteristics of masonry units. The results obtained for this study showed to be close to those found in literature, except for the ADB unit where no results could be determined. Even though results could not be obtained for the ADB unit, the test setup is deemed as acceptable and suitable for the two other AMUs investigated in this study.

6.1.5 Surface Roughness

The surface roughness of a masonry unit can have an influence on the bond development process at the joint interface. Literature has suggested that masonry units with an increase in surface roughness show an increase in bond strength (Reddy and Gupta, 2006; Tschegg *et al.*, 2008). The surface roughness of each material was investigated in this study to determine its effect on the bond strength of masonry.

Due to no standard being available to quantify the surface roughness of masonry units a method was adopted from literature (Reddy and Gupta, 2006), Section 5.1.5 discusses this method. Figure 6.5 represents the undisturbed surfaces and pores size distribution of each masonry material.

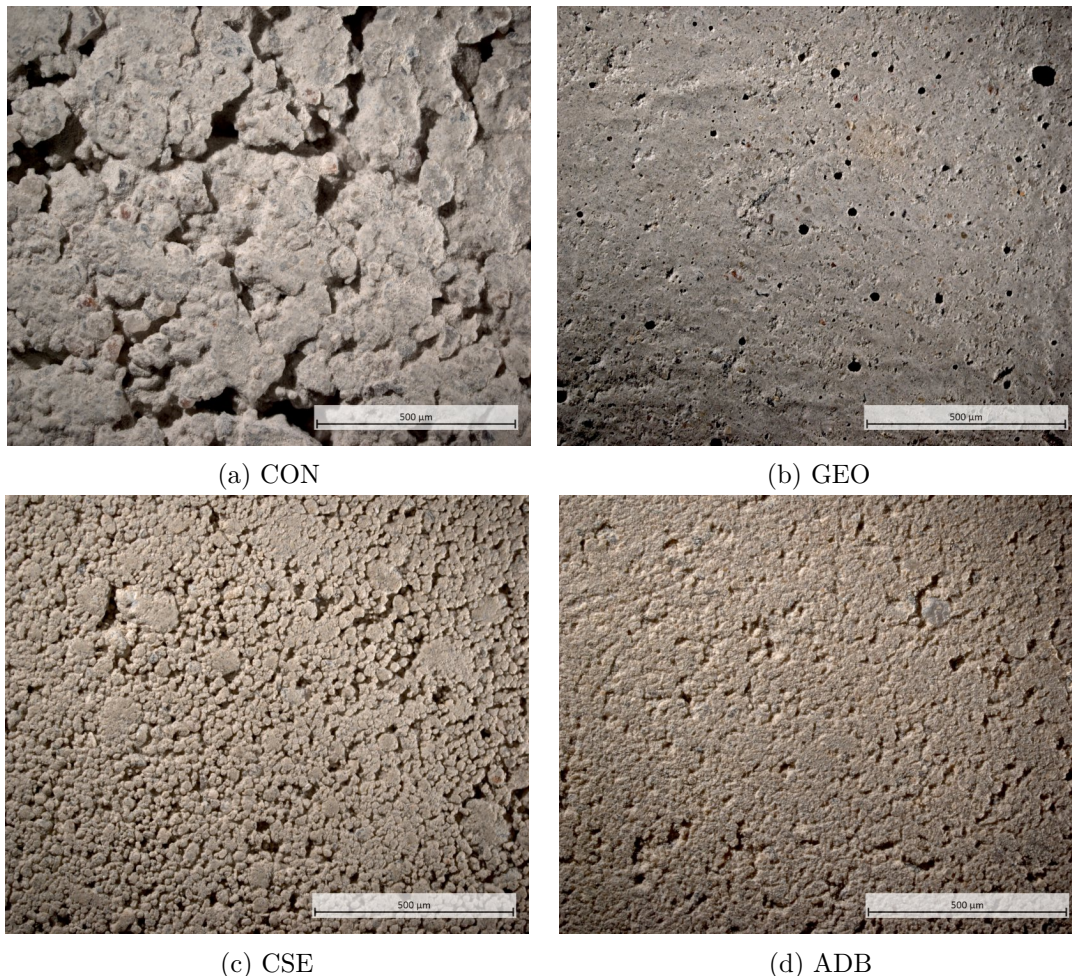


Figure 6.5: Surface images of typical CON, GEO, CSE and ADB unit

It can be seen from Figure 6.5 that the pore sizes differ significantly between the different types of masonry units. It can be clearly seen that the CON unit has the largest pores, and the CSE unit the most pores. The ADB surface look similar to the surface of the CSE unit, but with less

pores. The GEO unit by far has the least amount of pores and shows uniform pores with similar major and minor axis lengths. The major and minor axis lengths of the pores of the CON and CSE unit surfaces vary significantly. A possible reason for this could be attributed to the dry mix design of each unit at manufacturing. The method of manufacturing the units through the use of the manual Hydraform block press could also contribute towards forming these irregular pores. The ADB unit surface also contains irregular pores with some pores being more elliptical. It can be seen that the self compacting nature of the GEO material causes a much smoother surface for the end product.

Table 6.6 gives the pores size, number of pores and the surface porosity of each material as represented in Figure 6.5. It should be noted that the number of pores were determined for the same area and, therefore, the values are comparable against each other. Table 6.6 confirms that the pore size of the CON unit is the largest, followed by the CSE unit and then the ADB unit. The pore size of the GEO unit surface was the smallest. Interestingly, even though the pore sizes varied significantly between the CON and CSE unit surfaces the surface porosities were nearly the same, differing with only 0.5%. This could be attributed towards the significance difference in number of pores between the two materials.

The average pore sizes of the GEO and ADB units are similar. However, the ADB unit has 6 times more pores than the GEO unit. The CON unit showed half the amount of pores of the ADB unit, and the ADB unit more or less half the amount of pores of the CSE unit. It can be concluded from the number of pores and surface porosity results that the GEO unit has the lowest pore density of all the materials, and the CSE unit the highest.

Reddy and Gupta (2006) did research on soil-cement block masonry and found surface roughness parameters that are close to that of the CON and CSE unit of this study. Reddy and Gupta (2006) found average major and minor axis pore sizes of between 0.08 and 0.28 mm and surface porosities of between 14.1% and 14.9%. This shows that this test method is appropriate and in line with results from literature.

Table 6.6: Surface characteristics of masonry units

Material	CON	GEO	CSE	ADB
Average pore size - Major axis (mm)	0.21	0.03	0.08	0.05
Average pore size - Minor axis (mm)	0.08	0.03	0.02	0.02
Number of pores	142	49	536	294
Surface porosity (%)	14.7	0.9	14.2	8.0

6.2 Mortar Test Results

Mortar plays an important role in the bond strength of the joint interface of masonry (Groot, 1993; Grenley, 1969; Reddy and Gupta, 2006). Different mortar properties have different effects on the bond development process. Mortar in its fresh state usually has quite a large influence on the initial bond development of the joint interface and, therefore, tests are conducted on the mortars in both their fresh and hardened conditions. The following tests are conducted on fresh and hardened mortar and their results are discussed in this section: flow table tests, dry density tests, flexural strength tests, compressive strength tests and modulus of elasticity tests. All the mortar tests were conducted on mortars at 7 days. The reason for this is, all the masonry joint interface tests were conducted on 7 days \pm 1 day.

6.2.1 Flow Value of Mortar

The workability of a mortar can be quantified by conducting the flow table test. Varying flow values can effect the characteristics of the mortar, as well as the bond strength Reddy and Gupta (2006). Reddy and Gupta found that reducing the flow value of mortar increased its compressive strength, but led to a decrease in bond strength. Reddy and Gupta suggest that if the flow value of mortar is reduced below 100% the mortar becomes dry, which would reduce the mortar workability and it would then become difficult for the fresh mortar to effectively penetrate the pores on the masonry unit surface, leading to a weaker bond strength.

The test procedure proposed by the European testing standard, EN 1015-3 (1999), was adopted in this study to determine the flow value of both mortars used throughout this study. This test method and how it was executed is explained in Section 5.2.1. This test on the fresh mortar, along with the dry density and compressive strength test on the hardened mortar, were used as quality control tests throughout the construction phase of this study (building small masonry prisms for the joint interface masonry tests).

A target flow value of 100% was adopted for this study to keep the workability of both mortars constant and to aim for consistent bond development conditions throughout this study. Another reason for keeping the flow value constant was to remove a variable that could influence the bond strength or bond development process. Table 6.7 shows the average flow values of the two mortars used for the masonry specimen construction, with their respective COV values. It can be seen from Table 6.7 that the average flow values were close to 100% each with acceptable COV values.

Table 6.7: Flow value results of mortars

Mortar	7M	20M
Flow Value (%)	102	98
COV (%)	6.8	8.3

6.2.2 Dry Density of Mortar

The dry density values of both mortars were determined for this study to use as a measure of quality control. As explained earlier, the dry density values also represent a technique by which the consistency of the mix designs can be measured. The test procedure by the standard, EN 1015-10 (1999), was followed to determine the dry densities of both mortars.

Table 6.8 shows the dry density results for both 7M and 20M. It can be seen that 20M has a higher density than 7M, which is strange due to 7M having a larger water content than 20M. A larger water content usually leads to higher densities. A possible reason for the higher densities for 20M can be the higher cement content which increase the fines content in the mix ensuring better interlocking of particles in the material structures. A total of 10 mortar 100×100 cubes were tested to ensure a result that represents the mortar material as a whole.

Table 6.8: Average dry density results of mortars and the coefficient of variation (COV)

Mortar	7M	20M
Dry Density (kg/m ³)	1830	1990
COV (%)	0.7	0.5

6.2.3 Flexural and Compressive Strength of Mortar

Past research has suggested that there is a relationship between mortar compressive strength and mortar flexural strength. Lumantarna *et al.* (2014) found that the flexural bond strength and the initial shear strength of the joint interface is better characterised using the mortar compressive strength than using the masonry compressive strength (see Figures 3.6 and 3.9).

The reason for determining the compressive strength of both mortars is twofold. Firstly, for quality control measures and, secondly, to determine if these results are relatable to the masonry joint interface tests further conducted in this study. The mortar compressive strength tests served the same purpose as the flow table tests in this study. Mortar samples were taken throughout the masonry construction phase of this study and compressive strength tests were conducted on these mortars to ensure their quality and strength stayed consistent. Conventional cube tests were conducted to determine the compressive strength of the mortars at 7 days.

The test procedure proposed by EN 1015-11 (1999) was followed to determine the flexural strength of the mortar and is discussed in Section 5.2.3. The reasons for conducting the flexural strength test on both mortars are to determine if there is a relationship between the mortar compressive and flexural strength, as well as to investigate if any relationships exist between the mortar flexural strength and the tensile or shear characteristics of the joint interface of masonry.

Figure 6.6 shows the average compressive strength and average flexural strength results of both mortars. Columns on the left represent the flexural strength of each mortar and columns on the right the compressive strength. The variation in results is shown by standard deviation error bars at the top of each column.

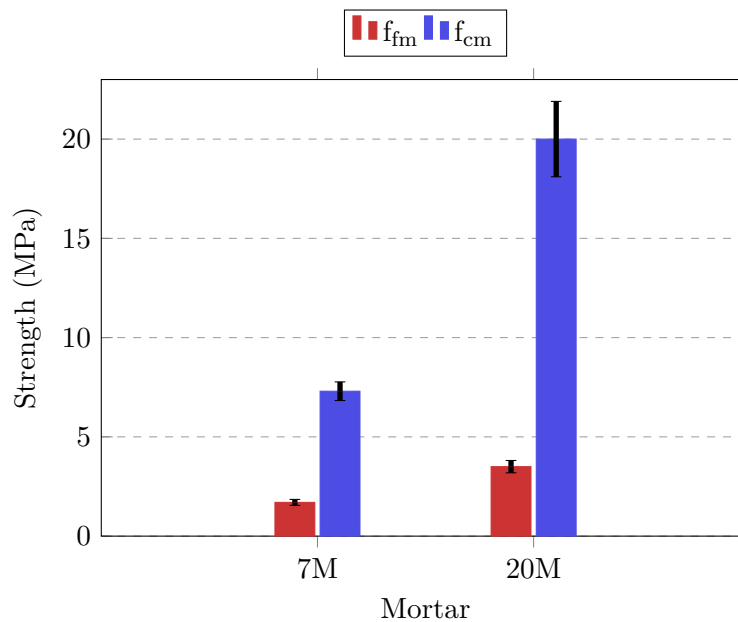


Figure 6.6: Average compressive (f_{cm}) and flexural (f_{fm}) strength of mortar measured at 7 days

The results shown in Figure 6.6 are also expressed in Table 6.9 with their respective COV values. The COV values for both tests and both mortars are acceptable, showing consistency in both the mix designs and quality of the mortars. It can be seen from Table 6.9 that the average strengths of both mortars throughout this study reached almost exactly the target strengths of 7 and 20 MPa.

Table 6.9: Average compressive (f_{cm}) and flexural strength (f_{fm}) values presented in Figure 6.6 and the coefficient of variation (COV)

Mortar	7M	20M
f_{cm} (MPa)	7.3	20.0
COV (%)	6.5	9.5
f_{fm} (MPa)	1.7	3.5
COV (%)	8.9	8.8

Due to the fact that only these two mortars can be used to determine if there is a relationship present between the compressive strength and the flexural strength, the relationship can only scarcely be proven if there is any. It can be concluded from Figure 6.6 and Table 6.9 that the flexural strength consists of 23.3% and 17.5% of the compressive strength for 7M and 20M, respectively. Even though these values are not close to each other they are still close enough to suggest that there is a relationship present.

As stated in Section 4.3, mortars with compressive strengths as high as that of 20M are not commonly used in industry and 7M presents a better replica of what is used in industry. This could have an effect on the flexural-compressive strength relationship. Literature usually uses mortars with compressive strengths between 1.5 and 7 MPa (Lumantarna *et al.*, 2014; Reddy and Gupta, 2006).

EN 1996-1 (2005) defines mortar classes according to their compressive strengths and are classified by the letter M followed by the compressive strength in N/mm^2 at 28 days. Mortar classes from EN 1996-1 (2005) range from M1 to M20, and the most popular classes range between M2 and M9.

6.2.4 Modulus of Elasticity of Mortar

The modulus of elasticity of each mortar was obtained by the same test conducted on the cylindrical GEO specimens according to the EN 12390-13 (2013). The modulus of elasticity results were determined for both mortars to conclude if these results fall within ranges proposed by literature. Zengin *et al.* (2018) discussed the effect of mortar type and joint thickness on the mechanical properties of conventional masonry walls. Zengin *et al.* proposed that the modulus of elasticity of common cement and lime mortars range between 5.5 and 16.7 GPa.

Figure 6.7 and Table 6.10 shows the elastic modulus results of both mortars with the respective standard deviation error bars and COV values. It can be seen that 7M falls just above the range of elastic modulus values proposed by Zengin *et al.*. This can be attributed to the fact that 7M represent a conventional mortar more accurately than 20M. Higher COV values were observed and this can again be attributed towards the more complex nature of the test setup.

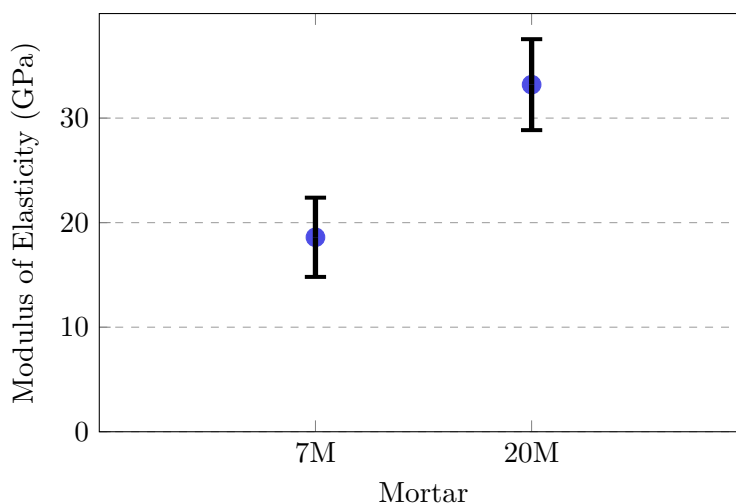


Figure 6.7: Average modulus of elasticity measured at 7 days for 7M and 20M

Interestingly, if the same method of $K_E F_{ck}$ is used as in Section 6.1.2 to determine the modulus of elasticity of the mortars, 7M would have a much more conservative results than 20M. The elastic modulus of 7M determined by testing is 165% higher than the elastic modulus predicted by $K_E F_{ck}$, where the elastic modulus of 20M by testing is only 66% higher than the value of $K_E F_{ck}$. From this can be concluded that the method proposed by EN 1996-1 (2005), to determine elastic modulus values of masonry in the absence of experimental data, is not applicable on mortar materials.

Table 6.10: Average modulus of elasticity values presented in Figure 6.7 and the coefficient of variation (COV)

Material	7M		20M	
	E (GPa)	COV (%)	E (GPa)	COV (%)
7 days	18.6	20.3	33.2	13.1

6.3 Joint Interface Test Results

Well known mechanical properties are regularly studied such as strength and stiffness, but the tensile and shear strength of the joint interface of masonry not as much. A reason for this can be due to more complex test setups needed to obtain these properties. However, for AMUs to replace CMUs on the housing market these properties would need to be known.

An aim of this section is to characterise the tensile and shear properties of the joint interface of the alternative masonry materials investigated in this study. For this, results from the crossed-brick couplet test and triplet test, on all four masonry materials, are presented and discussed in this section. These two tests are considered as the main tests of this study. Also discussed is the suitability of these test methods, usually applied on CMU, on alternative materials.

6.3.1 Direct Tensile Strength

The tensile bond strength of the joint interface was determined with the use of the crossed-brick couplet test. The test was conducted according to the standard ASTM C 952-12 (2012), as discussed in Section 5.3.1, on eight specimens of each material at 7 days.

The crossed-brick couplet test presents a straight forward test method to determine the direct tensile strength of the joint interface. The tensile strength is calculated from the maximum load achieved at failure divided by the area of the mortar interface.

As predicted in Section 3.1.2 problems were encountered with determining the tensile fracture energy from the crossed-brick couplet test results. The quasi-brittle behaviour of the joint interface at failure prevents the determination of the fracture energy. The load-deformation diagrams of the results show a sudden drop at failure and not a descending branch as desired. Therefore, the tensile fracture energy results were discarded for this study.

Figure 6.8 shows the average tensile strengths of the four masonry materials with both mortars. The first column at each material represents the average tensile bond strength of the masonry materials constructed with 7M, and the second column those constructed with 20M. The standard deviation error bars again show the variation in results obtained from each set of eight specimens.

From the figure a few observations are obvious. The order from greatest to smallest tensile bond strengths, for both mortars, was: CON, GEO, CSE and then the ADB masonry. In terms of mortar, 20M showed higher tensile bond strengths for the CON and GEO masonry than 7M. The opposite was shown for the CSE and ADB masonry, these masonry materials with 7M reached higher tensile bond strengths than with 20M.

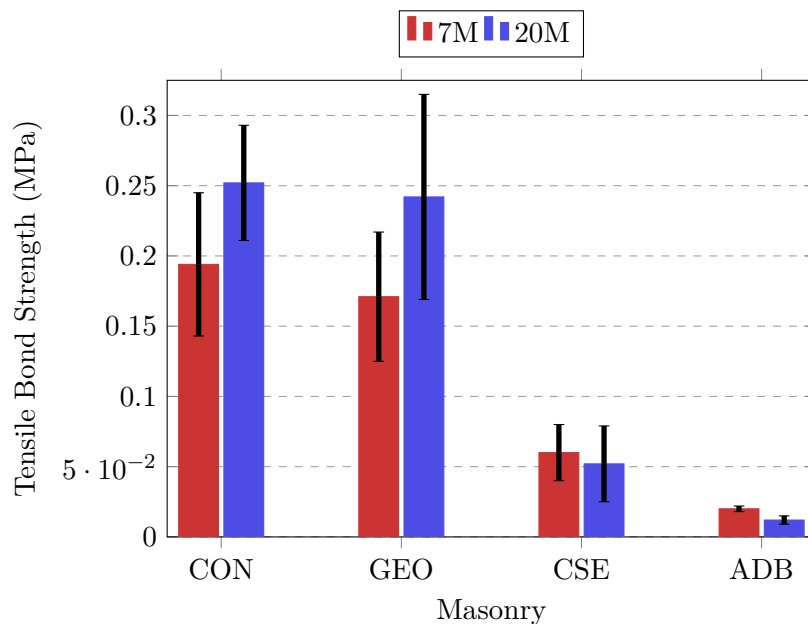


Figure 6.8: Average tensile bond strength of the joint interface measured at 7 days

Comparing mortars for each masonry material showed that the tensile bond strength of the CON masonry with 7M was 77% of that with 20M. For the GEO masonry, 7M reached 71% of that with 20M. As stated earlier, the opposite mortar produced higher bond strengths for the CSE and ADB masonry. 20M showed an average tensile bond strength of 87% of that with 7M, for CSE masonry. For ADB masonry 20M showed a tensile bond strengths of 60% compared to ADB masonry with 7M.

Table 6.11 shows the average tensile bond strength values from Figure 6.8 with their respective COV values. This table shows that the average tensile bond strength values of the CON and

GEO masonry were almost the same for 7M and 20M. The tensile bond strength between the CON and GEO masonry differed with 0.023 MPa and 0.01 MPa, for 7M and 20M respectively. This was an unexpected finding due to the big difference in surface roughness between these two masonry materials. The CSE and ADB masonry units also have higher surface roughness values than the CON unit, in terms of number of pores and surface porosity, but show much lower tensile bond strengths than the CON masonry. These results could mean that for tensile strength of the joint interface other factors play a larger role in bond strength development than surface roughness.

Another material parameter that could have a larger influence on the bond strength is water absorption. Even though CON showed a higher IRA value than GEO (refer to Table 6.5), these materials showed similar long term water absorption characteristics by mass (refer to Figure 6.4) which could explain the similar bond strengths between the CON and GEO masonry.

Table 6.11: Average tensile bond strength values presented in Figure 6.8 and the coefficient of variation (COV) for each mortar

Material	CON		GEO		CSE		ADB	
	f_t (MPa)	COV (%)	f_t (MPa)	COV (%)	f_t (MPa)	COV (%)	f_t (MPa)	COV (%)
7M	0.194	26.4	0.171	26.9	0.060	33.5	0.020	10.2
20M	0.252	16.2	0.242	30.1	0.052	53.0	0.012	24.8

The water absorption characteristics of the CSE and ADB materials could explain the reason for their weaker bond strengths. These materials have higher water absorption characteristics than the CON and GEO material and, as stated in Section 6.1.4, mortar workability problems were encountered upon construction of the CSE and ADB masonry test specimens. The high absorption characteristics led to stiffening and dewatering of the mortar which could cause low water-cement ratios, leading to an incomplete hydration process of the cement binder. This could explain why the CSE and ADB masonry with 20M have a lower tensile strength than the same masonry materials with 7M. Due to the large cement content in 20M, dewatering of the mortar in its fresh condition could mean there is not enough water to fully hydrate all of the cement particles present in 20M and this could lead to a weaker bond.

Another parameter that can influence the bond strengths of the CSE and ADB materials is the tensile strength of the masonry units. Walker (1999) suggests when the bond is limited by the block strength there is little benefit to increase the cement content of a mortar. Selecting a mortar similar to block characteristics better optimises the bond strength. The high COV values can be due to a number of reasons. A reason can be human error (inconsistency of the mason's construction technique) or inconsistencies in the test setup. Nonetheless, even though conclusions can be made considering the influences of different masonry unit and mortar characteristics on the joint interface it is evident that more research still needs to be conducted in this area.

As stated in Section 5.3.1 the failure modes from the bond wrench test, as per the European testing standard, was adopted for this test. Most tensile failures that occurred were failure Type B1 (failure at the joint interface between the upper unit and mortar), only a distinct few failure Type B2's (failure at the joint interface between the lower unit and mortar) were observed. The ADB unit was the only exception where almost all the couplets showed failure Type B5 (failure within unit near the interface). Figure 6.9 shows examples of failure Types B1, with CON masonry, and B5, with ADB masonry, from crossed-brick couplet tests conducted in this study.

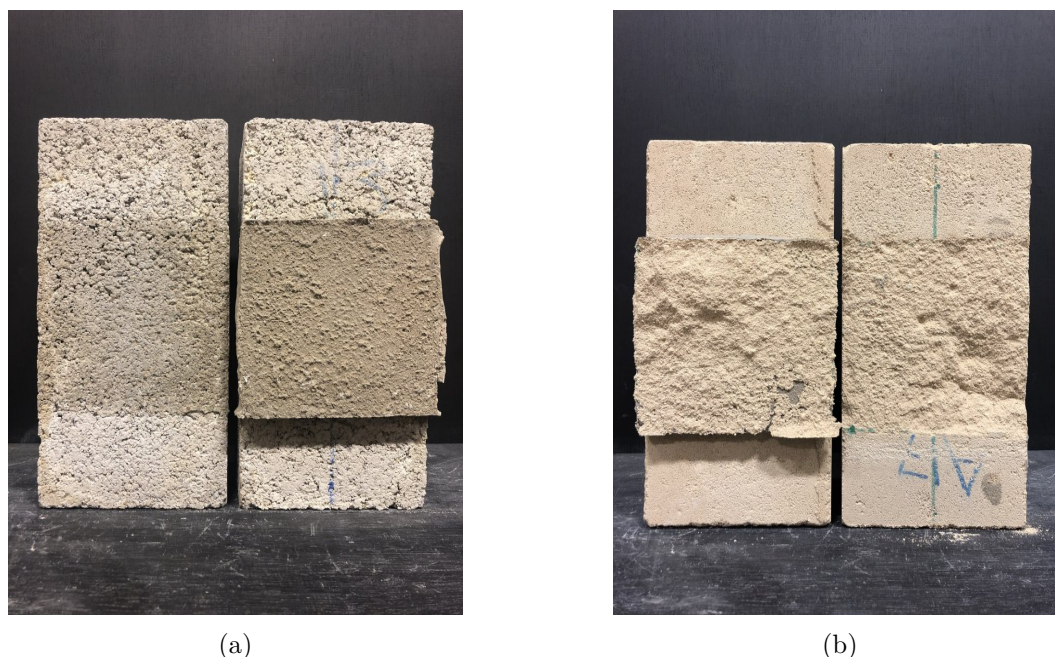


Figure 6.9: Crossed brick couplet test failure types (a) B1 and (b) B5

The reason for this type of failure for the ADB couplet could be that the masonry unit tensile strength was less than the bond strength. This is supported by the tensile strength values obtained for similar ADB units by Fourie (2017). Fourie (2017) determined the indirect tensile strength of similar ADB units with the wedge splitting test method proposed by Brühwiler and Wittmann (1990) and values of 0.03 MPa were obtained, similar to the tensile bond strength values of the ADB masonry in this study. This can suggest that the bond strength of the ADB masonry is limited by the unit's tensile strength and not by factors influencing the bond strength. However, there is still a 40% difference in the tensile bond strength of the ADB masonry with 20M compared to that with 7M. This could indicate that the tensile bond strength of the ADB masonry is a function of the bond development of the joint interface and the tensile strength of the masonry unit.

The failure types also confirm that, for the CSE couplet, the weaker bond strengths were due to the masonry unit characteristics and not the tensile strength of the unit. Literature proposes that the tensile strength of the CSE unit is approximately one tenth of that in compression (Morel and Pkila, 2002). One tenth of the compression strength of the CSE unit is 0.63 MPa which is ten times larger than the tensile bond strength obtained in this study.

When compared to literature similar values are obtained than those from this study. As stated in Section 3.1.2, Sugo *et al.* (2001) tested the tensile strength of the joint interface for CON masonry and found an average tensile strength of 0.51 MPa. The CON masonry reached half the tensile strength of Sugo *et al.* (2001) and it is not clear if Sugo *et al.* (2001) increased the moisture content of the masonry units before construction which could lead to higher bond strength values. Reddy and Gupta (2006) conducted similar crossed-brick couplet tests on three types of soil cement blocks. Reddy and Gupta (2006) found tensile bond strengths for various combinations of mortar and soil-cement blocks in the range of 0.09 to 0.18 MPa. The tensile bond strengths of almost all the materials and mortar combinations in this study fell within this range, except those from the ADB masonry.

The soil-cement block tested by Reddy and Gupta (2006) was similar to the CSE units of this study in terms of compressive strength. The results for these two type masonry units also showed to be similar. Reddy and Gupta (2006) also tested crossed-brick couplets that had a zero moisture content at the time of construction of the couplet, with a mortar similar to this study, and found tensile bond strength values between 0.09 and 0.11 MPa.

The traditional ADB masonry investigated by De Almeida (2012) showed similar characteristics to the ADB masonry material of this study. De Almeida (2012) investigated the tensile strength of ADB masonry and found the tensile strength to be 0.01 MPa. This value compliment the findings of this study, due to the fact that the tensile strengths of the ADB masonry in this study are close to (with 20M) and above (with 7M) the value by De Almeida (2012) (see results in Table 6.11).

The test procedure laid out by ASTM C 952-12 (2012) presented an easy and quick method to test for the tensile bond strength of the joint interface. This test method proves to give satisfactory results when compared to literature for the masonry materials investigated in this study. Therefore this test method is deemed suitable for conventional masonry, as well as the alternative masonry materials investigated in this study.

6.3.2 Shear Strength

Triplet tests were conducted according to, EN 1015-3 (1999), as discussed in Section 5.3.2, and provided the initial shear strength, friction coefficient, shear fracture energy and dilatancy values for the four different masonry materials and two mortars. The initial shear strength and friction coefficient are acquired by plotting the maximum shear strength of each test against the normal pre-compressive stress. Three triplet specimens were tested at each of the four pre-compression levels. If the test results or test setup gave erroneous results the test was disregarded and another specimen was tested until three valid tests were obtained for each pre-compression level which satisfies the standard requirements.

A line of best fit is plotted against the shear data using linear regression. The average initial shear strength is determined from the intercept of the linear regression line with the vertical axis. The friction coefficient is obtained from the slope of the linear regression line. This relationship is explained as the Mohr-Coulomb's friction law and Equation 3.1 in Section 3.1.3 shows this law in equation form and defines each variable. Therefore, this equation is not again represented here. This equation represents the sliding failure line of triplet specimens.

Figure 6.10 shows the maximum shear stress results against the pre-compressive stress levels as data points for each masonry material and mortar. Figure 6.10, therefore, represents a total of 8 data sets. A linear regression line is fitted to each one of these data sets from which the average initial shear strength and friction coefficient are obtained. The shear strength results are each plotted against the true pre-compression stress at time of failure. Each set of triplet tests at a pre-compression level is indicated with a different shape and colour to easily identify the difference in pre-compression. From the results can be seen that a better linear relationship exist between the shear stress and pre-compression stress, for a pre-compression stress of up to 2 N/mm^2 , compared to that of only 0.5 N/mm^2 .

The maximum shear stress, for each pre-compression level, was obtained from the shear stress at the failure of the first interface of the triplet specimen, even though higher shear stresses were sometimes obtained at the failure of the second interface. After failure occurred at one of the two interfaces of the triplet specimen, moment forces seemed to occur which disrupted the pure shear values. Results were only added to the data set if a failure type of A1/1, A1/2 or A2 occurred (refer to Section 5.3.2 for the explanation of these failure modes).

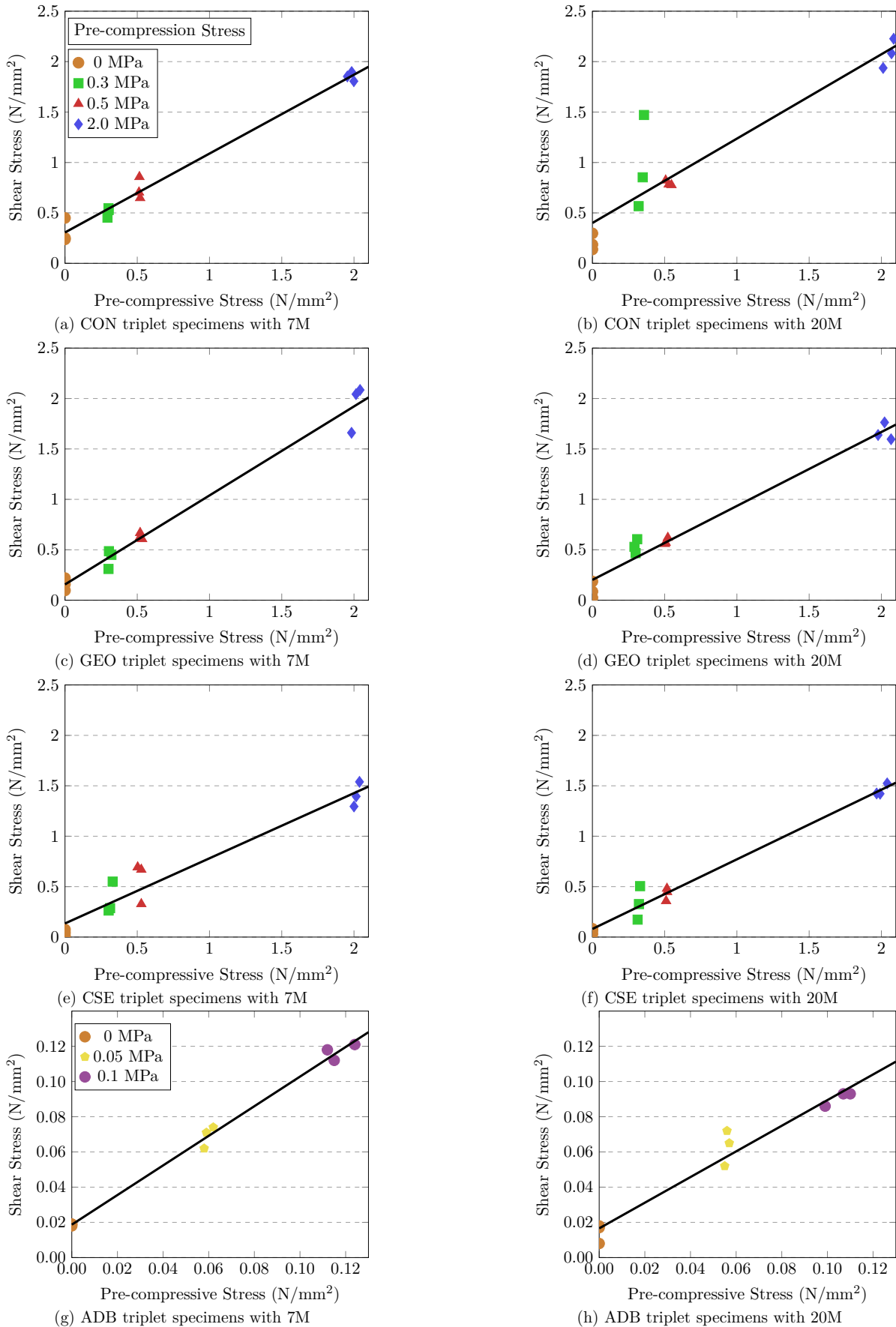


Figure 6.10: Shear bond strength of the joint interface at different pre-compression levels from the triplet tests for both mortars

It can be seen from Figure 6.10 that the results appear reasonably similar when comparing the linear regression lines of the same masonry material between the two different mortars. However, it is somewhat difficult to compare the linear regression lines of different materials to each other and, therefore, Figure 6.11 presents the data points and linear regression lines of all the materials for both mortar on their own respective plots. An unexpected result is that the linear regression line shows a better fit to the data points with the inclusion of the shear stresses obtained from the highest pre-compression level, which was 2 N/mm^2 , than without it. This was the case for most of the tests. The highest pre-compression load proposed by the standard, EN 1052-3 (2002), is 1 N/mm^2 for masonry units with compressive strengths greater than 10 N/mm^2 . Therefore, there was uncertainty about what the results would show at higher pre-compression levels.

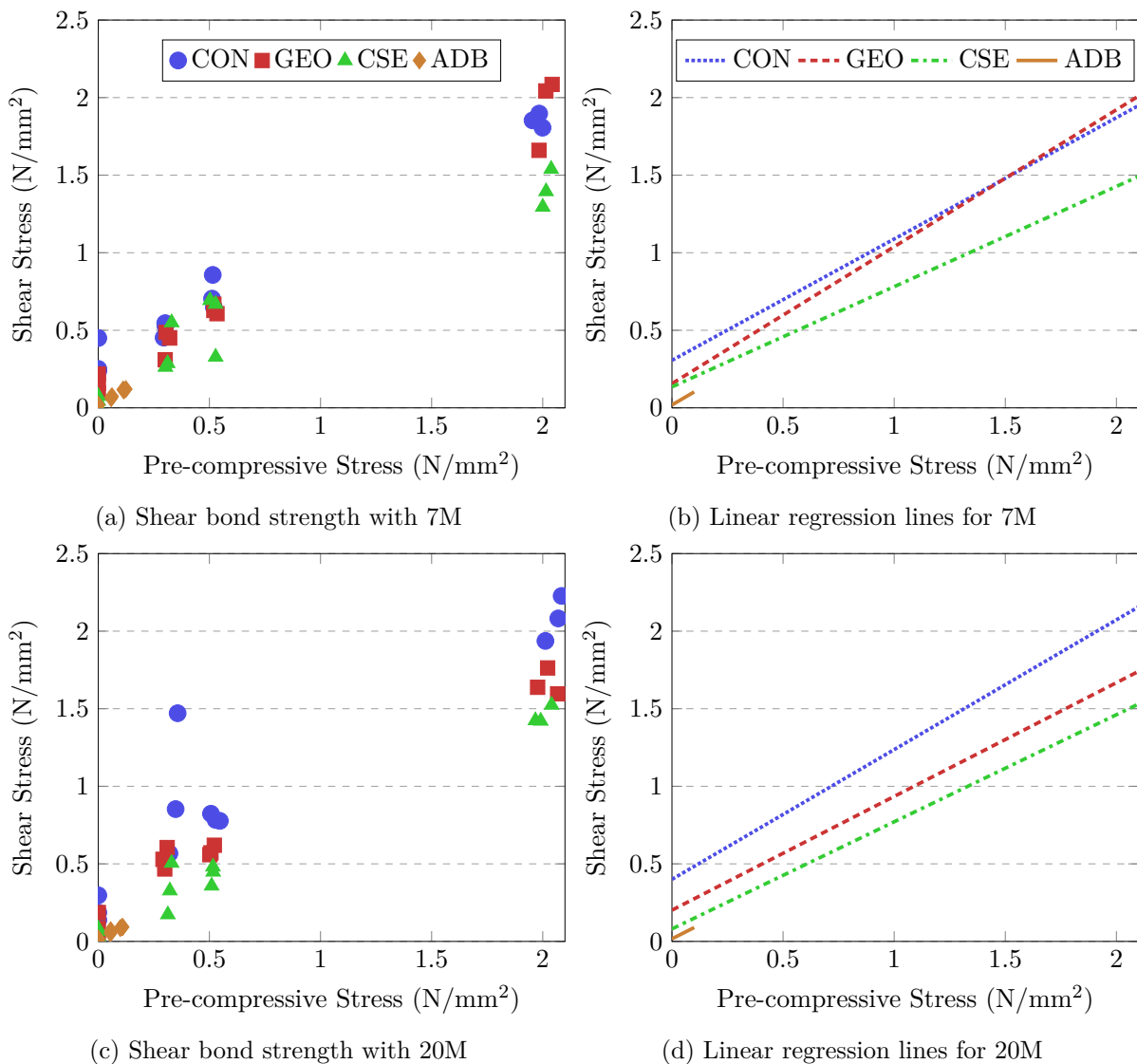


Figure 6.11: Shear bond strength of the joint interface at different pre-compression levels for all materials and both mortars

It can be seen from this figure that the CON masonry with 20M showed the highest initial shear strength. The ADB masonry showed the lowest initial shear strength for both mortars. The linear regression line of the ADB masonry, for 7M and 20M, is only plotted up to a pre-compression stress of 0.1 N/mm^2 due to it being unrealistic to test ADB masonry at such high levels of pre-compression. The GEO masonry showed the highest internal angle of friction for all

of the materials tested with 7M, and the CON masonry the highest internal angle of friction for the materials tested with 20M. The CSE masonry showed the lowest internal angle of friction for both mortars, however, for 7M it showed a similar initial shear strength to the GEO masonry. The ADB masonry showed a similar internal angle of friction to the GEO masonry for both mortars.

Table 6.12 shows the initial shear strength, coefficient of friction and coefficient of determination (R^2) for all of the materials and both mortars. The results represented in Table 6.12 are reproduced from Figure 6.11. The internal angle of friction is also given for comparison to literature. The value of R^2 quantifies how closely the line of best fit, fits the data points. The value of R^2 is expressed as a value between 0 and 1. The closer R^2 is to one the better the fit of the line to the data points. The R^2 is a key output of regression analysis, and it gives the variance in the dependant variable that is predicted from the independent variable. It can be seen from Table 6.12 that all of the materials have similar R^2 values except the CON masonry with 20M.

Table 6.12: Triplet test results

Material	CON		GEO		CSE		ADB	
	7M	20M	7M	20M	7M	20M	7M	20M
Initial Shear Strength (N/mm ²)	0.306	0.400	0.156	0.202	0.135	0.081	0.019	0.017
Coefficient of Friction	0.78	0.84	0.88	0.73	0.65	0.69	0.84	0.73
Internal Angle of Friction (°)	38.0	39.9	41.4	36.2	32.9	34.6	40.1	36.1
Coefficient of Determination - R^2	0.98	0.87	0.93	0.98	0.99	0.96	0.98	0.97

The Eurocode, EN 1996-1 (2005), states that an initial shear strength of 0.20 N/mm² can be assumed for aggregate masonry and a mortar with strength range of 10 to 20 MPa when experimental data is not available. The masonry material that most closely resembles the initial shear strength proposed by the Eurocode is the GEO masonry with 0.202 N/mm² for 20M and 0.156 N/mm² for 7M. The CON masonry showed higher initial shear strengths, for both mortars, than the value proposed by EN 1996-1 (2005). The CSE masonry with 7M showed an initial shear strength that is almost equal to the GEO masonry material with 20M. The other masonry materials with their respective mortars all showed initial shear strengths lower than 0.20 N/mm².

Interestingly, 20M gave higher initial shear strength results for the CON and GEO masonry materials than the 7M and this, however, was reversed for the initial shear strength results of the CSE and ADB masonry materials. For both the CSE and ADB masonry materials 7M produced higher initial shear strengths than 20M. A possible reason why the CON masonry gives higher initial shear strengths than the GEO masonry can be attributed towards the higher surface roughness of the CON masonry units (discussed in Section 6.1.5). It should be noted that even though the initial shear strength of the CON masonry with 7M is double that of the GEO masonry with 7M, the linear regression lines predict that the maximum shear strengths of both masonry materials with 7M will be equal to one another at a pre-compression stress of 1.5 N/mm². This could mean that the surface roughness has the highest influence at lower pre-compression levels, and that the influence of surface roughness diminishes as the pre-compression levels increase.

Surface roughness, however, did not seem to have an effect on the bond strength of the CSE and ADB masonry. According to the results from Section 6.1.5 the CSE and ADB units has higher

surface roughness's than the GEO unit, but results in Table 6.12 show that they has weaker initial shear strengths. The same were found for the tensile bond strengths in Section 6.3.1. This contributes towards the validity of the assumption made in Section 6.3.1, that the water absorption characteristics of the CSE and ADB masonry causes weaker bonds to form due to the dewatering of the mortar and insufficient hydration of the cement binder. As also stated in Section 6.3.1, this could explain why 7M produced higher initial shear strength results than 20M for the CSE and ADB masonry. Upon dewatering 20M, due to the large cement content in the mix, can easier experience un-hydrated binder products than 7M, which leaves 20M with a weaker bond.

Failure of the triplet specimens mostly occurred at the joint interface or in the mortar layer, this is explained as failure Type A1/1 (failure in the joint interface on one unit face) and A1/2 (failure in the joint interface divided between two unit faces). Failure Type A3 and A4 only occurred in the ADB specimens, and this can be attributed towards the weak nature of the material. For one or two instances failure Type A4 occurred at the highest pre-compression level (2 MPa) in the CSE and GEO specimens. All failure Types A3 and A4 were disregarded from the results and another specimen was tested until a valid failure type was recorded. Problems were, however, encountered with the ADB specimens where failure Type A3 occurred for most of the specimens. This could mean that the shear strength of the joint interface is stronger than the shear strength of the ADB unit, which is similar to findings in Section 6.3.1. This can be confirmed with the initial shear strengths results of the ADB masonry. Both mortars showed almost exactly the same results. The initial shear strength between the two mortars differed with only 0.002 N/mm^2 , showing that their initial shear strength is dependent on the shear strength of the unit and not of the joint interface. Therefore, failure Type A3 was taken as a valid failure type only for the ADB specimens.

Figure 6.12 shows examples of shear failure Types A1/1 and A1/2 from triplet tests conducted in this study. No failure Type A2 was encountered for any of the triplet tests conducted in this study. This could mean that the shear strength of both mortars is stronger than the shear strength of the joint interfaces.

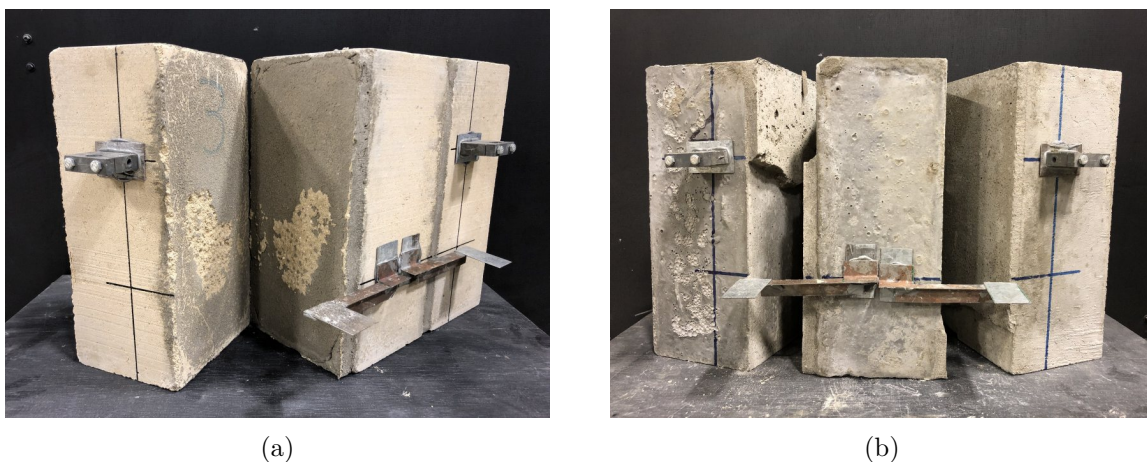


Figure 6.12: Triplet test failure types (a) A1/1 and (b) A1/2

Even though the triplet test setup proposed by, EN 1052-3 (2002), was designed for conventional masonry units it was shown in this study that the test provided acceptable and consistent results for all the materials investigated in this study. Adjustments were made to the test setup, and testing procedure, provided by EN 1052-3 (2002) and this is discussed in Section 5.3.2. EN 1052-3 (2002) states that the pre-compression level shall be kept within $\pm 2\%$ of the initial value. A steel spring was used to try and ensure that the pre-compression levels were kept as

close as possible to the initial value during the triplet tests when pre-compression loads of up to 0.5 N/mm^2 were applied, due to this being the maximum capacity of the spring. Once the higher pre-compression loads of 2 N/mm^2 were applied a technique of manually adjusting the pre-compression was applied. To determine the effectiveness of these two techniques the average percentage change over and under the initial pre-compression value was recorded for each test. The summary of the change in pre-compression during the triplet tests of each material is represented in Table 6.13.

Table 6.13: Summary of change in pre-compression during triplet tests

Change Value	CON		GEO		CSE		ADB	
	20M	7M	20M	7M	20M	7M	20M	7M
Over Initial Value (%)	12.93	7.76	6.10	5.94	5.44	5.79	14.53	21.31
Under Initial Value (%)	1.70	6.40	3.46	3.31	1.42	3.10	4.55	0.32

It can be seen from Table 6.13 that the pre-compression levels increased more than it decreased and this was expected due to the phenomenon of dilatancy. The values of most of the materials under the initial value were close to the recommended 2%, but for all of the material the pre-compression loads increased to between 6 and 21% of the recommended value. A reason for this can be due to the many loose parts that form part of the triplet test setup for this study. The material that experienced the largest change in pre-compression, over the initial value, was the ADB material with 7M. This can be attributed to the low pre-compression levels of the ADB triplet specimens, where relative to the other materials, more or less the same change in N/mm^2 was experienced.

It should be noted that the largest pre-compression changes for most tests only occurred after the failure of the first interface of the triplet specimens. As stated earlier in this section, the initial shear strength, cohesion and friction angle were all obtained from the shear stress at failure of the first interface of the triplet specimen. Therefore, the pre-compression changes were not as high for these values as shown in Table 6.13 and possibly did not have any significant influence on these values. The shear fracture energy and dilatancy results, however, were calculated over the period of failure of both interfaces of the triplet specimen and these results could have been influenced by these changes in pre-compression. It is expected that higher pre-compression values could increase the shear strength results (this is explained by the Mohr-Coulomb friction law, see Section 3.1.3) and decrease the dilatancy results. As stated in Section 3.1.3 dilatancy is dependent on the confining pressure, higher confining pressures lead to a decrease in dilatancy, as shown in Figure 3.11. This could mean that some of the shear strength results presented in this section are slightly higher than their actual values and some of the dilatancy results slightly lower.

Even though the test procedure deviated from the standard, the test results from this study still showed that this test setup provides acceptable results which are consistent. Therefore, this test setup is deemed satisfactory for this study on the CON masonry and alternative masonry materials. The shear fracture energy of each triplet specimen is calculated as the area under the load-deformation graph from the point where the first interface failed until the end of the test. The specific shear fracture energy ($G(f, t)$) is then calculated by dividing the shear fracture energy by the projected fracture area. Figure 6.13 shows the load-displacement diagrams of all the triplet tests conducted in this study. Eight load-displacement diagrams are shown, each with load-displacement data for a specific masonry material and mortar, at the different pre-compression levels.

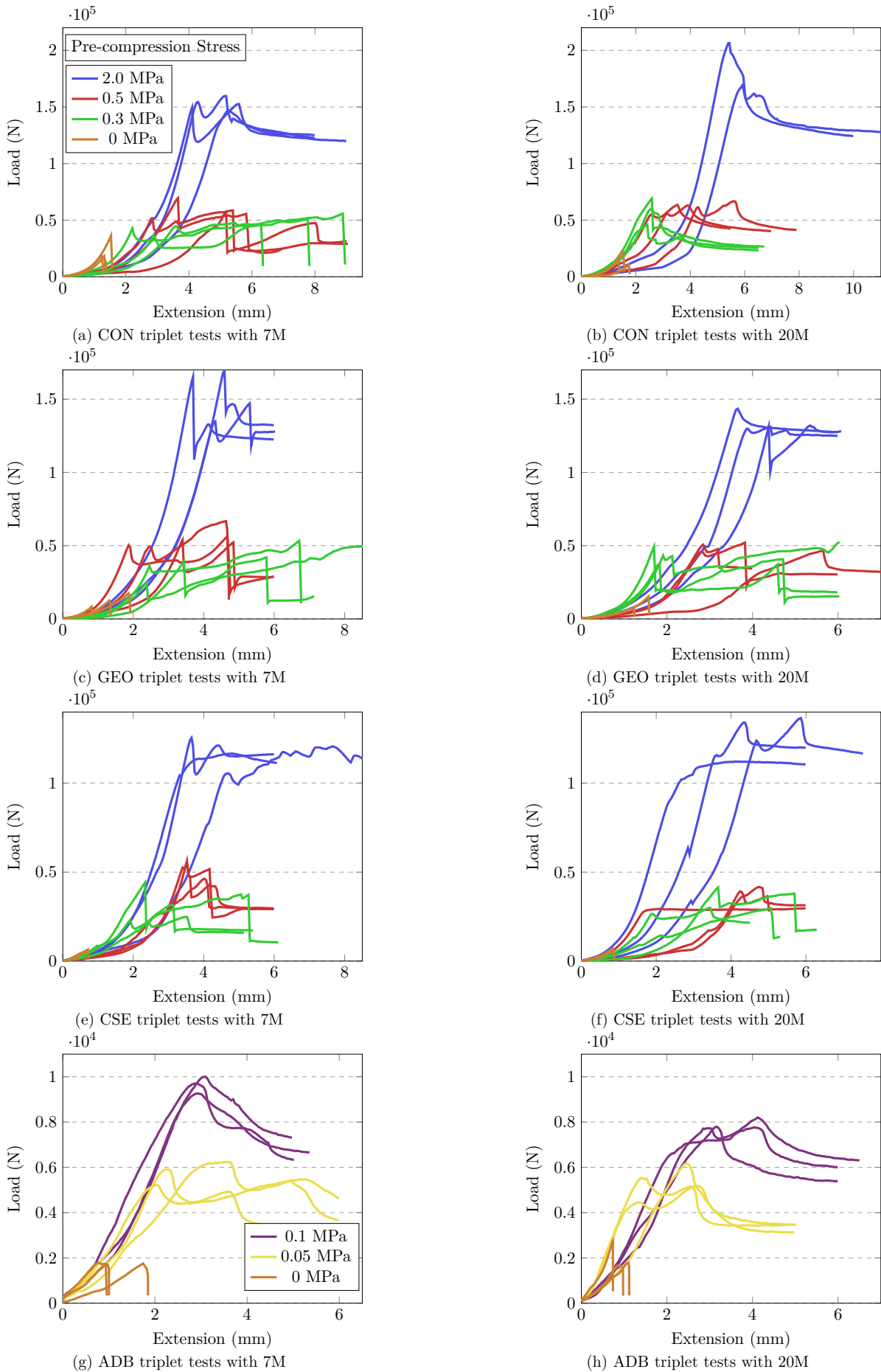


Figure 6.13: Load vs displacement diagrams for each triplet test and each mortar

It can be seen from Figure 6.13 that a stable descending branch is not always obtained after the peak load is reached. This caused problems with determining $G_{f,s}$ values for some of the tests. Observations that could immediately be made from the figure is that the maximum achieved shear load varied greatly for different materials and different pre-compression load. A consistent occurrence was that higher pre-compression loads led to higher maximum shear loads. It is also evident that failure modes differed for different materials. The ADB specimens showed the best results in terms of fracture mechanics and presented consistent $G_{f,s}$ values at each pre-compression level. No $G_{f,s}$ values could be calculated at zero pre-compression levels for any of the materials, the reason for this is a sudden drop in the load-displacement diagram.

Table 6.14 represents the $G_{f,s}$ values calculated from the load-displacement diagrams for each specimen, as presented in Figure 6.13. It can be seen that the shear fracture energies present a large scatter in results. A trend that can be seen from Table 6.14 is that the $G_{f,s}$ values are higher for lower pre-compression loads. This was, however, not expected. It would be expected that the $G_{f,s}$ values would be higher for higher pre-compression loads. It can be seen from Figure 6.13 that higher loads are required for shear failure at higher pre-compressions, therefore, it would be expected that more energy is dissipated at higher shear failure loads leading to larger $G_{f,s}$ values.

Table 6.14: Shear fracture energy results

Material	CON							
Mortar	7M				20M			
Pre-compression (N/mm ²)	0	0.3	0.5	2.0	0	0.3	0.5	2.0
$G_{f,s}$ (N/m)	0	3820.9	1814.2	631.2	0	474.5	270.4	549.5
	0	2577.3	529.4	567.5	0	307.5	457.7	1070.9
	0	2968.5	1277.1	138.6	0	327.2	363.7	335.9
	GEO							
$G_{f,s}$ (N/m)	0	0.0	347.1	140.9	0	88.4	102.8	113.5
	0	2081.9	2205.6	104.8	0	1388.4	222.7	66.2
	0	1343.1	640.3	188.3	0	330.1	357.9	12.1
	CSE							
$G_{f,s}$ (N/m)	0	327.1	410.4	68.8	0	114.1	0.8	25.3
	0	166.6	251.8	91.5	0	734.1	42.1	62.1
	0	1871.5	163.7	24.2	0	594.3	68.8	187.6
Material	ADB							
Mortar	7M				20M			
Pre-compression (N/mm ²)	0	0.05	0.1	-	0	0.05	0.1	-
$G_{f,s}$ (N/m)	0	20.0	30.0	-	0	21.7	39.4	-
	0	58.0	46.1	-	0	25.5	35.7	-
	0	42.3	35.0	-	0	29.1	20.3	-

Another phenomenon that was regularly observed was a sudden drop in the load-deformation diagram upon failure of the second interface of the triplet specimens. This occurred for most of the masonry specimens except for the ADB specimens and CON specimens with 20M. The fact that there are two interfaces that can fail for the triplet test makes this test less stable in terms of fracture mechanics. After the failure of the first interface a pressure build up usually occurs that leads to a sudden failure in the second interface where a lot of energy is dissipated, which leads to large $G_{f,s}$ values. Even though this could still be an accurate representation of the energy dissipated at the shear of the interface, these values could be scattered. A reason for this can be due to the many loose parts (also referred to earlier) that form part of the triplet test setup used in this study.

The reason for higher $G_{f,s}$ values at lower pre-compression levels could be due to the sudden failures that occurred for most masonry materials at these pre-compression levels. These sudden failures could increase the area under the load-deformation graph significantly and cause higher $G_{f,s}$ values. Figure 6.14 displays (a) the area under the load deformation graph of a triplet test where a sudden failure occurred at the failure of the second interface of the triplet specimen and (b) the area under the load deformation graph of a triplet test where a descending branch was obtained after the peak load was reached. These areas were used to calculate the $G_{f,s}$ for both tests and as a result of the sudden failure in Figure 6.14(a) the $G_{f,s}$ was much larger than that of Figure 6.14(b).

The only masonry material where higher $G_{f,s}$ values were obtained for higher pre-compression loads was for the ADB material with 20M. The ADB masonry showed a descending branch for most of the tests after the peak load was reached.

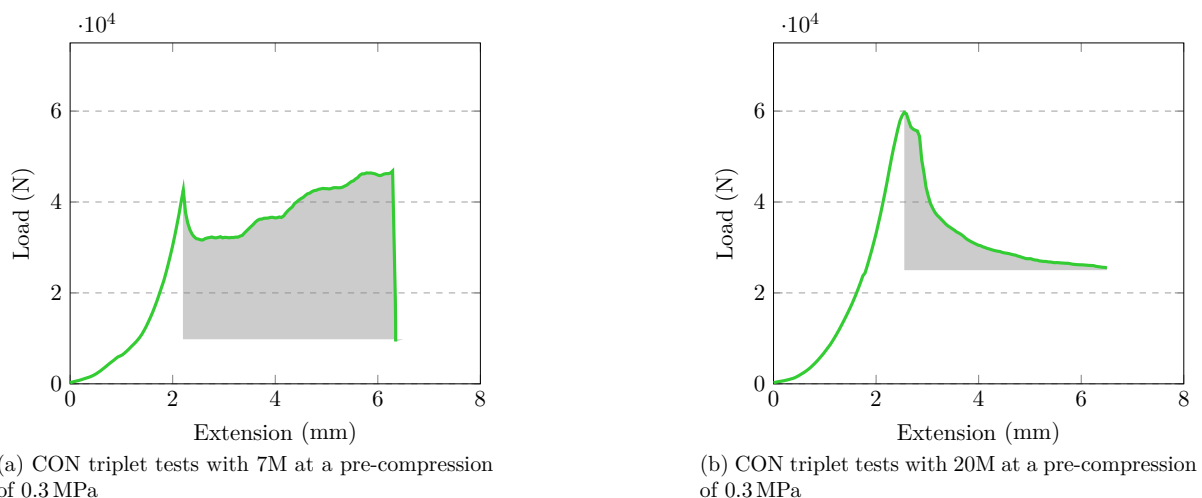


Figure 6.14: Load vs displacement diagrams for triplet test with sudden failure vs triplet test with descending branch

As stated in Section 3.1.3, De Almeida (2012) obtained shear fracture energy results between 400 and 625 N/m for traditional ADB masonry with pre-compression levels between 0.1 en 0.3 MPa. Van der Pluijm (1993) reported shear fracture energy results ranging from 12 to 188 N/m for solid clay prisms and calcium-silicate prisms at pre-compression loads of 0.1, 0.5 and 1 MPa. These results show that a wide range in shear fracture energy results can be expected for the joint interface of masonry. It can be seen that the shear fracture energy results from the CON, GEO and CSE masonry of this study is scattered within and above the range of results obtained by Van der Pluijm (1993) and De Almeida (2012).

The ADB masonry results fall within the bottom of the range of values obtained by Van der Pluijm (1993). Therefore, even though the $G_{f,s}$ results from this study are scattered it can still represent acceptable $G_{f,s}$ values for the masonry materials investigated in this study.

The dilatancy of the joint interface of the masonry materials was determined through the use of linear variable differential transducers (LVDTs) connected to the triplet test specimens. The methodology behind taking LVDT readings from the triplet specimens and calculating the dilatancy of each interface is discussed in Section 5.3.2. Dilatancy results were obtained from each valid triplet test for both interfaces of the triplet specimens.

Figure 6.15 shows the dilatancy values of the CON, GEO, CSE and ADB masonry materials for both mortars at different pre-compression levels. The pre-compression values used in Figure 6.15 were calculated as the average pre-compression value for the duration of each triplet test. The dilatancy value of each triplet specimen was calculated as the average of the two dilatancy values obtained from each interface of the triplet specimen.

It can be seen from Figure 6.15 that a partially linear relationship exists between the dilatancy coefficient and pre-compression stress values, for pre-compression stress levels between 0 and 0.5 N/mm^2 . A decrease in the dilatancy coefficient is observed for higher pre-compression levels. Linear regression lines (for the data points between pre-compression values of 0 and 0.5 N/mm^2) indicated that all the materials, except CSE, showed higher R^2 values with 20M. Larger negative gradients were obtained for the linear regression lines of all the masonry materials with 20M, compared to the same material with 7M. This shows a larger decrease in dilatancy for higher pre-compression levels for the masonry materials with 20M compared to 7M.

Pre-compression loads of up to 2 MPa are not usually tested for in literature. The highest pre-compression load normally tested for is 1 MPa. Literature suggest a linear regression line, with a negative gradient, as the best fit for dilatancy values at pre-compression levels between 0 and 1 MPa (Van der Pluijm, 1993). Therefore, linear regression lines were only applied to the data points between pre-compression values of 0 and 0.5 MPa in Figure 6.15.

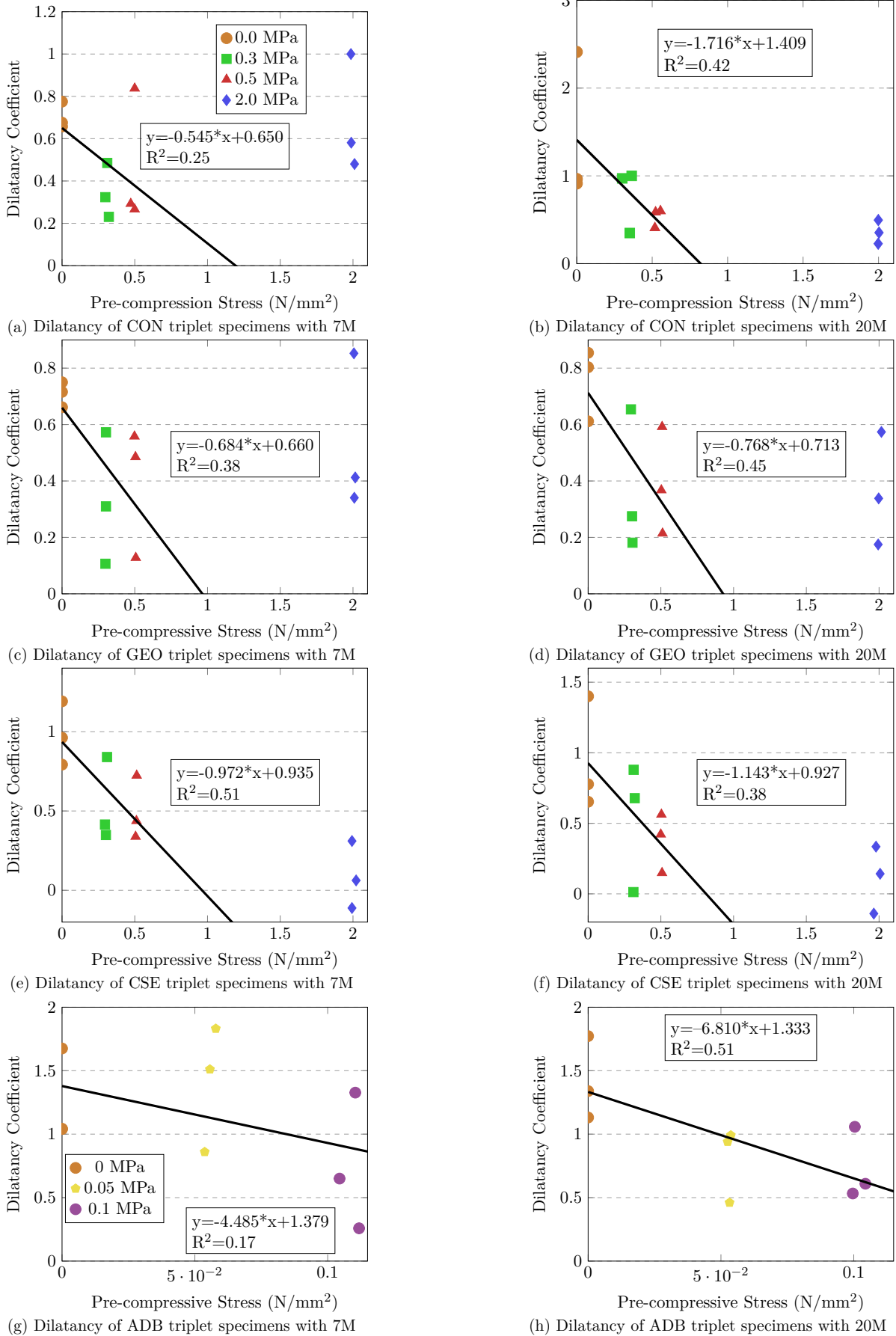


Figure 6.15: Dilatancy results of the joint interface from triplet tests

Table 6.15 represents the average dilatancy value of the three dilatancy values obtained per pre-compression level in Figure 6.15. As stated in Section 3.1.3, the surface roughness is one of the physical characteristics of masonry units that influences dilatancy the most (Lourenço, 1996). This is confirmed by the results from Table 6.15 where the dilatancy coefficients of the CON masonry were higher than the dilatancy coefficients of the GEO masonry and, CSE masonry with 20M. Interestingly, the CSE masonry with 7M showed larger and similar dilatancy values than the CON masonry with 7M. This could be due to the similarities in surface porosity between the two materials.

Table 6.15: Dilatancy results

Material	CON							
	7M				20M			
Mortar								
Pre-compression (N/mm ²)	0	0.3	0.5	2.0	0	0.3	0.5	2.0
Dilatancy Coefficient	0.70	0.35	0.47	0.69	1.43	0.77	0.53	0.36
COV (%)	9.0	37.2	69.3	40.1	59.5	47.6	20.2	37.5
Dilatancy Angle (ψ)	35.1	19.1	25.0	34.5	55.0	37.7	28.0	19.7
	GEO							
Dilatancy Coefficient	0.71	0.33	0.39	0.54	0.76	0.37	0.39	0.36
COV (%)	6.3	70.8	59.0	51.8	16.9	67.6	48.6	55.3
Dilatancy Angle (ψ)	35.3	18.2	21.3	28.2	37.1	20.3	21.4	19.9
	CSE							
Dilatancy Coefficient	0.98	0.53	0.50	0.09	0.94	0.52	0.38	0.11
COV (%)	20.4	49.9	40.0	243.3	42.5	86.7	55.8	212.6
Dilatancy Angle (ψ)	44.5	28.1	26.6	5.0	43.3	27.6	20.7	6.4
	ADB							
Mortar								
Pre-compression (N/mm ²)	0	0.05	0.1	-	0	0.05	0.1	-
Dilatancy Coefficient	1.25	1.40	0.75	-	1.41	0.80	0.73	-
COV (%)	29.2	35.3	72.6	-	23.1	36.7	38.7	-
Dilatancy Angle (ψ)	51.4	54.5	36.7	-	54.7	38.6	36.2	-

Interestingly, higher dilatancy values than expected were obtained for the triplet specimens tested at a pre-compression load of 2 N/mm². Literature states that for high pre-compression loads the dilatancy tends to zero. Lourenço (1996) proposed that confining pressures between 1 and 2 N/mm² are sufficient to reduce the dilatancy angle to zero. Van der Pluijm (1993) predicts zero dilatancy for confining pressures of 1.37 N/mm² and 2.44 N/mm² for two types of clay bricks. Therefore, the dilatancy values obtained at a pre-compression load of 2 N/mm² were unexpected. The only masonry material that showed such reduction in dilatancy at higher pre-compressions is the CSE masonry. A reason for this occurrence in the CSE masonry and

not in the CON and GEO masonry can be due to the lower strength of the CSE masonry unit. This could mean that surface of the CSE units experience crushing or shear slipping at the joint interface at shear failure. From this can be concluded that not only the surface roughness influences dilatancy but also the compressive strength of the masonry unit.

However, if predictions were to be made on the basis of the linear regression lines in Figure 6.15 it would be predicted for most masonry materials (except the ADB masonry), a zero dilatancy coefficient at a pre-compression load of 1 N/mm^2 as suggested by literature. Another observation was higher dilatancy coefficient values, with a larger scatter in results were obtained for most masonry materials with 7M, compared to the same materials with 20M. The reason for this is unknown.

Another phenomenon that was realised from the dilatancy results is that similar dilatancy values were obtained for both mortars per material. The only material where this was not the case is the CON masonry. Higher dilatancy values were obtained for the CON masonry with 20M than with 7M except at a pre-compression load of 2 N/mm^2 . A concern from the dilatancy results are the low R^2 values from Figure 6.15, especially for the CON and ADB triplet specimens with 7M. This shows a weak relationship between the dilatancy coefficient and the pre-compressive stress for these materials. However, due to the nature of experimental results and the scarcity of dilatancy data in literature the low R^2 values were accepted.

Most of the dilatancy results from this study fall within a range of results from literature. Van der Pluijm (1993) obtained dilatancy angle results which varied between 11.3 and 35° for solid clay and calcium masonry. Other literature found dilatancy angle results between 7.1 and 36.5° for clay brick, concrete block masonry and calcium silicate masonry (Burnett *et al.*, 2007; Haach *et al.*, 2011; Van Zijl, 2004). Most of the results from this study fall within this range. The only masonry material that showed consistent values outside this range was the ADB masonry material. The reason for this could be due to the low pre-compression levels used for testing the ADB material (refer to Section 5.3.2), allowing larger normal displacement (perpendicular to the joint interface) upon failure. Even though accurate conclusions cannot be obtained for most of the dilatancy results and large variations are present (considering the COV values), definite trends in the data could still be seen. This with the fact that most results fall within the range of acceptable results from literature shows that the dilatancy results obtained from this study are acceptable.

6.4 Conclusion

This chapter presented the results from tests conducted on masonry units, mortar and masonry specimens. The masonry materials included CON, GEO, CSE and ADB. The tests conducted on the masonry specimens were also known as the joint interface masonry tests. Tests conducted on the masonry units included: compressive strength, modulus of elasticity, dry density, water absorption and surface roughness tests. Mortar tests included: flow table, dry density, compressive strength, flexural strength and elastic modulus tests. Lastly the joint interface tests consisted of the crossed-brick couplet test and the triplet test.

The tests were conducted successfully in most cases and the test setups were satisfactory, bar certain aspects, which are discussed further in Chapter 7.

Chapter 7

Conclusions and Recommendations

The tensile and shear characterisation of the joint interface of alternative masonry was investigated in this study. This study has two main objectives. The first objective is to determine whether standards and benchmark tests used on conventional masonry can be applied successfully to alternative masonry. It aims to determine previously mentioned mechanical properties and if unsuccessful, to adopt tests from literature or develop new tests. The alternative masonry units (AMUs) included in this study are the geopolymer (GEO) unit, cement stabilised earth (CSE) unit and adobe (ADB) unit. Results from the AMUs are compared to concrete (CON) units which act as the benchmark material in this study. Two mortars are compared in this study, a weaker and a stronger mortar of approximately 7 MPa and 20 MPa. These mortars are further referred to as 7M and 20M.

The second objective is the tensile and shear characterisation of the joint interface of three types of alternative masonry materials. The goals of this objective are summarised as follows:

- To add reliable data to literature of mechanical properties of the joint interfaces of alternative masonry;
- To complement other studies in developing a finite element model (FEM) to simulate and analyse structures with different geometries constructed out of AMU's on a performance basis;
- To contribute towards the development of regional and national standards for AMU construction in South Africa.

The second objective of this study was achieved by a number of tests that were conducted on the CON and alternative masonry materials. The tests can be grouped as companion tests, the joint interface tensile test and the joint interface shear test. The mechanical properties tested in the companion tests include: the compressive strength, modulus of elasticity, dry density, water absorption and surface roughness of masonry units; the consistence, dry density, flexural strength, compressive strength and modulus of elasticity of mortars. The mechanical property tested with the joint interface tensile test include: the tensile strength of joint interface. These mechanical properties were tested with the crossed-brick couplet test. The triplet test was used for the joint interface shear test, and the mechanical properties tested include: the initial shear strength, cohesion, friction angle, shear fracture energy and initial dilatancy angle of joint interfaces.

7.1 Conclusions

This study shows that tests were conducted successfully in most cases on the alternative masonry materials and the test setups were satisfactory, bar certain aspects. In conjunction with the first objective, hereby follow conclusions made with regards to the suitability of applying standard and benchmark tests, used on conventional masonry, on different alternative masonry materials. Recommendations are also provided for adjustments to obtain more accurate results.

- The compressive strength tests could be applied successfully on both the CON units and AMUs in this study. No issues were observed with this test method on the AMUs. The consistency in the size of the AMUs facilitated convenience in result comparison. Adjustment of the loading rate was required for the weak ADB units, otherwise failure occurred before the time period specified by the standard. Typically for concrete and conventional masonry, as the loading rate increases, the compressive strength and elastic modulus increase. Therefore reducing the loading rate for the ADB may well reduce the compressive strength determined. The test showed consistent results for the CON, CSE and ADB units. A larger variation in results were obtained for the GEO units. This was attributed to the number of factors influencing the strength of the GEO unit and not to inconsistencies in the test setup.
- Even though challenges were encountered with the modulus of elasticity tests, it was still found that the test method is suitable for AMUs. A large variation in results was found for the CON and ADB materials. The reason for this can be attributed to the small prismatic specimens cut from existing masonry units. Cutting these small specimens by hand could lead to inequalities in the specimen geometry and inconsistencies in results. The GEO material was cast in conventional cylindrical moulds and gave acceptable results with small variations. Adjusting the test method from a load controlled test to a displacement controlled test, was required for the weak ADB material. However, these tests still yielded acceptable results. It is recommended that a cylindrical press mechanism is designed where weight batched cylinders can be manufactured from dry masonry mix designs. This would allow the production of alternative masonry cylinders with the same densities as AMUs for more consistent elastic modulus testing.
- The dry density tests could be successfully applied on the AMUs in this study. Consistent results were obtained with low variations, showing that the dry density test is suitable for AMUs.
- Due to the simplicity of the water absorption test this test method could be successfully applied on the CON, GEO and CSE materials without any issues. This test could not be applied on the ADB units, due to the lack of binder material present in its mix design. However, consistent results were obtained for the other materials showing that this test is suitable for application on AMUs. It is recommended that other methods are investigated to determine the water absorption characteristics of masonry units without binders.
- No standard test method is currently available for quantifying the surface roughness of masonry units, and a meagre amount of literature investigates this material property. However, a test method was found in literature and adopted in this study. This test method provided similar results to literature for the CSE units (the only applicable material with surface roughness values from literature). This indicated that this method is suitable for use on AMUs.
- The crossed-brick couplet test was successfully applied to the masonry materials in this study to determine the tensile strength of the joint interface. Due to the weak nature of

the joint interface, of the ADB masonry, the loading rate was adjusted to avoid premature failure. Higher variations in results were obtained in the tensile strength values. This was expected due to so many variables influencing the bond developing process.

- Problems were encountered while determining the tensile fracture energy of the joint interface from the crossed-brick couplet test results. The sudden drop in the load-deformation diagram at failure (due to the quasi-brittle nature of masonry) prevented the determination of the fracture energy. It is recommended that more stable tensile fracture mechanic tests are investigated where the load-deformation diagram shows a descending branch after failure. A possible solutions to this is using the wedge-splitting test. The design of such a test specimen, with mortar layer in the middle, is however complex.
- The triplet test was successfully applied to the CON and alternative masonry materials. A few adjustment were made to the test method specified by the standard. To avoid crushing of the ADB triplet specimens, three pre-compression levels were chosen (lower than specified by the standard), with a lower shear loading rate. The same shear loading rate applied to the ADB specimens was also applied to the other materials. Four pre-compression levels (different from those suggested by the standard and those selected for the ADB material) were chosen for the CON, GEO and CSE materials. Another deviation from the standard was the addition of a second steel roller at each of the two bottom support plates. The addition of the second steel roller was to aid with the placement of triplet specimens inside the test setup, especially with the weak ADB specimens where failure under self weight sometimes occurred. Even though the test method deviated from the standard, consistent results were obtained, concluding that this test method is suitable for use on alternative masonry materials.
- The triplet test setup consisted of many loose parts and it is suggested that this could have played a role in increasing the variabilities in the test results. A reason for the loose part in the test setup was to control the initial pre-compression value, but this showed to be unsuccessful as the initial pre-compression values changed with more than 2% during testing, which is the maximum change in pre-compression allowed by the standard. It is recommended that the loose parts of the test setup are attached to each other to ensure a more stable setup with less movement. Another recommendation is to use servo-hydraulics of a portable instron the control the normal pre-compression load, while the same instron still applies the vertical shear stress.
- The two failure planes of the triplet test setup increased the difficulty of obtaining consistent shear fracture energy results from this test. After failure of the first interface a pressure build up usually occurred that led to a sudden failure of the second interface. This caused a large scatter in fracture energy results. This shows that the triplet test is not the best test for obtaining shear fracture mechanics of masonry. It is recommended that other, more stable, shear tests are investigated to obtain more consistent shear fracture energies. A test that is recommended is the couplet test. The reason for recommending the couplet test is twofold. Firstly, this test only has one shear failure plane and, secondly, throughout literature valid and consistent shear fracture energy results have been obtained with this test setup.

The mechanical properties obtained for most of the companion and joint interface tests showed results that either fall within ranges of acceptable results from literature, or were comparable to values suggested by standards. In conjunction with the second objective of this study, hereby follow the conclusions made with regards to the mechanical properties of the masonry materials obtained from the experimental procedure in this study.

- The compressive strengths of the CON, GEO, CSE and ADB units at 28 days were 13.3 MPa, 37.4 MPa, 6.3 MPa and 0.5 MPa, respectively. These results showed that the CON, CSE and ADB units fell within ranges found in literature. The high strength of the GEO unit was attributed to its mix design. After a number of trial mixes this mix design showed a workable mix. The aim of this study was not to optimise the mix designs of AMUs, but rather to focus on the mechanical properties of the joint interface. Therefore, the GEO unit mix design was accepted. All the units, except the ADB unit, exceeded the minimum strength requirement of 4 MPa for single storey buildings with solid masonry units according to SANS 10400-K (2015).
- The elastic modulus results for the CON and alternative masonry materials were similar to elastic modulus values suggested by EN 1996-1 (2005) for masonry structures, in the absence of experimental data, with the formula $K_E f_{ck}$. Interestingly, the experimental results of the CON material varied most from the value suggested by EN 1996-1 (2005), with a variance of 21%. Even though larger variations in results were present for some of the AMUs, the results were still similar to those obtained by literature and previous research at Stellenbosch University.
- Water absorption results for the CON, GEO and CSE units were similar to those found in literature for the respective materials. The density and clay content of masonry units seemed to have an influence on the water absorption characteristics. Low densities and high clay content increased the initial rate of absorption. Workability problems were encountered by the masons upon masonry prism construction with the AMUs that had higher absorption characteristics (the CSE and ADB unit). This confirms that the ADB unit has high water absorption characteristics even though it cannot be tested by the method presented by the European testing standard.
- The crossed-brick couplet test provided the tensile strength of the joint interface. From these results it is concluded that the water absorption characteristics of the masonry unit have a larger influence on the bond strength development than the surface roughness. It was seen that the CON and GEO masonry showed similar tensile bond strengths for 7M and 20M even though their surface roughnesses varied greatly. On the other hand, the CSE and ADB masonry with similar surface roughness values to CON masonry showed much lower tensile bond strengths.
- Also concluded from the tensile strength results of the joint interface, is that low strength mortars improve the bond strength of the joint interface for masonry units with higher absorption values. In mortars with a higher cement content, the dewatering of the mortar (due to the water absorption characteristics of the masonry units) could lead to an incomplete hydration process of the cement binder, causing weaker bonds. This is possibly the reason for higher tensile bond strengths for the CSE and ADB masonry with 7M than 20M.
- An additional finding from the tensile strength results of the ADB masonry, is that the bond strength can be limited by the strength of the masonry unit. This is confirmed by literature.
- Literature suggests that surface roughness and water absorption are not the only material parameters that influence the bond strength, but parameters like the water retentivity characteristics and rheology of the mortar also play a role. These parameters were not investigated in this study and it is recommended that these parameters are investigated to understand the complex nature of the bond development process.

- The shear properties provided by the triplet test included the initial shear strength, friction coefficient, shear fracture energy and initial dilatancy angle. The Eurocode EN 1996-1 (2005) recommends that an initial shear strength of 0.20 N/mm^2 can be assumed for masonry. The initial shear strength of the CON masonry was double the recommended value with 20M. The initial shear strength of the GEO, CSE and ADB masonry was similar, half and much lower than recommended, respectively.
- The triplet test results indicated that the linear relationship, defined by Mohr's Coulomb friction law, continues up to a pre-compression level of 2 N/mm^2 for the CON, GEO and CSE materials. The highest pre-compression load specified by the standard is 1 N/mm^2 . This is also the highest pre-compression load implemented by most literature for shear tests. The results also showed that surface roughness has the highest influence at lower pre-compression levels in terms of shear strength, and the influence of surface roughness diminishes as the pre-compression load increases.
- The ADB triplet specimens and CON triplet specimens with 20M showed the most consistent shear fracture energy results that fell within acceptable ranges from literature. The other materials showed a large scatter in results, however, this was attributed to test setup and not due to inconsistencies in the triplet specimens. The only masonry material where higher shear fracture energies were obtained for higher pre-compression loads was for the ADB masonry. It is recommended that this mechanical property of alternative masonry is further investigated in future studies.
- A partially linear relationship was found from the dilatancy results, between the dilatancy coefficient and pre-compression stress, for a pre-compression stress up to 0.5 N/mm^2 for the CON, GEO and CSE masonry. Dilatancy results further indicated, in contradiction to values predicted by literature, non-zero dilatancy values at a pre-compression level of 2 N/mm^2 . The CSE masonry showed the lowest dilatancy values at the highest pre-compression level. This can indicate that not only the surface roughness influences the dilatancy, but also the compressive strength of the masonry unit.
- Literature suggests that surface roughness has the largest influence on dilatancy and this was confirmed by the results from this study.

7.2 Recommendations

Through observations made over the course of this study, recommendations for future studies were identified and these recommendations are presented here.

- One of the reasons why standardised compressive tests for AMUs have not been developed, is due to the fact that the influence of testing alternative masonry of different shapes and sizes are not fully understood. Therefore, it is recommended that future studies test different sizes of AMUs to understand these affects and adopt or develop new shape factors for universal application to these materials.
- Efflorescence can become a problem for the industrial production of GEO units and, therefore, further investigations to prevent efflorescence, or at least reduce it, are required.
- It is recommended that more research is conducted on the material property of the surface roughness of masonry units to aid the development of standardised tests for this material property in the future. As well as the reason this material property has a large influence on the bond development process of the joint interface of masonry.

Chapter 7. Conclusions and Recommendations

- The wedge splitting test currently presents the best method for determining the tensile fracture energy of the joint interface of masonry. Constructing wedge splitting specimens that keeps the material properties of the respective AMUs and are joint together with mortar, however, is complex. It is recommended that methods are investigated to construct these type of masonry specimens for more accurate tensile fracture mechanic testing.
- This study only investigated certain mechanical properties of alternative masonry and not any non-structural aspects which would be needed if these AMUs were to be adopted onto the housing market of South Africa. Therefore, it is recommended that a complete economic analysis and an environmental impact study is conducted on each AMU and compared to conventional masonry.
- In industry masons would usually wet the surface of masonry units before using them for construction. A number of sources from literature also suggest that the initial moisture content of the masonry units at the time of construction optimises the bond strength. It is recommended that other studies investigate the influence on the initial moisture content on the bond strength for the AMUs of this study.
- Literature suggests that soil-cement mortars outperform lime-cement mortars and sand-cement mortars (like 7M and 20M used in this study). It is recommended that soil-cement mortars are investigated for AMU construction to determine the influence on the bond strength of the joint interface.

References

- Ahmari, S. and Zhang, L. (2015). The properties and durability of alkali-activated masonry units. In: *Handbook of Alkali-Activated Cements, Mortars and Concretes*, chap. 24, pp. 643–660. Woodhead Publishing, Arizona.
- Almeida, J.C., Lourenço, P.B. and Barros, J.a. (2002). Characterization of brick and brick – mortar interface under uniaxial tension. In: *VII International Seminar on Structural Masonry for Developing Countries*. Belo Horizonte, Brazil.
- Annenberg Foundation (2017). Major Greenhouse Gasses. URL: <https://www.learner.org/courses/envsci/unit/text.php?unit=2&secNum=4>. (Visited: 2019/08/03).
- ASTM C 1072-06 (2006). Standard Test Method for Measurement of Masonry Flexural Bond Strength. In: *American Section of the International Association for Testing Materials*. West Conshohocken, USA.
- ASTM C 1531-09 (2009). Standard Test Methods for In Situ Measurement Of Masonry Mortar Joint Shear. In: *American Section of the International Association for Testing Materials*. West Conshohocken, USA.
- ASTM C 952-12 (2012). Standard Test Method for Bond Strength of Mortar to Masonry Units. In: *American Section of the International Association for Testing Materials*. ASTM, West Conshohocken, USA.
- Aymerich, F., Fenu, L. and Meloni, P. (2011). Effect of reinforcing wool fibres on fracture and energy absorption properties of an earthen material. *Construction and Building Materials*, vol. 27, no. 1, pp. 66–72.
- Baker, I. (1902). *A treatise on masonry construction*. 9th edn. Wiley, New York.
- Barnard, R. (2014). *Mechanical properties of fly ash/slag based geopolymers concrete with the addition of macro fibres*. MEng Thesis, University of Stellenbosch.
Available at: <http://scholar.sun.ac.za/handle/10019.1/95866>
- Barr, B.I.G., Abusiaf, H.F. and Sener, S. (1998). Size effect and fracture energy studies using compact compression specimens. *Materials and Structures/Materiaux et Constructions*, vol. 31, no. February, pp. 36–41.
- Benhelal, E., Zahedi, G., Shamsaei, E. and Bahadori, A. (2013). Global strategies and potentials to curb CO₂ emissions in cement industry. *Journal of Cleaner Production*, vol. 51, pp. 142–161.
- Bloom, D.E. (2011). Population Dynamics in India and Implications for Economic Growth.
- Boshoff, W., de Klerk, M., Coetzee, G., de Villiers, W. and Tolêdo Filho, R. (2013). Alternative Materials for Masonry Units. In: *The South African Housing Foundation International Conference, Exhibition & Housing Awards*.
- Brühwiler, E. and Wittmann, F.H. (1990). The wedge splitting test, a new method of performing stable fracture mechanics tests. *Engineering Fracture Mechanics*, vol. 35, no. 1, pp. 117–125.
- Buchanan, A.H. and Honey, B.G. (1994). Energy and carbon dioxide implications of building construction. *Energy and Buildings*, vol. 20, no. 3, pp. 205–217.

- Burnett, S., Gilbert, M., Molyneaux, T., Beattie, G. and Hobbs, B. (2007). The performance of unreinforced masonry walls subjected to low-velocity impacts: Finite element analysis. *International Journal of Impact Engineering*, vol. 34, no. 8, pp. 1433–1450.
- Centre for Affordable Housing Finance in Africa (2019). *Housing Finance in Africa: A Review of Africa's Housing Finance Market*. 10th Edition.
- Cheah, C.B., Part, W.K. and Ramli, M. (2015). The hybridizations of coal fly ash and wood ash for the fabrication of low alkalinity geopolymer load bearing block cured at ambient temperature. *Construction and Building Materials*, vol. 88, pp. 41–55.
- Concrete Society of Southern Africa (2019). Concrete Society of Southern Africa. URL: <https://concretesociety.co.za/faqs/cement#Q10> (Visited: 2019/08/05).
- Davidovits, J. (1989). Geopolymers and geopolymeric materials. *Journal of Thermal Analysis*, vol. 35, pp. 429–441.
- Davidovits, J. (1994). High-Alkali Cements for 21st Century Concretes. Tech. Rep. 19.
- Davidovits, J. (2008). *Geopolymer Chemistry and Application*.
- Davidovits, J. (2013). Geopolymer cement: A review. Tech. Rep., Institut Geopolymer, France.
- D'Ayala, D.F. (2008). Numerical modelling of masonry structures. *Structures & Construction in Historic Building Conservation*, pp. 151–172.
- De Almeida, J.A.P.P. (2012). *Mechanical characterization of traditional adobe masonry elements*. MEng Thesis, University of Minho.
- De Vasconcelos, G.d.F.M. (2005). *Experimental investigations on the mechanics of stone masonry: Characterisation of granites and behaviour of ancient masonry shear walls*. PhD Thesis, Universidade do Minho.
- Debnath, A., Singh, S. and Singh, Y. (1995). Comparative assessment of energy requirements for different types of residential buildings in India. *Energy and Buildings*, vol. 23, no. 2, pp. 141–146.
- Deboucha, S. and Hashim, R. (2011). A review on bricks and stabilized compressed earth blocks. *Scientific Research and Essays*, vol. 6, no. 3, pp. 499–506.
- Dobbs, R. (2010). Megacities. URL: <https://foreignpolicy.com/2010/08/16/megacities/>. (Visited: 2018/08/15).
- Domone, P.L.J. and Illstone, J.M. (2001). *Construction Materials Their nature and behaviour. 3rd Edition*. Spon Press, London and New York.
- Dowling, D. (2004). Improved adobe mudbrick in application: Child - care centre construction in El Salvador. In: *13th World Conference on Earthquake Engineering*, 705.
- EBANZ (2015). Earth Building Standards. Earth Building Association of New Zealand. URL: http://www.earthbuilding.org.nz/?page_id=15. (Visited: 2018/08/20).
- EN 1015-10 (1999). Methods of test for mortar for masonry. Part 10: Determination of dry bulk density of hardened mortar. In: *Brussels: European Committee for Standardization*. BSi.
- EN 1015-11 (1999). Methods of test for mortar for masonry. Part 11: Determination of flexural and compressive strength of hardened mortar. In: *Brussels: European Committee for Standardization*. BSi.
- EN 1015-3 (1999). Methods of test for mortar for masonry. Part 3: Determination of consistence of fresh mortar (by flow table). In: *Brussels: European Committee for Standardization*. BSi.
- EN 1052-1 (1999). Methods of test for masonry Part 1: Determination of compressive strength. In: *Brussels: European Committee for Standardization*. BSi.

- EN 1052-3 (2002). Methods of test for masonry. Part 3: Determination of initial shear strength. In: *Brussels: European Committee for Standardization*. BSi.
- EN 1052-5 (2005). Methods of test for masonry. Part 5: Determination of bond strength by the bond wrench method. In: *Brussels: European Committee for Standardization*. BSi.
- EN 12390-13 (2013). Testing hardened concrete: Determination of the secant modulus of elasticity in compression. In: *Brussels: European Committee for Standardization*. BSi.
- EN 1996-1 (2005). General rules for reinforced and unreinforced masonry structures. In: *Brussels: European Committee for Standardization*.
- EN 5930 (2015). Code of practice for ground investigations. In: *Brussels: European Committee for Standardization*. BSi.
- EN 771-1 (2011). Specification for masonry units. Part 1: Clay masonry units. In: *Brussels: European Committee for Standardization*. BS.
- EN 771-3 (2011). Specification for masonry units. Part 3: Aggregate concrete masonry units. In: *Brussels: European Committee for Standardization*. BSi.
- EN 772-1 (2011). Masonry units Part1: Determination of compressive strength. In: *Brussels: European Committee for Standardization*. BSi.
- EN 772-11 (2011). Methods of test for masonry units. Part 11: Determination of water absorption of aggregate concrete, manufactured stone and natural stone masonry units due to capillary action and the initial rate of water absorption of clay masonry units. In: *Brussels: European Committee for Standardization*. BSi.
- EN 772-13 (2013). Methods of test for masonry units. Part 13: Determination of net and gross dry density of masonry units (except for natural stone). In: *Brussels: European Committee for Standardization*. BSi.
- Evonik Industries (2011). GPS Safety Summary. Tech. Rep. November, Evonik.
- Fourie, J. (2017). *Characterisation and Evaluation of the Mechanical Properties of Alternative Masonry Units*. MEng Thesis, Stellenbosch University.
Available at: <http://scholar.sun.ac.za/handle/10019.1/100880>
- Fratini, F., Pecchioni, E., Rovero, L. and Tonietti, U. (2011). The earth in the architecture of the historical centre of Lamezia Terme (Italy): Characterization for restoration. *Applied Clay Science*, vol. 53, no. 3, pp. 509–516.
- Garcia-Lodeiro, I., Palomo, A. and Fernández-Jiménez, A. (2014). An overview of the chemistry of alkali-activated cement-based binders. In: *Handbook of Alkali-Activated Cements, Mortars and Concretes*, chap. 2, pp. 19–47. Woodhead Publishing, Madrid.
- Government Gazette No.42483 (2019). Carbon Tax Act No. 15. Tech. Rep..
- Grenley, D.G. (1969). Study of the effect of certain modified mortars on compressive strength and flexural strength of masonry. *Designing, engineering, and constructing with Masonry Products*, pp. 28–33.
- Groot, C.J. (1993). Effects of water on mortar-brick bond. pp. 57 – 70.
- Haach, V.G., Vasconcelos, G. and Lourenço, P.B. (2011). Parametrical study of masonry walls subjected to in-plane loading through numerical modeling. *Engineering Structures*, vol. 33, no. 4, pp. 1377–1389.
- Hamid, A.A. (1978). *Behaviour characteristics of concrete masonry*. Ph.D. thesis, McMaster University.
- Hardjito, D., Wallah, S.E., Sumajouw, D.M.J. and Rangan, B.V. (2005). Introducing Fly Ash-Based Geopolymer Concrete : Manufacture and Engineering Properties. In: *OUR WORLD IN CONCRETE & STRUCTURES*, August, pp. 271–278. Singapore.

- Harrison, S.W. and Sinha, B.P. (1995). A study of alternative building materials and technologies for housing in Bangalore, India. *Construction and Building Materials*, vol. 9, no. 4, pp. 211–217.
- Hasanbeigi, A., Menke, C. and Price, L. (2010). The CO₂ abatement cost curve for the Thailand cement industry. *Journal of Cleaner Production*, vol. 18, no. 15, pp. 1507–1516.
- Hughes, D.M. and Zsembery, S. (1980). A Method of Determining the Flexural Bond Strength of Brickwork at Right Angles to the Bed Joint. In: *Paper presented at the Proceedings of the 2nd Canadian Masonry Symposium*, pp. 105–115. Ottawa.
- Huntzinger, D.N. and Eatmon, T.D. (2009). A life-cycle assessment of Portland cement manufacturing : comparing the traditional process with alternative technologies. *Journal of Cleaner Production*, vol. 17, no. 7, pp. 668–675.
- Illampas, R., Ioannou, I. and Charmpis, D.C. (2011). A study of the mechanical behaviour of adobe masonry. *WIT Transactions on the Built Environment*, vol. 118, pp. 485–496.
- Jablonski, N. (1996). Mix design for concrete block. Tech. Rep. 100, The Aberdeen Group.
- Katiyar, A. (2015). *Bond strength measurements from a tamu unbalanced bond wrench in comparison to brick prism ASTM E518 beam test*. MEng Thesis, Texa A&M University.
- Khan, S.U., Nuruddin, M.F., Ayub, T. and Shafiq, N. (2014). Effects of Different Mineral Admixtures on the Properties of Fresh Concrete. *The Scientific World Journal*, vol. 2014, p. 11.
- Kota-Fredericks, Z. (2013). Deputy Minister Zou Kota-Fredericks : South Africa Netherlands research programme on alternatives in development conference. URL: <https://www.gov.za/speaking-notes-human-settlements-deputy-minister-zou-kota-frederickss-south-africa-netherlands>.
- Kuhl, H. (1908). Slag cement and process of making the same.
- Laing, H. (2011). The CMA House: Bringing detail and durability to affordable housing. In: *International housing & construction conference & exhibition 2011*. Concrete Manufacturers Association, Cape Town.
- Lawrence, S. and Page, A. (1994). Bond studies in masonry. In: *10th IB²Mac*, pp. 909–918. Calgary, Canada.
- Leading Architecture (2011). Leading Architecture & Design. URL:<https://www.leadingarchitecture.co.za/tag/low-cost-housing/> (Visites:2019/11/16).
- Lippiatt, B. and Ahmad, S. (2004). *Measuring the life-cycle environmental and economic performance of concrete - The bees approach*. Building and Fire Research Laboratory, National Institute of Standards and Technology, USA.
- Lloyd, N. and Rangan, B. (2010). Geopolymer Concrete with Fly Ash. In: *Second International Conference on Sustainable Construction Materials and Technologies*, vol. 7, pp. 1493–1504.
- Lourenço, P.B. (1996). *Computational strategies for masonry structures*. Ph.D. thesis.
- Lourenço, P.B. (1998). Experimental and numerical issues in the modelling of the behaviour of masonry. *Structural analysis of historical constructions II*, pp. 58–91.
- Lourenço, P.B., Barros, J.O. and Oliveira, J.T. (2004). Shear testing of stack bonded masonry. *Construction and Building Materials*, vol. 18, no. 2, pp. 125–132.
- Lumantarna, R., Biggs, D.T. and Ingham, J.M. (2014). Compressive, Flexural Bond, and Shear Bond Strengths of In Situ New Zealand Unreinforced Clay Brick Masonry Constructed Using Lime Mortar between the 1880s and 1940s. *Journal of Materials in Civil Engineering*, vol. 26, no. 4, pp. 559–566.
- Mahr (2005). Production-Related Roughness Measuring . Mobile With Marsurf.
- Malherbe, D. (2016). *The Characterisation of Compressed Earth Blocks Stabilised with Cement and Agro-industrial Residues*. MEng Thesis, Stellenbosch University. Available at: <http://scholar.sun.ac.za/handle/10019.1/98356>

- Meukam, P., Jannot, Y., Noumowe, A. and Kofane, T.C. (2004). Thermo physical characteristics of economical building materials. *Construction and Building Materials*, vol. 18, no. 6, pp. 437–443.
- Meyer, C. (2009). The greening of the concrete industry. *Cement and Concrete Composites*, vol. 31, no. 8, pp. 601–605.
- Minke, G. (2009). *Building with Earth: Design and Technology of a Sustainable Architecture*. Birkhauser.
- Montazerolghaem, M. and Jaeger, W. (2014). A Comparative Numerical Evaluation of Masonry Initial Shear Test Methods A Comparative Numerical Evaluation of Masonry Initial Shear Test Methods and Modifications Proposed for EN 1052-3. In: *9th International Masonry Conference 2014 in Guimarães*, August.
- Morel, J.C. and Pkla, A. (2002). A model to measure compressive strength of compressed earth blocks with the ‘ 3 points bending test ’. *CONSTRUCTION & BUILDING MATERIALS*, vol. 16, pp. 303–310.
- Morel, J.-C. and Walker, P. (2007). Compressive strength testing of compressed earth blocks. *Construction and Building Materials*.
- Najafgholipour, M.A., Maheri, M.R. and Lourenço, P.B. (2013). Capacity interaction in brick masonry under simultaneous in-plane and out-of-plane loads. *Construction and Building Materials*, vol. 38, pp. 619–626.
- NEN 3835 (1991). Mortels voor metselwerk van stenen, blokken of elementen van baksteen, kalkzandsteen, beton en gasbeton. In: *Nederlands Normalisatie-instituut*, p. 16.
- Neumann, J.V., Bernales, J.B. and Blondet, M. (1984). Seismic resistance of adobe masonry. *Pontificia University Católica of Peru*, p. 19.
- Nichols, J. and Holland, N.L. (2011). A comparative study of balanced bond wrench testing and unbalanced bond wrench testing. In: *NAMC*, 11.
- Owens, G. (2009). *Fulton’s Concrete Technology. 9th ed.* Midrand, South Africa: Cement and Concrete Institute.
- Pacheco-Torgal, F. (2015). Introduction to Handbook of Alkali-activated Cements, Mortars and Concretes. In: *Handbook of Alkali-activated Cements, Mortars and Concretes*, chap. 1, pp. 1–18. Woodhead Publishing, Minho.
- Pacheco-torgal, F., Abdollahnejad, Z., Camões, A.F., Jamshidi, M. and Ding, Y. (2012). Durability of alkali-activated binders : A clear advantage over Portland cement or an unproven issue ? *CONSTRUCTION & BUILDING MATERIALS*, vol. 30, pp. 400–405.
- Pacheco-Torgal, F. and Jalali, S. (2012). Earth construction: Lessons from the past for future eco-efficient construction. *Construction and Building Materials*, vol. 29, pp. 512–519.
- Provis, J.L. (2013). Geopolymers and other alkali activated materials: Why, how, and what? *Materials and Structures*, vol. 47, no. 1-2, pp. 11–25.
- Provis, J.L. and van Deventer, J.S. (2009). Introduction to geopolymers. *Geopolymers: Structure, processing, properties and industrial applications*, pp. 1–11.
- Purdon, A.O. (1940). The action of alkalis on blast-furnace slag. *Journal of the Society of Chemical Industry*, vol. 59, no. 9, pp. 191–202.
- Quagliarini, E., Stazi, A., Pasqualini, E. and Fratolocchi, E. (2010). Cob construction in Italy: Some lessons from the past. *Sustainability*, vol. 2, no. 10, pp. 3291–3308.
- Rao, K.M., Reddy, B.V. and Jagadish, K. (1996). Flexural bond strength of masonry using various blocks and mortars. *Materials and Structures*, vol. 29, no. 2, pp. 119–124.
- Reddy, B.V. and Gupta, A. (2006). Tensile Bond Strength of Soil-Cement Block Masonry Couplets Using Cement-Soil Mortars. *Journal of Materials in Civil Engineering*, vol. 18, no. 1, pp. 36–45.

- Reddy, B.V.V. (2012). Stabilised soil blocks for structural masonry in earth construction. In: *Modern earth buildings: Materials, engineering, construction and applications*, chap. 13, pp. 324–363. Woodhead Publishing.
- Reddy, B.V.V. and Jagadish, K.S. (2003). Embodied energy of common and alternative building materials and technologies. *Energy and Buildings*, vol. 35, pp. 129–137.
- Riddington, J.R., Fong, K.H. and Jukes, P. (1997). Numerical study of failure initiation in different joint shear tests. *Masonry International*, vol. 11, no. 2, pp. 44–50.
- Rigassi, V. (1995). *COMPRESSED EARTH BLOCKS : MANUAL OF PRODUCTION*, vol. I.
- RILEM (1996). MS-B.4: Determination of shear strength index for masonry unit/mortar junction. *Materials and Structures/Materiaux et Constructions*, vol. 29, no. 3, pp. 459–475.
- Rogers, C.D.F. and Smalley, I.J. (1995). The adobe reaction and the use of loess mud in construction. *Engineering Geology*, vol. 40, no. 3-4, pp. 137–138.
- Sakulich, A.R. (2011). Reinforced geopolymer composites for enhanced material greenness and durability. *Sustainable Cities and Society*, vol. 1, no. 4, pp. 195–210.
- SANS 0400 (1990). The application of the National Building Regulations. In: *South African National Standard*. The Council of the South African Bureau of Standards, Pretoria.
- SANS 10145 (2011). Concrete masonry construction. In: *South African National Standard*. SABS Standards Division, Pretoria.
- SANS 10400-A (2016). The application of the National Building Regulations Part A: General principles and requirements. 3rd Edition. In: *South African National Standard*. SABS Standards Division, Pretoria.
- SANS 10400-K (2015). The application of the National Building Regulations Part K : Walls. 3rd Edition. In: *South African National Standard*. SABS Standards Division, Pretoria.
- SANS 1215 (2008). Concrete masonry units. In: *South African National Standard*. SABS Standards Division, Pretoria.
- SANS 201 (2008). Sieve analysis fines , content and dust content of aggregates. In: *South African National Standard*. SABS Standards Division, Pretoria.
- SANS 3001-GR30 (2015). Civil engineering test methods. Part GR30: Determination of the maximum dry density and optimum moisture content. In: *South African National Standard*. SABS Standards Division, Pretoria.
- SANS 5844 (2006). Particle and relative densities of aggregates. In: *South African National Standard*. SABS Standards Division, Pretoria.
- Sarangapani, G., Reddy, B.V.V. and Jagadish, K.S. (2005). Brick-Mortar Bond and Masonry Compressive Strength. *Journal of Materials in Civil Engineering*, vol. 17, no. 02, pp. 229–237.
- Schneemayer, A., Schranz, C., Kolbitsch, A. and Tschegg, E.K. (2014). Fracture-Mechanical Properties of Mortar-to-Brick Interfaces. *Journal of Materials in Civil Engineering*, vol. 26, no. 1997, pp. 1–8.
- Schneider, M., Romer, M., Tschudin, M. and Bolio, H. (2011). Sustainable cement production-present and future. *Cement and Concrete Research*, vol. 41, no. 7, pp. 642–650.
- Schubert, P. (1998). Properties of masonry, bricks and mortar. *Mauerwerk*, pp. 89–105.
- Shafiqh, P., Mahmud, H.B., Jumaat, M.Z. and Zargar, M. (2014). Agricultural wastes as aggregate in concrete mixtures - A review. *Construction and Building Materials*, vol. 53, pp. 110–117.
- Shakir, A.A. and Mohammed, A.A. (2013). Manufacturing of Bricks in the Past, in the Present and in the Future: A state of the Art Review. *International Journal of Advances in Applied Sciences*, vol. 2, no. 3, pp. 145–156.

- Shi, C., Krivenko, P. and Roy, D. (2006). *Alkali-Activated Cements and Concretes*. Taylor & Francis, New York.
- Shiso, E.P. (2019). *In-Plane Structural Response of Single-Storey Unreinforced Walls Constructed Using Alternative Masonry Units*. MEng Thesis, Stellenbosch University.
Available at: <http://scholar.sun.ac.za/handle/10019.1/105889>
- Sinha, B.P. (1967). *Model studies related to loadbearing brickwork*. Ph.D. thesis, University of Edinburgh.
- Sitton, J.D., Zeinali, Y., Heidarian, W.H. and Story, B.A. (2018). Effect of mix design on compressed earth block strength. *Construction and Building Materials*, vol. 158, pp. 124–131.
- South African Human Rights Commission (1997). The Right to Adequate Housing Factsheet. Tech. Rep..
- Stone, L. (2017). *Tensile fracture energy of Alternative Masonry Units*. Bachelors Dissertation, University of Stellenbosch.
- Sugo, H.O., Page, A. and Lawrence, S.J. (2001). The development of mortar / unit bond. In: *Canadian Masonry Symposium*, 9. UNB, Canada.
- Tennant, A.G., Foster, C.D. and Reddy, B.V.V. (2012). Verification of Masonry Building Code to Flexural Behavior of Cement-Stabilized Soil Block. *Journal of Materials in Civil Engineering*, vol. 25, no. 3, pp. 303–307.
- Tschegg, E.K., Jamek, M. and Schouenborg, B. (2008). Fracture properties of marble - Mortar compounds. *Bulletin of Engineering Geology and the Environment*, vol. 67, no. 2, pp. 199–208.
- Van der Pluijm, R. (1992a). Deformation controlled shear tests on masonry. Tech. Rep., TNO Buildings and Construction, Delft, The Netherlands.
- Van der Pluijm, R. (1992b). Material properties of masonry and its components under tension and shear. In: *Proceedings 6th Canadian Masonry Symposium*, pp. 675–686. Saskatoon, Canada.
- Van der Pluijm, R. (1993). Shear behavior of bed joints. In: *Proceedings 6th North American Masonry Conference*, pp. 125–136. Drexel University, Philadelphia, Pennsylvania, USA.
- Van der Pluijm, R. (1999). *Out-of-Plane Bending of Masonry Behaviour and Strength*. Ph.D. thesis.
- Van Jaarsveld, J., Van Deventer, J. and Lukey, G. (2003). The characterization of source materials in fly ash-based geopolymers. *Materials Letters*, vol. 57, pp. 1272–1280.
- Van Zijl, G.P.A.G. (2004 nov). Modeling Masonry Shear-Compression: Role of Dilatancy Highlighted. *Journal of Engineering Mechanics*, vol. 130, no. 11, pp. 1289–1296.
- Varum, H., Costa, A., Martins, T., Pereira, H., Almeida, J.A., Rodrigues, H. and Silveira, D. (2007). Structural behaviour characterization of existing adobe constructions in Aveiro. In: *First Euro-Mediterranean Regional Conference - Traditional Mediterranean Architecture: Present and Future - Reference no. 090*, pp. 470–471. Civil Engineering Department, University of Aveiro, Aveiro.
- Velde, B. (2008). Formation of Earthen Materials. *Terra Literature Review - An overview of research in earthen architecture conservation*, pp. 15–20.
- Walker, P. (1999). Bond Characteristics of Earth Block Masonry. *Journal of Engineering Mechanics*, vol. 11, pp. 249–256.
- Walker, P. and Stace, T. (1996). Properties of some cement stabilised compressed earth blocks and mortars. *Materials and Structures*, vol. 30, no. 9, pp. 545–551.
- Wang, T. (2019). Cement production globally and in the U.S. from 2010 to 2018 (in million metric tons). URL: <https://www.statista.com/statistics/219343/cement-production-worldwide/> (Visited: 2019/08/03).
- Yip, C.K., Lukey, G.C., Provis, J.L. and van Deventer, J.S.J. (2008). Effect of calcium silicate sources on geopolymerisation. *Cement and Concrete Research*, vol. 38, no. 4, pp. 554–564.

- Zengin, B., Toydemir, B., Ulukaya, S., Oktay, D., Yüzer, N. and Kocak, A. (2018). The effect of mortar type and joint thickness on mechanical properties of conventional masonry walls. *Structural Engineering and Mechanics*, vol. 67, no. 6, pp. 579–585. ISSN 12254568.
- Zeranka, S. and Van Zijl, G. (2018). *Steel fibre-reinforced concrete: Multi-scale characterisation towards numerical modelling*. Ph.D. thesis.
Available at: <http://scholar.sun.ac.za/handle/10019.1/102734>
- Zhang, S., Richart, N. and Beyer, K. (2019). Numerical evaluation of test setups for determining the shear strength of masonry. *Materials and Structures*, vol. 51, no. 4, pp. 1–12.
- Zhang, Z., Wang, H., Provis, J.L. and Reid, A. (2013). Efflorescence : A Critical Challenge for Geopolymer Applications ? In: *Concrete Institute Australia's Biennial National Conference*. Gold Coast, Australia.
- Zhao, Z., Hee, S. and Shah, S.P. (2008). Effect of specimen size on fracture energy and softening curve of concrete : Part I . Experiments and fracture energy. *Cement and Concrete Research*, vol. 38, pp. 1049–1060.